Space plasmas: Numerical simulation

Jörg Büchner

with thanks to the members of the TSSSP group at the MPS Göttingen: Neeraj Jain & Patrick Kilian & Patricio Munoz & Jan Skala

Max-Planck-Institut für Sonnensystemforschung (MPS)

and

Georg August University Göttingen, Germany

Max-Planck -Princeton Center for Plasma Physics

Princeton-Garching

Outline / lecture plan

1. MHD
   - basic equations, discretization, accuracy order, convergence
   - conservative and dissipative equations- solution schemes
   - parallelization
   - examples for exercises:
     - Magnetopaus and magnetotail reconnection
     - Kelvin Helmholtz instability
2. Kinetic simulation of collisionless plasmas
   - basic equations: Vlasov;
   - Vlasov codes: finite volume discretization
   - reversibility, filamentation and dissipation problem
   - examples for exercises

Invitation

There is an long series of „International Schools and Symposia of Space Plasma Simulation“, founded by M. Ashour-Abdalla, R. Gendrin, H. Matsumoto and H. Sato. Since their time, when simulation was till at its infancy, it trained the actual generations of „simulationists“. Next in Prague, June 2014

Opened February 1st 2014: new building of the MPS in Göttingen

Resistive two-fluid theory

$$\frac{\partial n}{\partial t} + \nabla \cdot (n\mathbf{v}) = 0$$

$$\frac{\partial (nm\mathbf{v})}{\partial t} + \nabla \cdot (nm\mathbf{v}\mathbf{v}) = -\nabla \cdot \mathbf{P} + \rho\mathbf{E} + \mathbf{j} \times \mathbf{B}$$

$$\mathbf{E} + \mathbf{v} \times \mathbf{B} = \eta\mathbf{j} + \frac{1}{ne}\mathbf{j} \times \mathbf{B} - \frac{1}{ne}\nabla \cdot \mathbf{P}_e + \frac{m_e}{ne^2}\frac{\partial \mathbf{j}}{\partial t}$$

$$\nabla \times \mathbf{B} = \mu_0\mathbf{j} + \mu_0\epsilon_0\frac{\partial \mathbf{E}}{\partial t}$$

$$\nabla \times \mathbf{E} = -\frac{\partial \mathbf{B}}{\partial t}$$

$$\nabla \cdot \mathbf{B} = 0$$

+ an equation of state, closing for the pressure (e.g. adiabatic)

From two-fluid to MHD equations

$$\frac{\partial n}{\partial t} + \nabla \cdot (n\mathbf{v}) = 0$$

no charge separation e-i

$$\frac{\partial (nm\mathbf{v})}{\partial t} + \nabla \cdot (nm\mathbf{v}\mathbf{v}) = -\nabla \cdot \mathbf{P} + \rho\mathbf{E} + \mathbf{j} \times \mathbf{B}$$

$$\mathbf{E} + \mathbf{v} \times \mathbf{B} = \eta\mathbf{j} + \frac{1}{ne}\mathbf{j} \times \mathbf{B} - \frac{1}{ne}\nabla \cdot \mathbf{P}_e + \frac{m_e}{ne^2}\frac{\partial \mathbf{j}}{\partial t}$$

$$\nabla \times \mathbf{B} = \mu_0\mathbf{j} + \mu_0\epsilon_0\frac{\partial \mathbf{E}}{\partial t}$$

$$\nabla \times \mathbf{E} = -\frac{\partial \mathbf{B}}{\partial t}$$

only slow processes – no displacement currents

$$\nabla \cdot \mathbf{B} = 0$$

+ an equation of state, closing for the pressure (e.g. P = *n* ^{gamma} or a more complete energy equation

Equation of state, e.g. an energy eq.

$$\frac{\partial p}{\partial t} = -\nabla \cdot p\boldsymbol{u} - (\gamma - 1)p\nabla \cdot \boldsymbol{u} + (\gamma - 1)S$$

heat conduction

along magnetic field

$$\nabla . \boldsymbol{q} = \nabla \left(\kappa_{\parallel} \nabla_{\parallel} T \right)$$

$$S = \eta j^2 - \nabla . \boldsymbol{q} - L_r \quad where\ \kappa_{\parallel} \sim 10^{-11} T^{5/2}$$

$$L_r = n\, n_n\, \chi T^{\alpha}\ W/m^3$$

radiative cooling

To obtain a conservative energy equation in the ideal MHD limit ->

$$p = 2h^{\gamma}$$

$$\frac{\partial h}{\partial t} = -\nabla \cdot h\boldsymbol{u} - \frac{(1-\gamma)}{\gamma} h^{1-\gamma} S$$

Problems have to be well posed

In mathematics a problem is called well posed, if

- **The solution exists**
- **The solution is unique**
- **The solution depends continuously on the input**

In numerical solutions a well posed problem is one for which three conditions are met:

- **Existence of the solution**
- **Uniqueness of the solution**
- **Continuous dependence on initial and boundary conditions**

Solutions for initial and boundary conditions (BCs)

Definition: A solution of a partial differential equation (PDE) is a particular function u(x,y,z,t) that 1. satisfies the PDE in the domain of interest R(x,y,z,t) and 2. satisfies given initial (in time) and/ or boundary (in space) conditions (functions f,g).

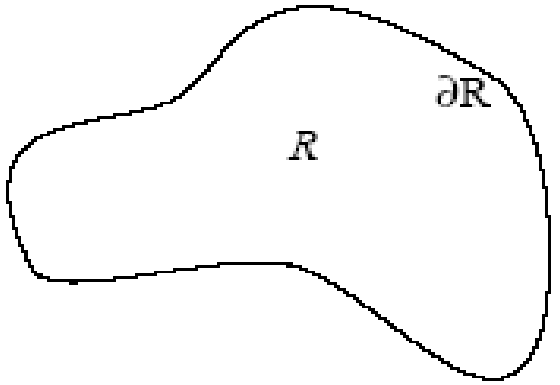

- Dirichlet conditions with $u = f$ on ∂R.
- Neumann conditions with $\partial u/\partial n = f$ or $\partial u/\partial s = g$ on ∂R.
- Mixed (Robin) conditions $\partial u/\partial n + ku = f$, $k > 0$, on ∂R.

Open and periodic BCs

Often: periodic boundary conditions

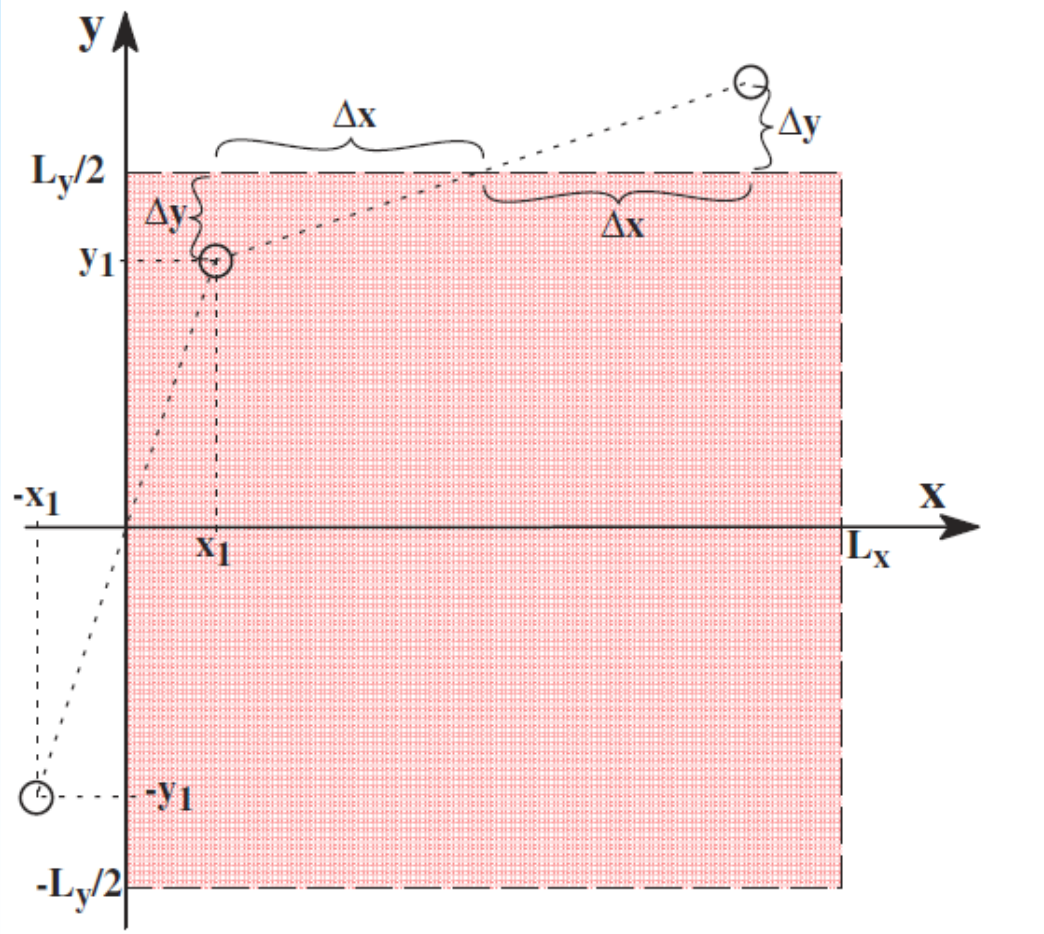

Illustration of the geometry of line symmetry.

Periodic with line symmetry compatible with 3D solar coronal extrapolated B-field compatible simulations, see [Otto, Büchner, Nikutowski, 2008]

Normalization of the equations

Normalization is needed since computers crunch numbers.

Goal: numbers close to unity to reduce the error.

Appropriate quantities for normalization are, e.g.,

Bo; rhoi=n Mi; Lo;

This gives you also a time scale (Lo/Vao).

$$\frac{\partial \rho}{\partial t} = -\nabla \cdot \rho \boldsymbol{u}$$

$$\frac{\partial \rho \boldsymbol{u}}{\partial t} = -\nabla \cdot \rho \boldsymbol{u}\boldsymbol{u} - \nabla h^{\gamma} + \boldsymbol{j} \times \boldsymbol{B}$$

$$\frac{\partial h}{\partial t} = -\nabla \cdot (h\boldsymbol{u}) + \frac{(\gamma - 1)}{\gamma h^{\gamma - 1}} \eta \boldsymbol{j}^2$$

$$\frac{\partial \boldsymbol{B}}{\partial t} = \nabla \times (\boldsymbol{u} \times \boldsymbol{B} - \eta \boldsymbol{j})$$

$$\boldsymbol{j} = \nabla \times \boldsymbol{B}$$

Note: Ideal MHD is scale free. Quantities like resistivity and/or viscosity (i.e. dissipation) introduce scales into MHD.

Eulerian vs Lagrangian

In fluid dynamics -> two ways of specification of the flow field / how to look at the fluid motion:

1. **Eulerian:** the observer focuses on specific locations in space through which the fluid flows passes with time.

Compare: you sit on the bank of a river and watch the water and boat passing your fixed location

2. **Lagrangian:** the observer follows an individual fluid element which moves through space and time.

Compare: you sit in a boat which drifts down a river.

Discretization of the PDEs

Eulerian approach: discrete grid (mesh) here for one spatial dimension (x) and time (t)

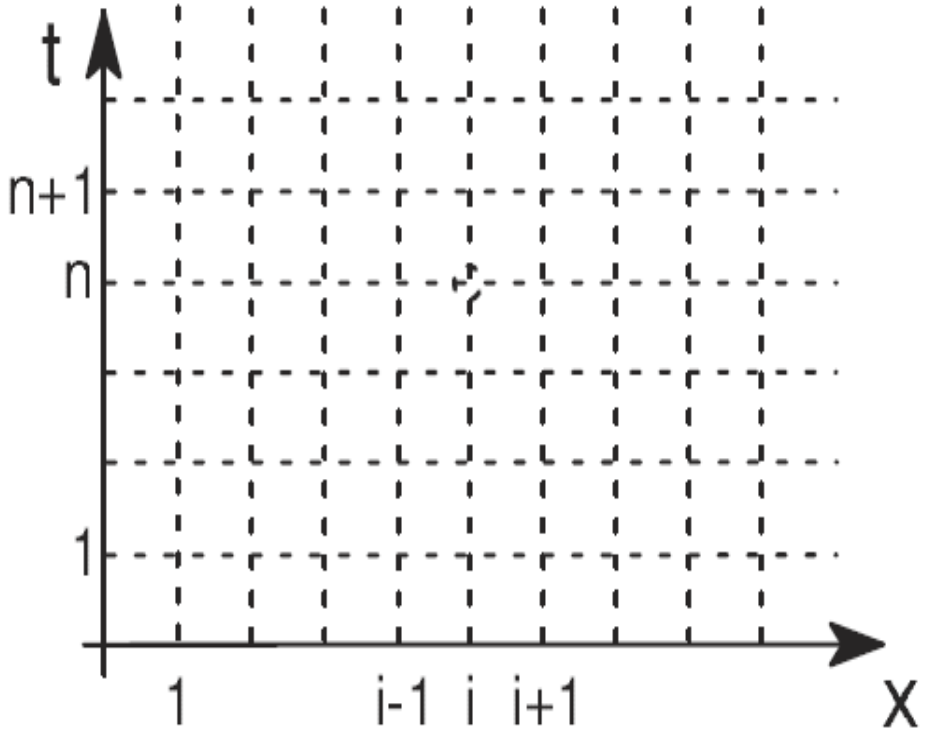

Discretization – simplest case: first order derivative

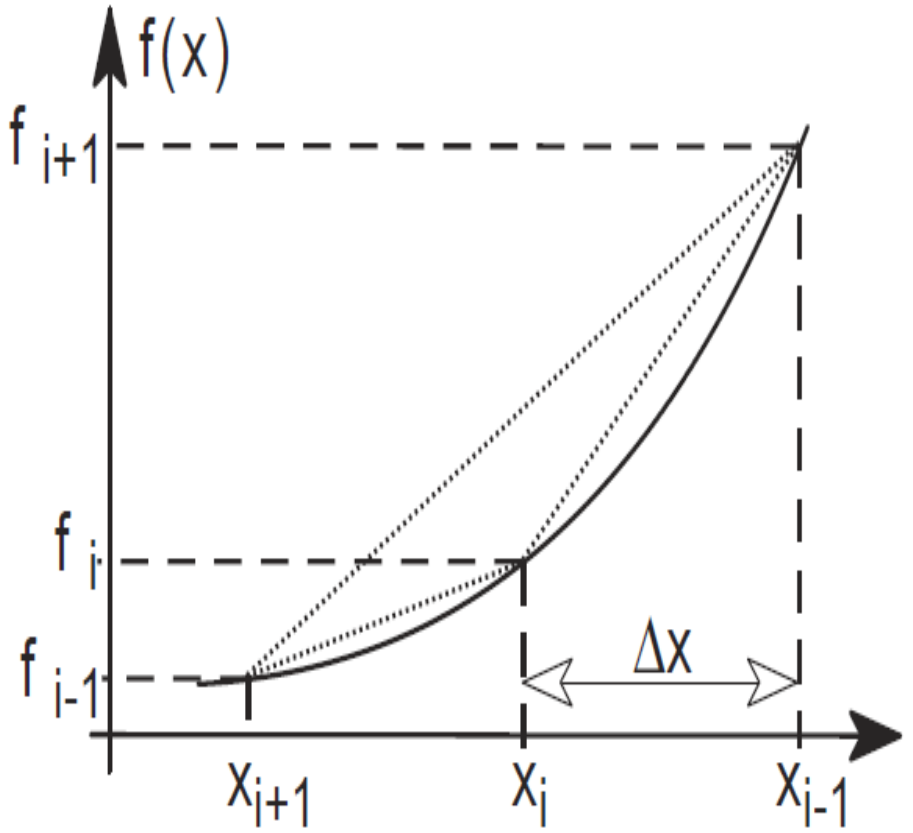

Schemes and accuracy

Different discretizations schemes have been developed,

- **Finite difference codes**
- **Finite elements codes**
- **Finite volume**
- **Fourier-mode based codes …**

Numerical error: depends on the step size Δ_x

Order of accuracy: Higher order schemes provide higher accuracy for the same step size

But higher order schemes:

- **require more complex programming**
- **inclusion of modifications i.e. of more physics are very difficult**
- **they are more error prone**
- **boundary conditions are more complicated to imply and change**
- **The Minimum should be second order in steps size** Δ_x
- **This is usually also the optimum between necessary accuracy and numerical costs / effort !**

Conservative equation solver

Conservative equations can be efficiently discretized, e.g., by a second order accurate Leap-Frog scheme (n= time, i=spatial step):

$$\frac{u_i^{n+1} - u_i^{n-1}}{\Delta t} = -\frac{u_{i+1}^{n} - u_{i-1}^{n}}{\Delta x}$$

Such scheme requires only a forward time derivation being first order accurate in time and second order accurate in space.

The Leap-Frog scheme requires two sets of initial values: in addition to the time step *n* one also has to prescribe a value for the time step *n*-1. While the values for the time step *n-1* are given by the initial conditions the values at the following time step *n* are obtained by a time integration using a Lax method.

Induction equation non-ideality

From the MHD and Maxwell's equations (Ohms law) an induction equation follows:

$$\frac{\partial \mathbf{B}}{\partial t} - \nabla \times (\mathbf{v} \times \mathbf{B}) + \nabla \times (\eta \nabla \times \mathbf{B}) = 0$$

Magnetic Reynolds Number

$$R_m = \frac{\mu_0 \, l \, v}{\eta}$$

In astrophysics, also in the solar corona mostly

$R_m \sim 10^{8\text{-}10}$ >>> 1 such plasma is called "ideal" ,

But non-ideality matters, e.g. for magnetic reconnection

Diffusion type equation solver

Since the Leap-Frog scheme does not solve a diffusive term, e.g. a DuFort-Frankel solver takes over for, e.g., calculating the resistive diffusion terms in the induction equation as well as the dissipation terms in the others equations - the diffusion equations are solved by utilizing a second order accurate DuFort-Frankel discretization.

$$u_i^{n+1} = u_i^{n-1} + 2\Delta t \left[w_1 u_{i-1}^n + w_3 u_{i+1}^n + \frac{1}{2} w_2 \left(u_i^{n-1} + u_i^{n+1} \right) \right]$$

Parallelization 1

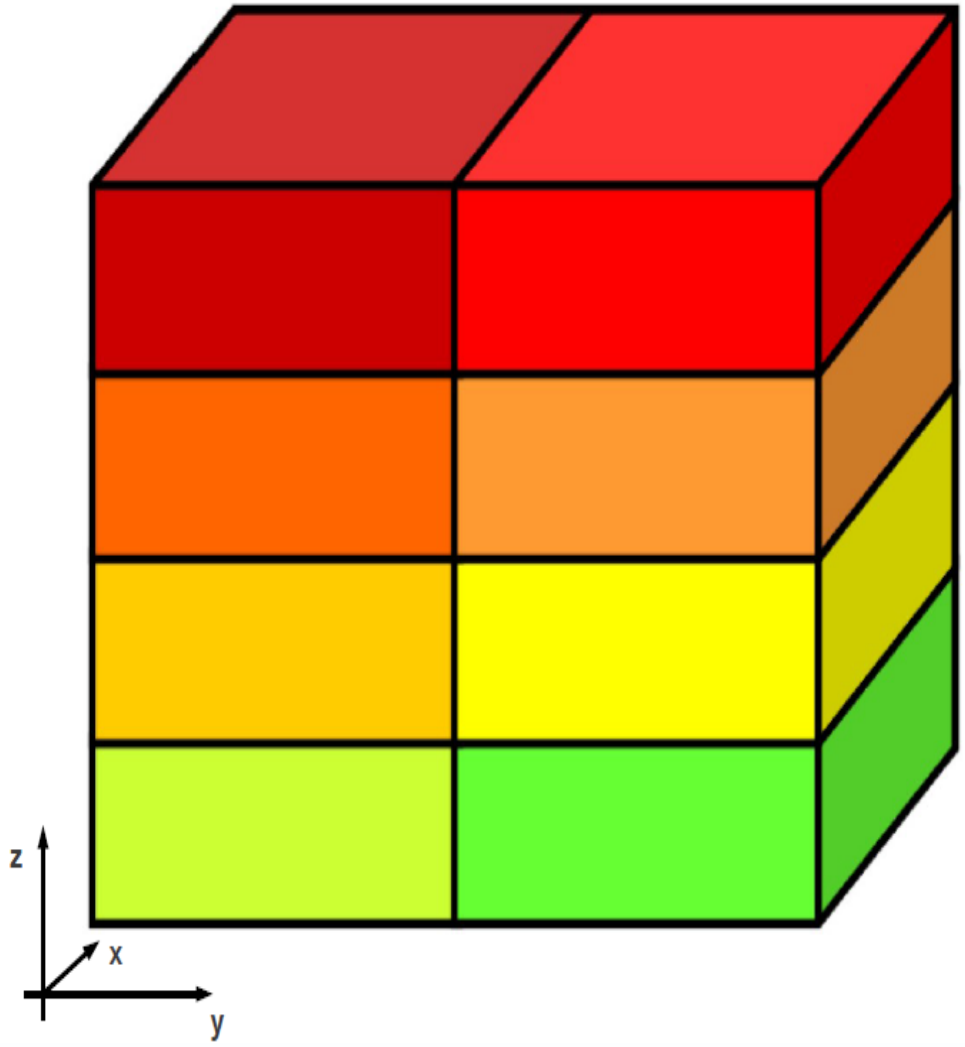

Modern computers allow the parallel use of many CPU cores. Example for there use is a 2D block data decomposition in the *y* and *z* directions for a 3D grid (individual domains are colored differently).

The domanis are assigned to different MPI- (Message Passing Instructions) tasks.

Parallelization 2

Block data decomposition (bold, black lines), 4 MPI tasks. The MPI rank of each sub-domain is given in the square brackets. Each rank has two coordinates, along the y and z direction. E.g. the sub-domain with rank 0 has Cartesian dimension (0,0), rank 1 has (0,1). The decomposition in this example is done into subdomains for a grid of 1620 points using 4 MPI tasks.

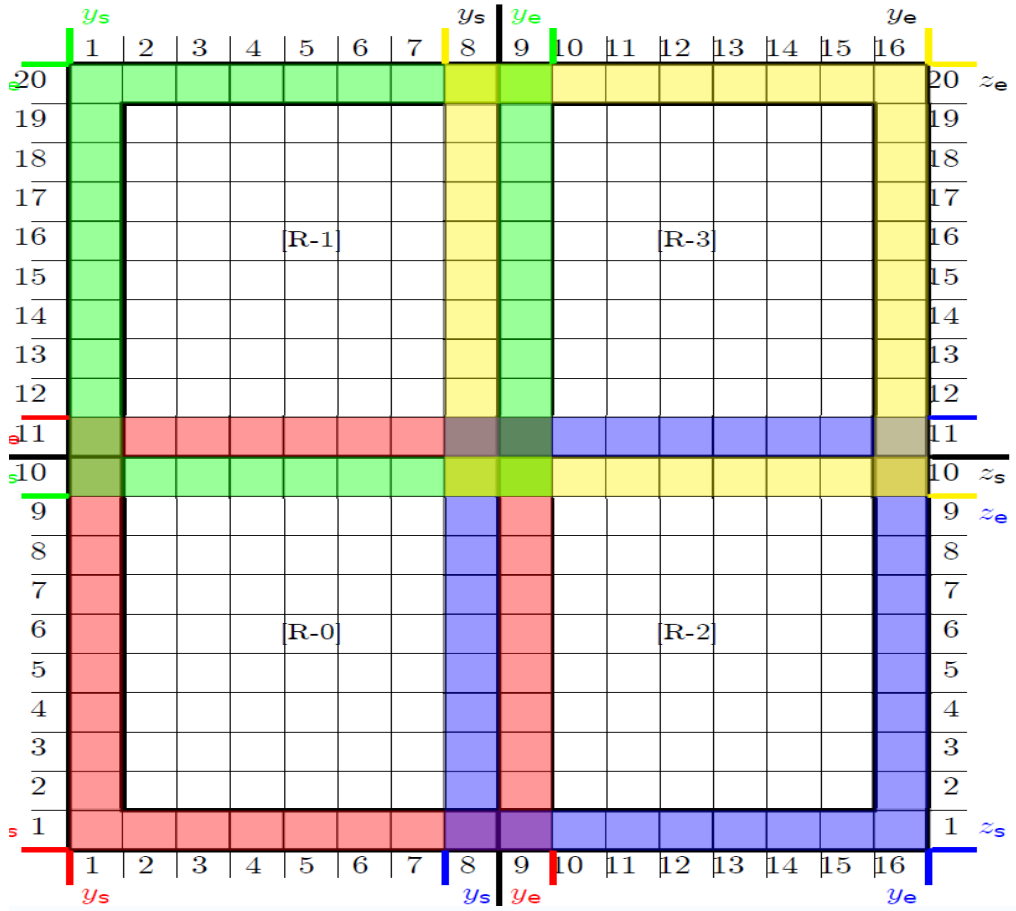

Different colors correspond to different subdomains and tasks. Starting and end points for each sub-domain are labeled Ys; Zs and Ye; Ze, respectively.

Parallelization 3

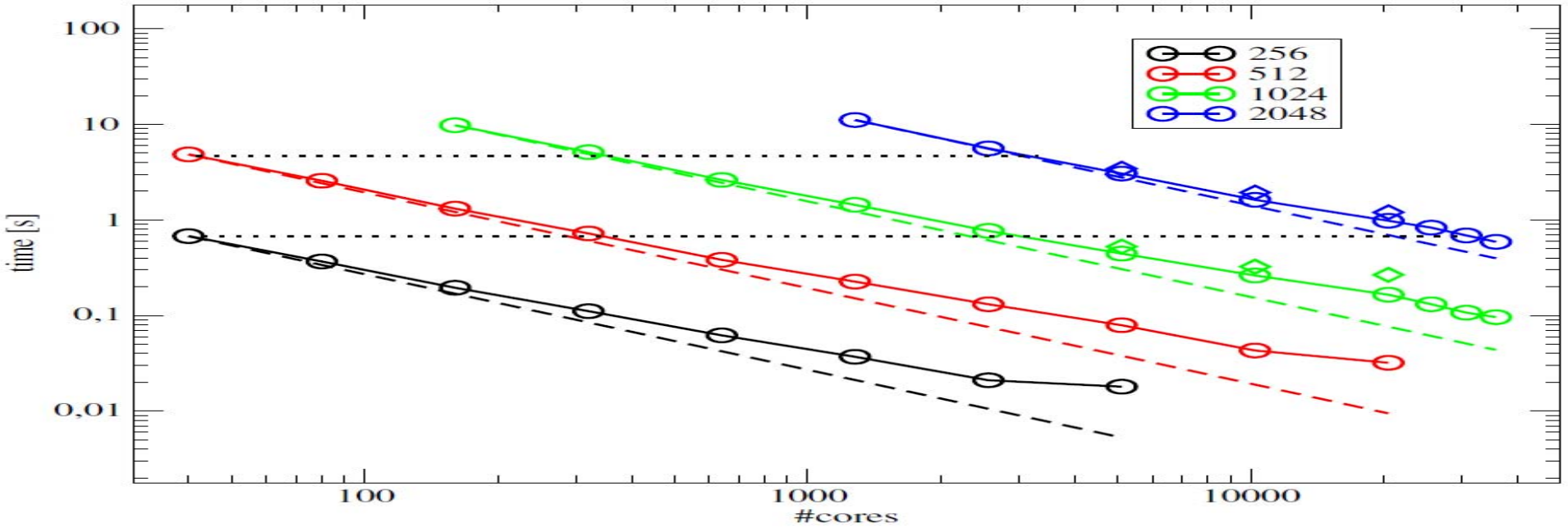

Computing time of a complete integration step versus the number of cores in logarithmic scale. Different colors correspond to different grid sizes. The dashed color lines are the ideal scaling for each grid. The horizontal dotted lines connects the points which belong to the weak scaling. The diamond symbols correspond to runs using an efficient MPI parallelization (GOEMHD3 code)

Ideal plasmas move together with the B-field (Alfven's theorem)

"If the magnetic flux through a circuit of fluid particles of the solar stream vanishes initially, it must vanish at all times."

I.e. if there us a flux at t=0 it moves together wit the plasma

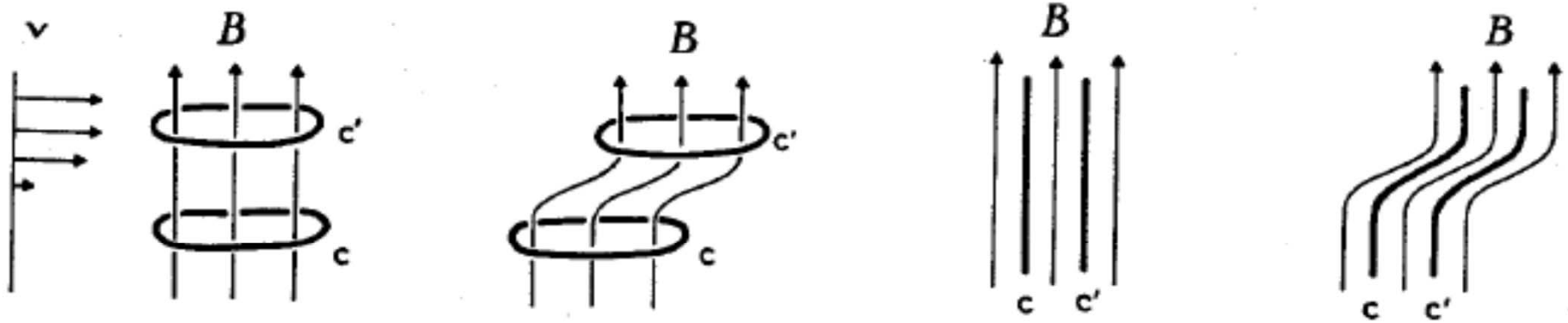

$$\frac{\partial B}{\partial t} = \nabla \times (v \times B) = -B\,\nabla \cdot v + (B \cdot \nabla)v - (v \cdot \nabla)B$$

Indeed 1930: 1. solar wind interaction model – a closed magnetic cavity is formed

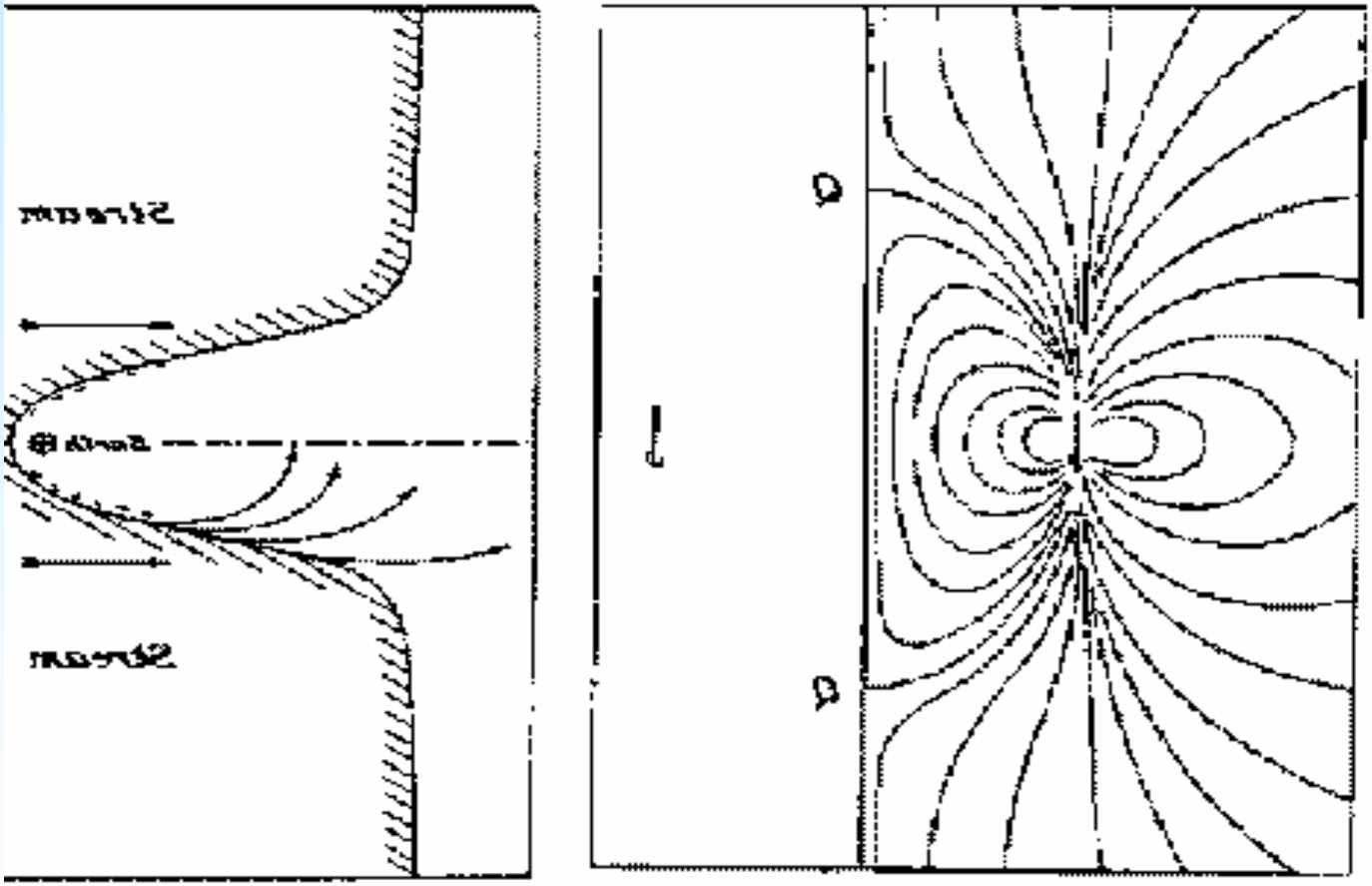

-> First models: interaction of an infinitely conducting gas of solar particles with a magnit – in the Earth -> closed magnetosphere (1950ties: "MAGNETOPAUSE"

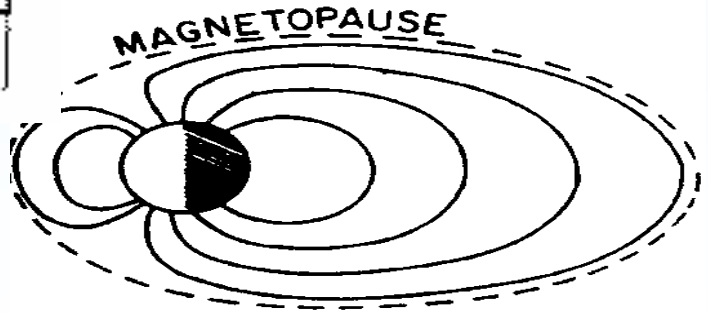

[Chapman and Ferraro, 1930]
Solar particle „*Stream*" - from the left toward the „*Earth*" (mirrored words)

Now we know: the magnetopause (MP) is opening to the solar wind

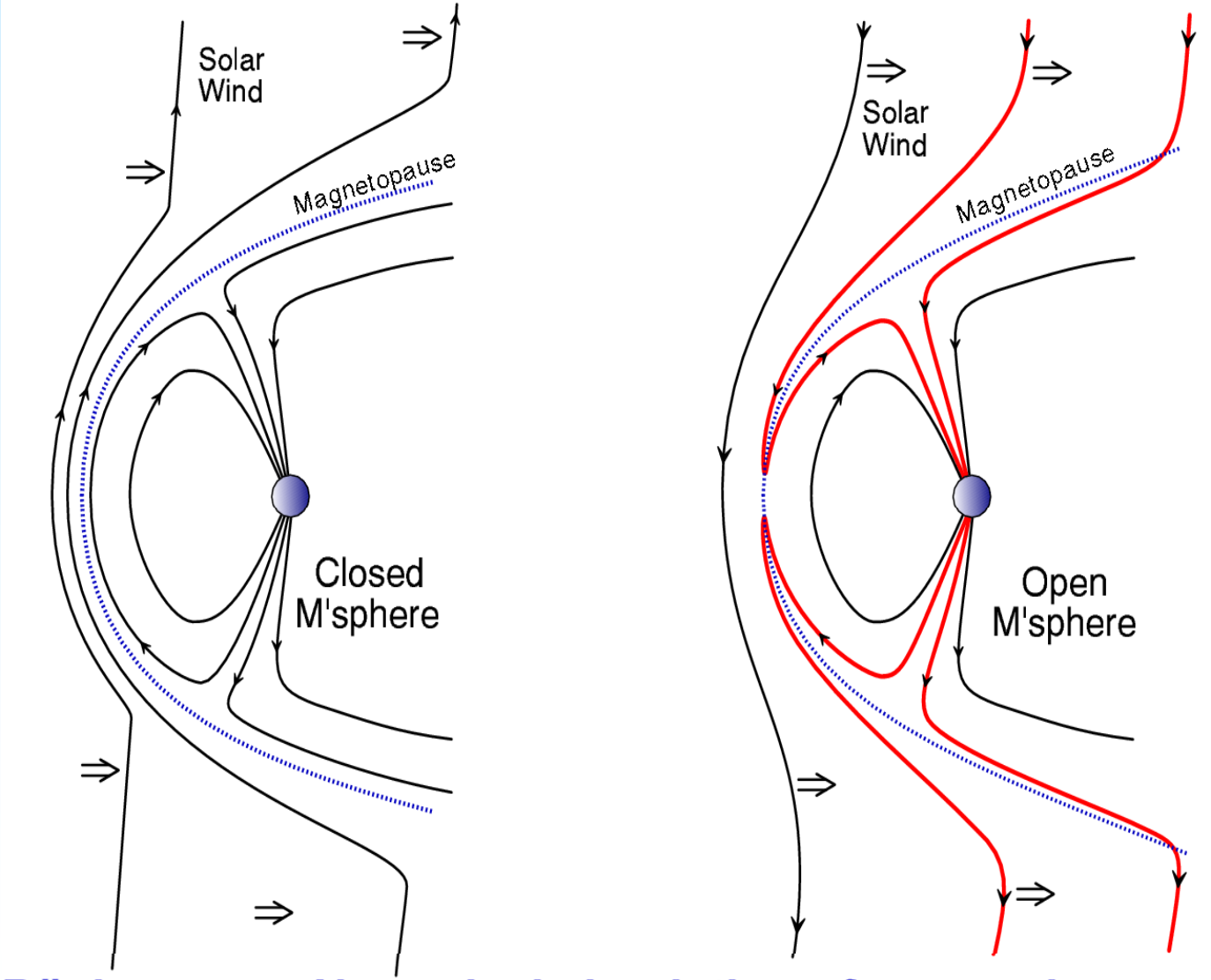

Left figure: "Closed" magnetosphere inside the blue dashed magnetopause

Right figure: Red: „Open" magnetospheric field lines: Reconnection connects

Plasma discontinuities

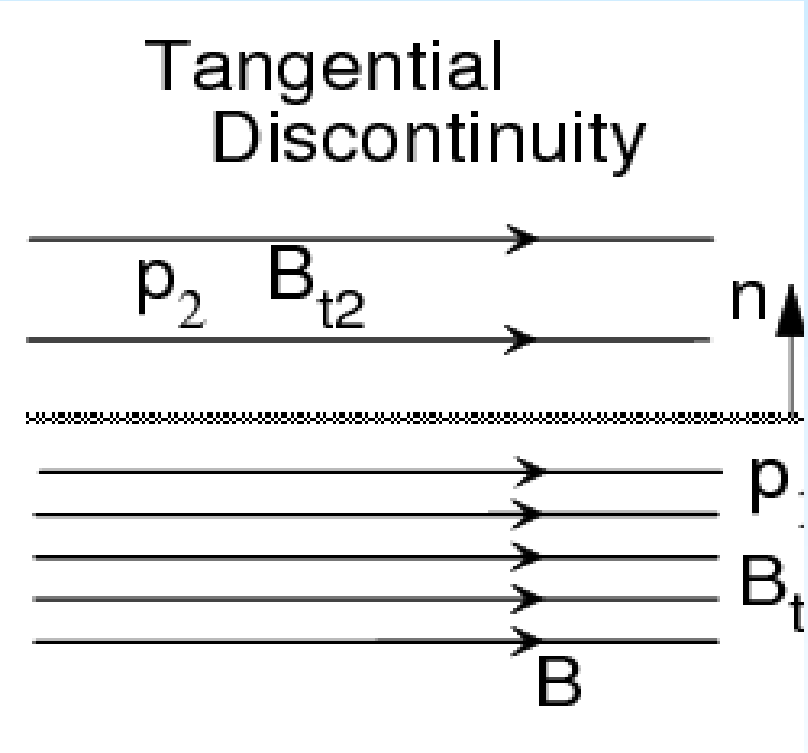

<- closed boundary

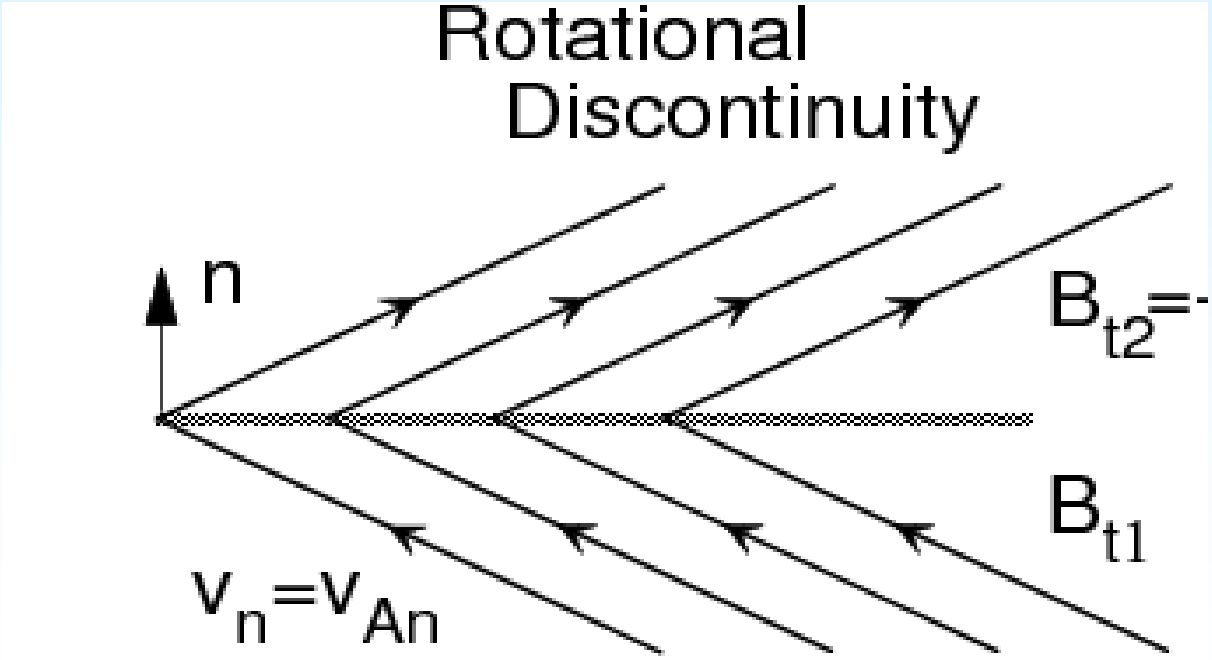

-> open boundary

Mechanism: Magnetic reconnection

Requires large anti-parallel magnetic field components
Delta Va > Va

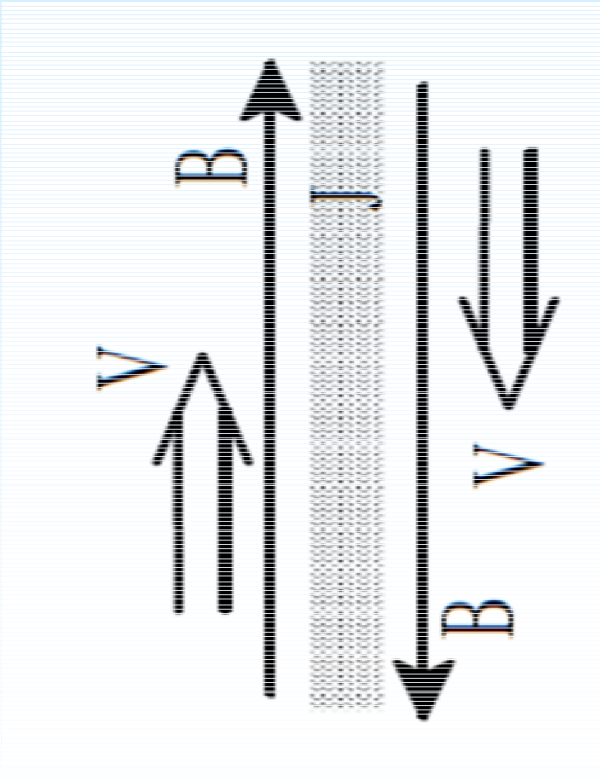

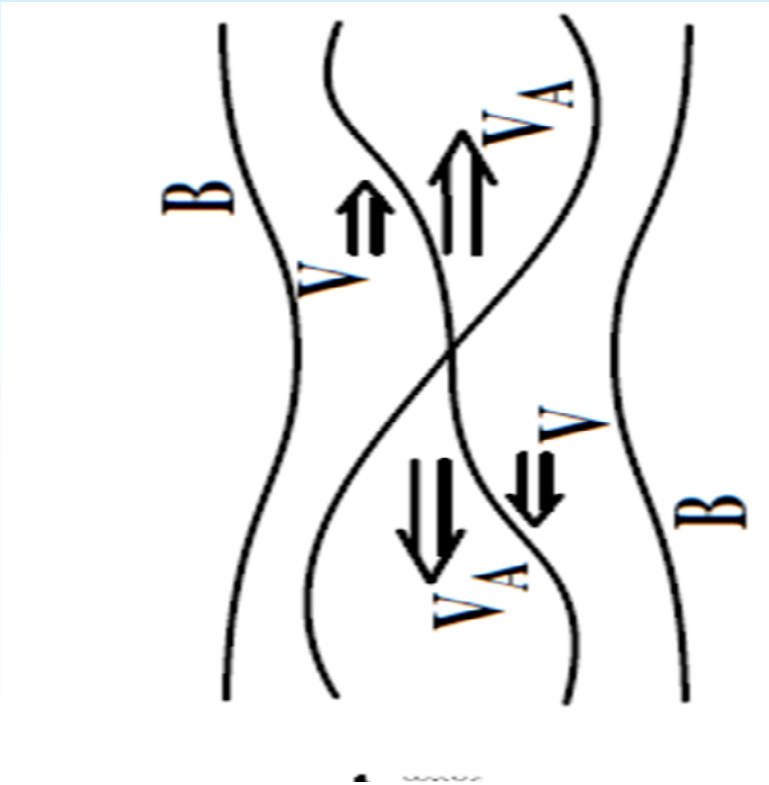

Allows transport of plasma across the MP

Simulation excercise No.1: Magnetopause reconnection

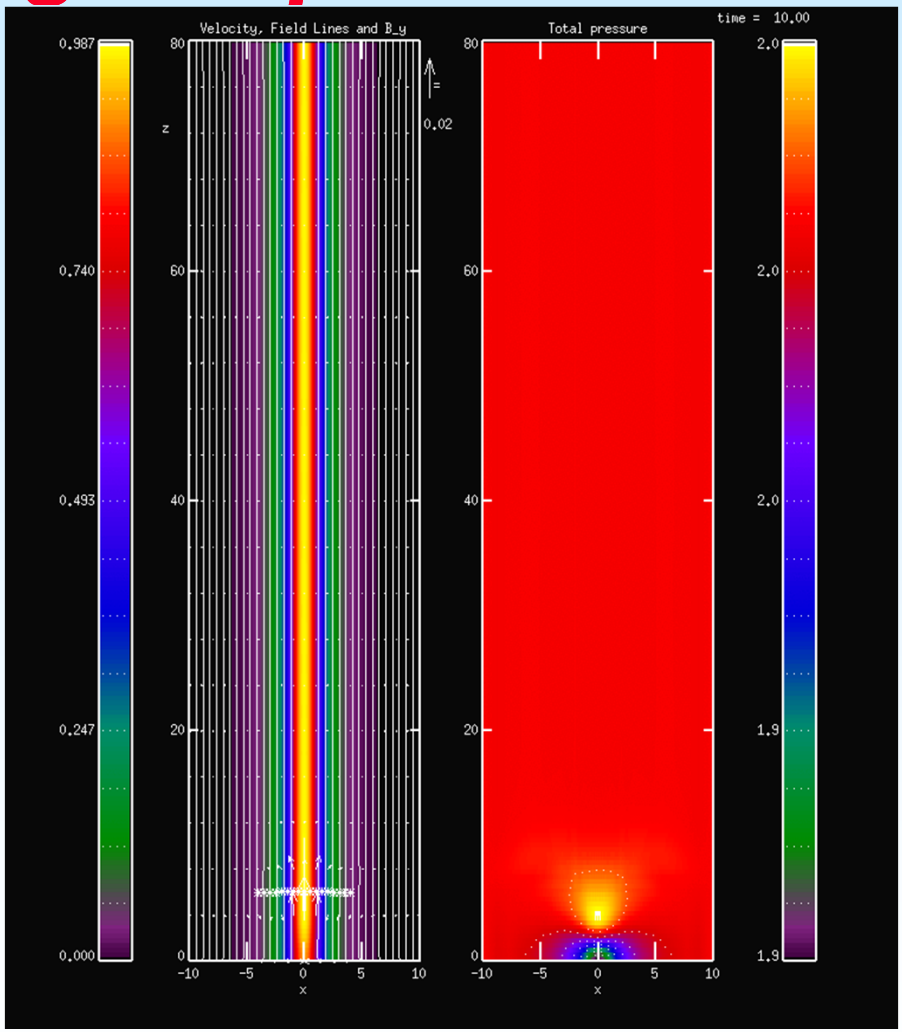

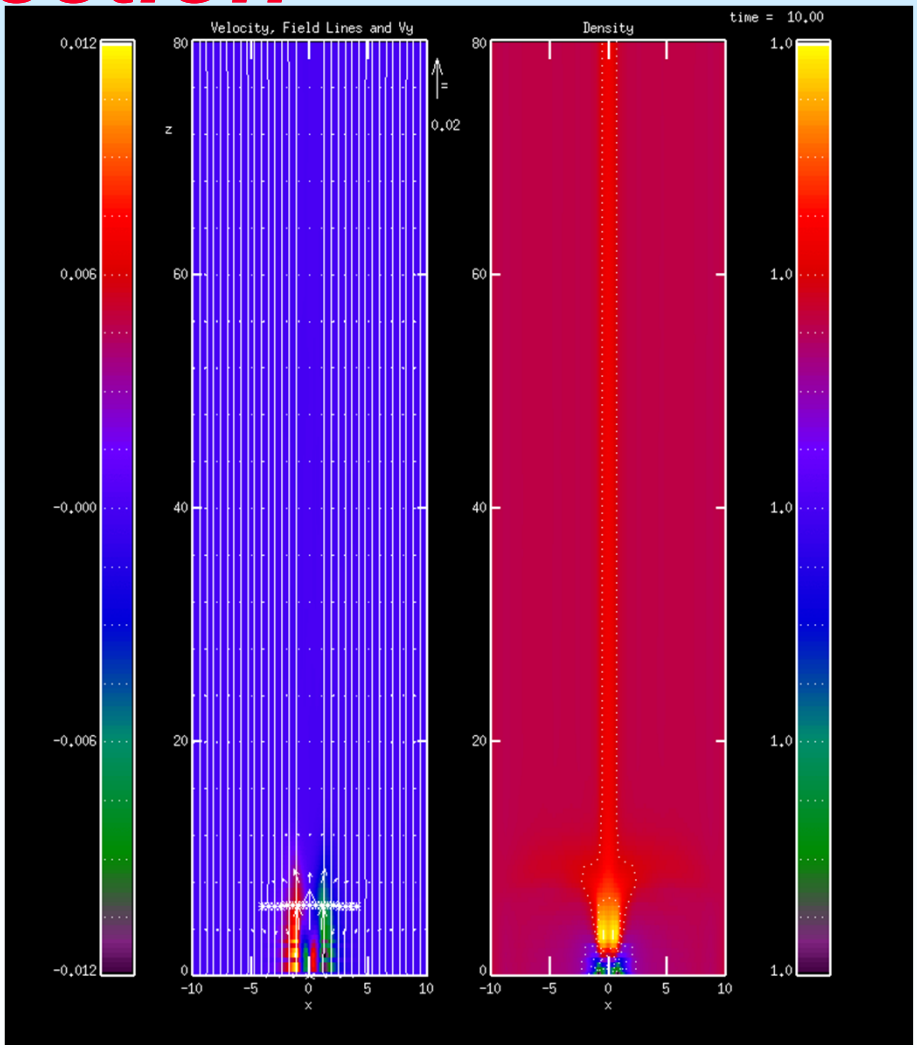

Velocity, B field lines, By; total pressure; velocity, B field lines, density

Single (bursty) MP reconnection

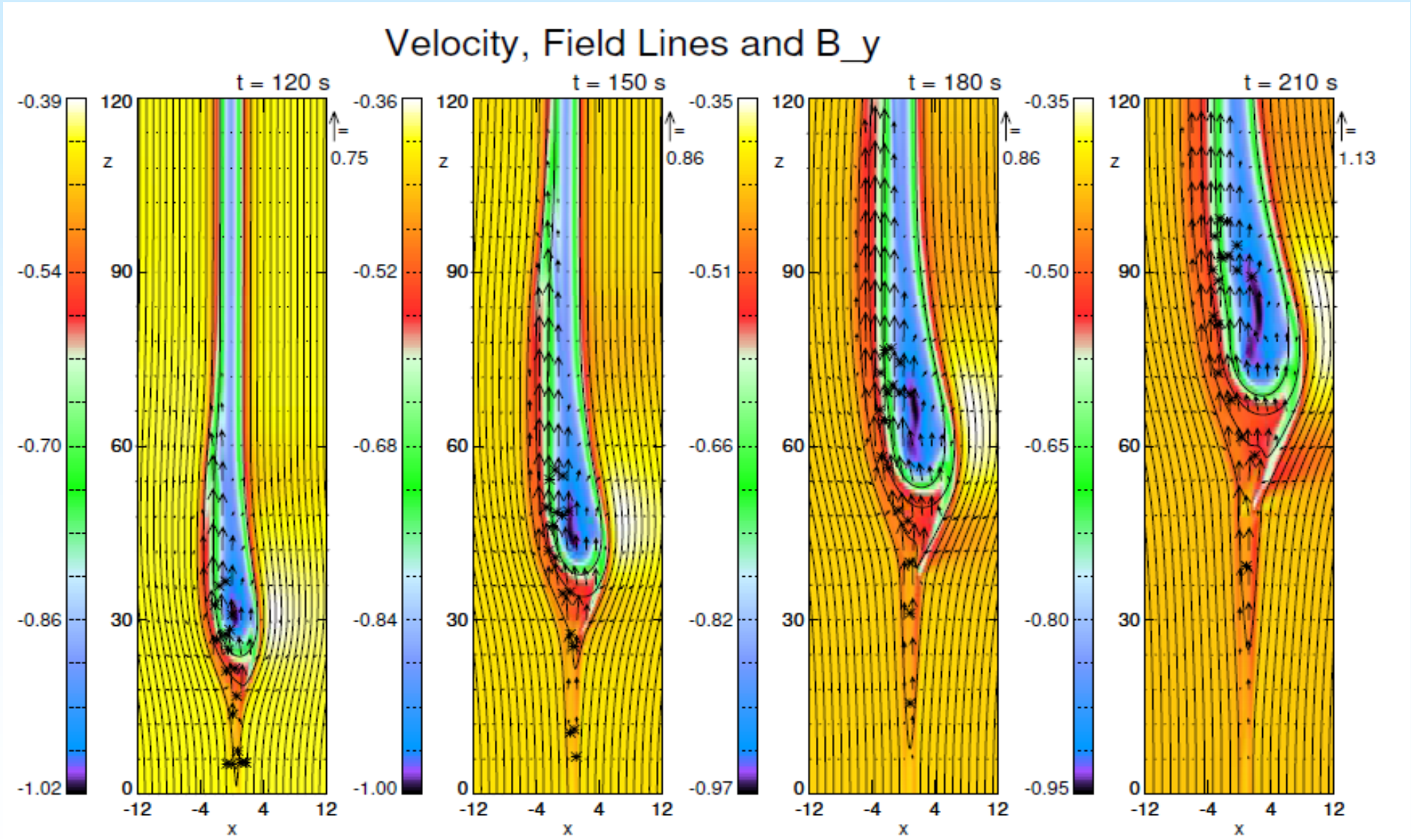

Bursty MP flux transfer events

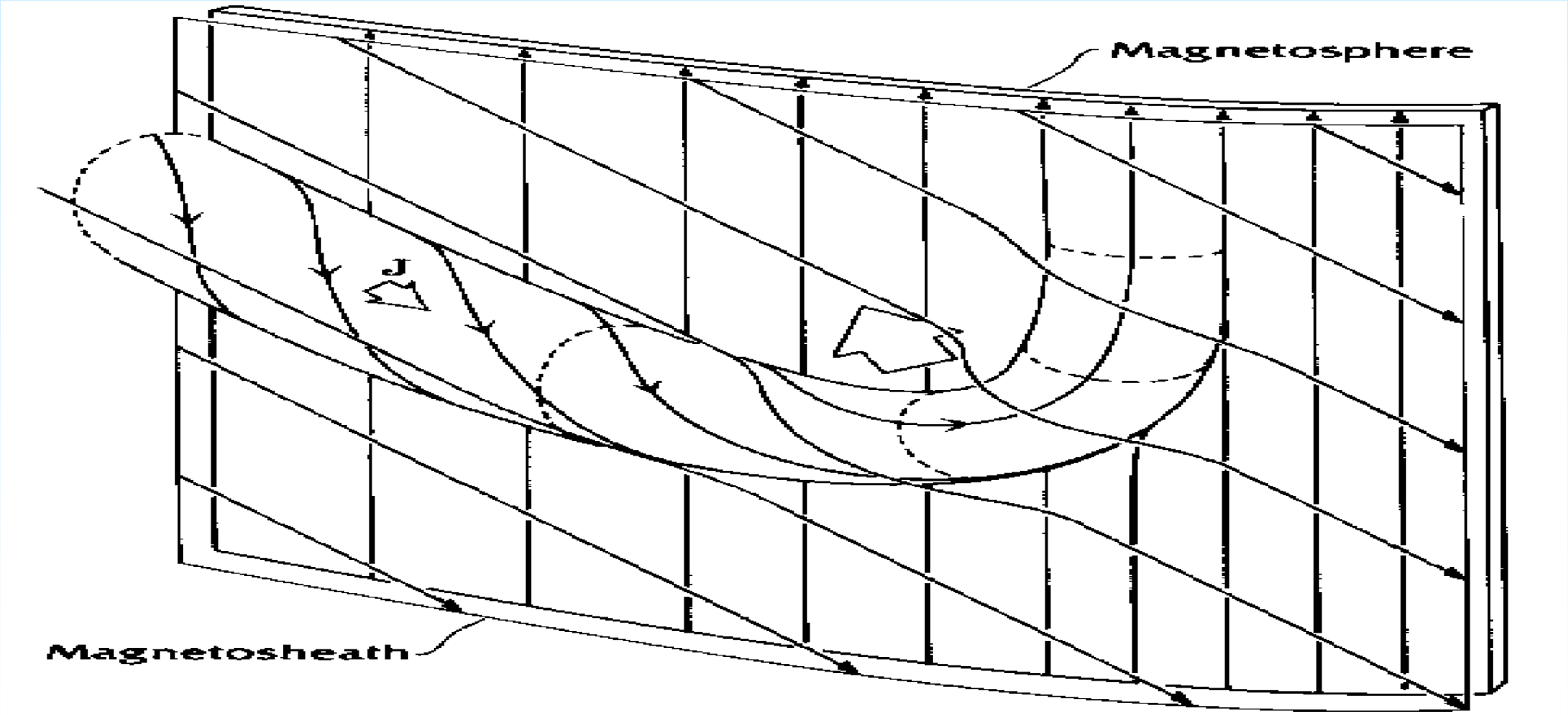

suggested by Russell and Elphic

Viscous interaction

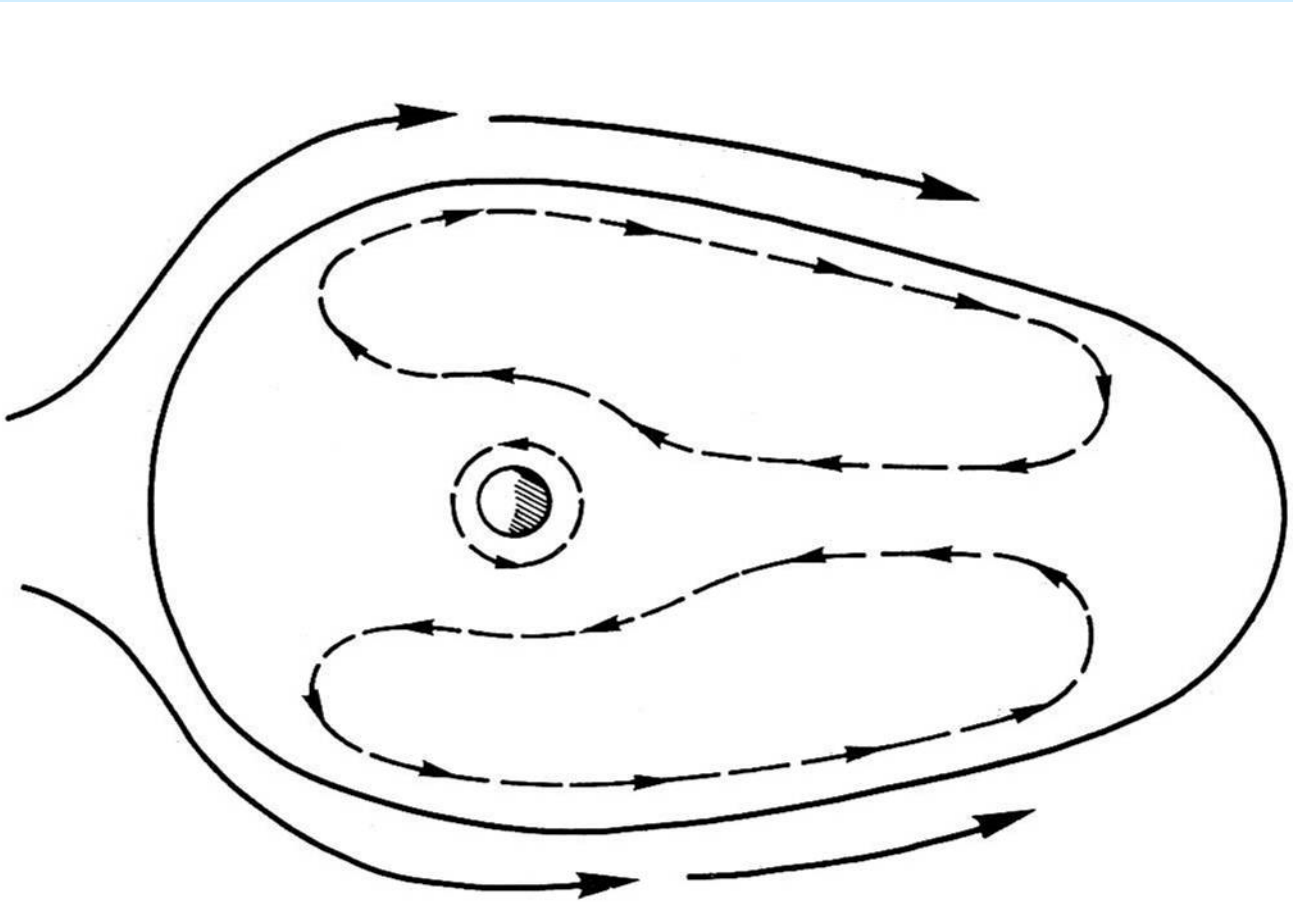

Pattern of the plasma convection driven by viscous interaction between the solar wind with a the earth's magnetosphe ric plasma [Axford and Hines, 1961]

Kelvin Helmholtz instability

A Kelvin–Helmholtz instability (after Lord Kelvin and Hermann von Helmholtz) occurs (a) due to a velocity shear in a single fluid/gas, or (b) due velocity differences across the interface between two fluids/gases of different density.

e.g. at boundaries in neutral atmospheric gases, in water:

(wind blowing over water cause water surface waves; cloud formation and Saturn's bands – see below - Jupiters red spot…)

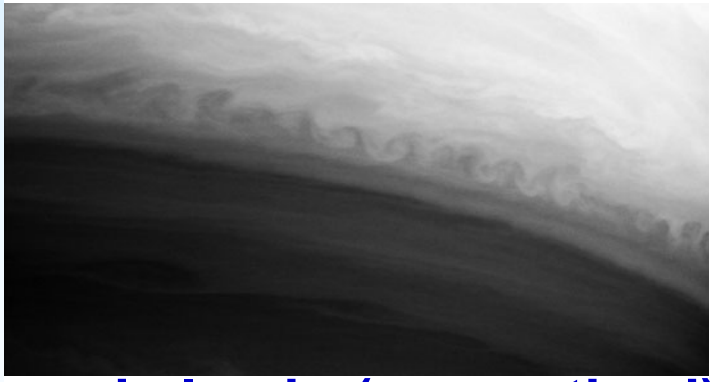

and also in (magnetized) plasmas like in the Sun's corona or at magnetopauses, the interfaces between stellar winds and magnetospheres ….

But: MHD waves are different

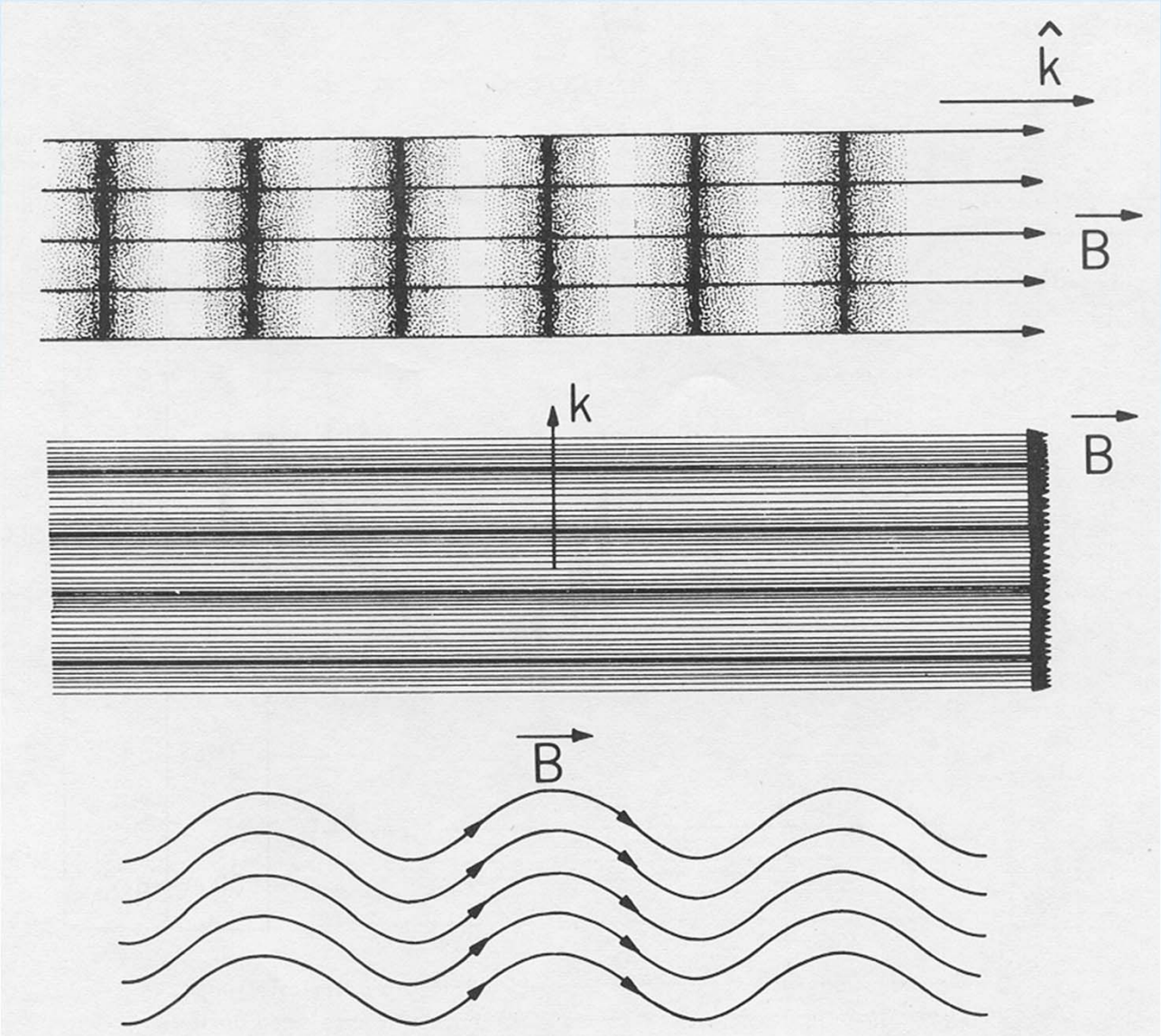

Compressible Magnetosonic waves

- parallel: slow and fast waves
- perpendicular: only fast waves

• $c_{ms} = (c_s^2 + v_A^2)^{1/2}$

Incompressible Schear Alfvén Welle; parallel propagation:

$v_A = B/(4\pi\rho)^{1/2}$

Kelvin Helmholtz instability – magnetopause case

Ideal MHD-instability, requires Delta V > Va along the k vector of the wave

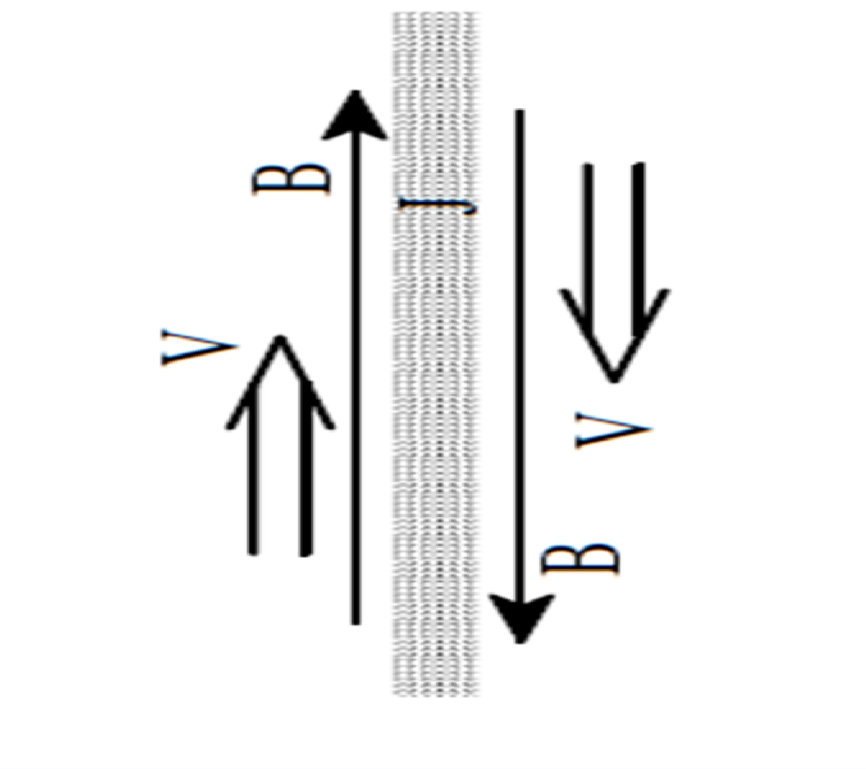

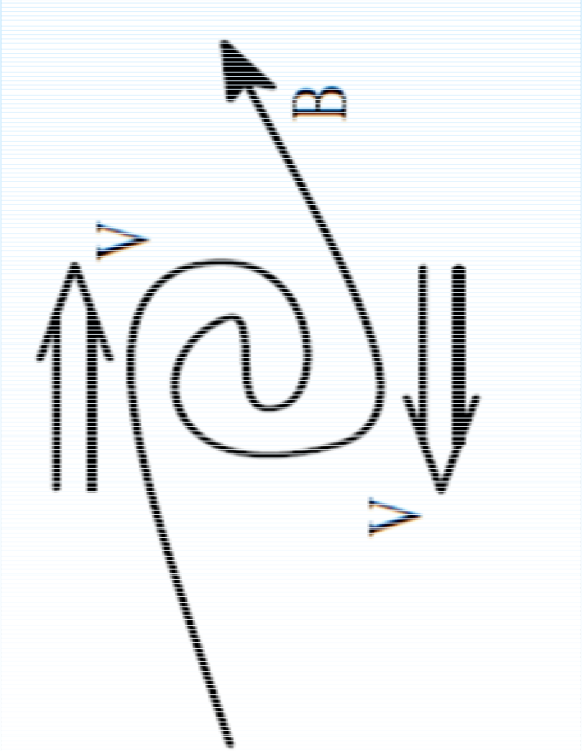

Causes transport of momentum and energy by turbulent viscosity

Simulation exercise No. 2: Kelvin-Helmholtz instability (MP)

Unstable growth, if Delta V > Va along the k vector of the mode
Plasma flow velocities and density evolution:

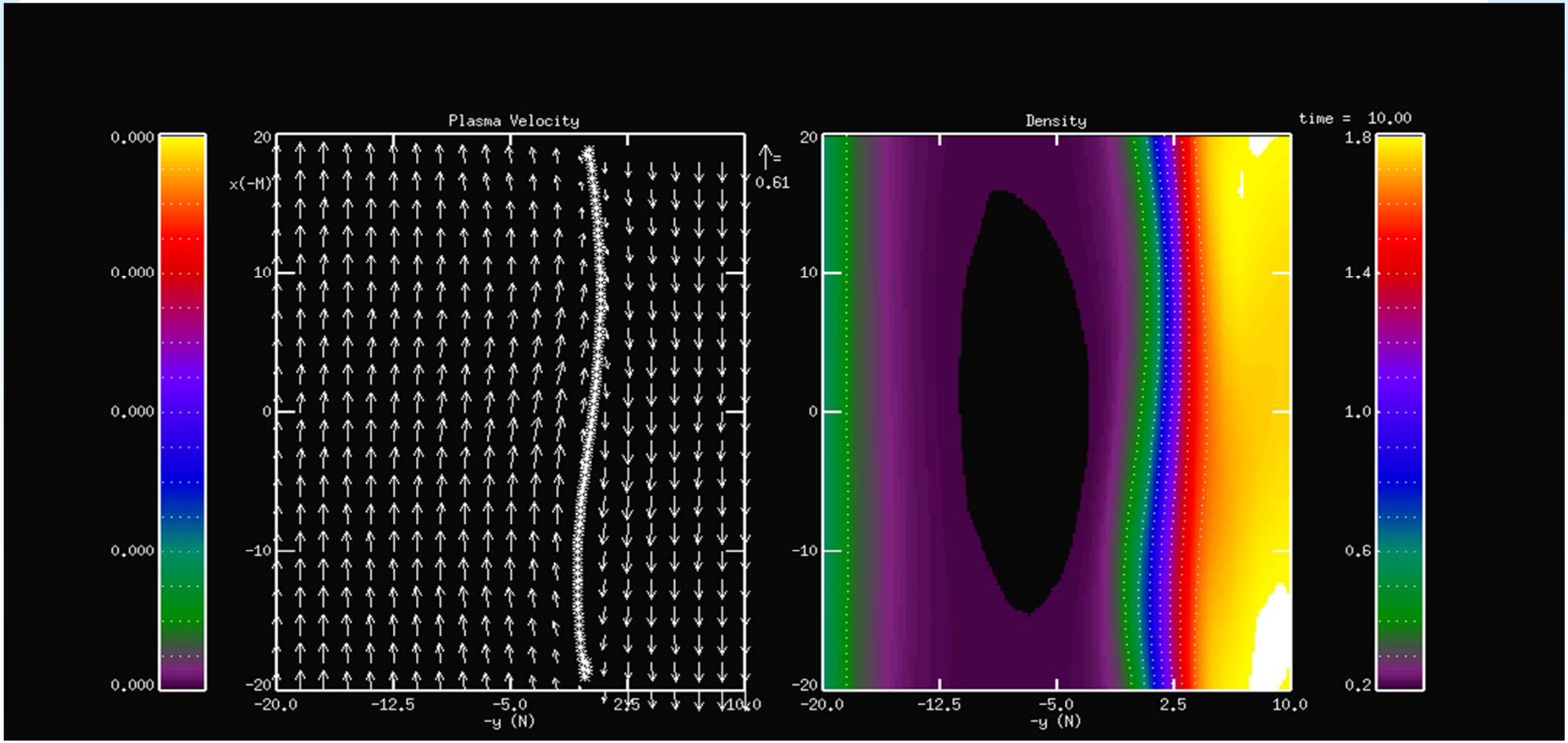

Reconnection in KH vortices

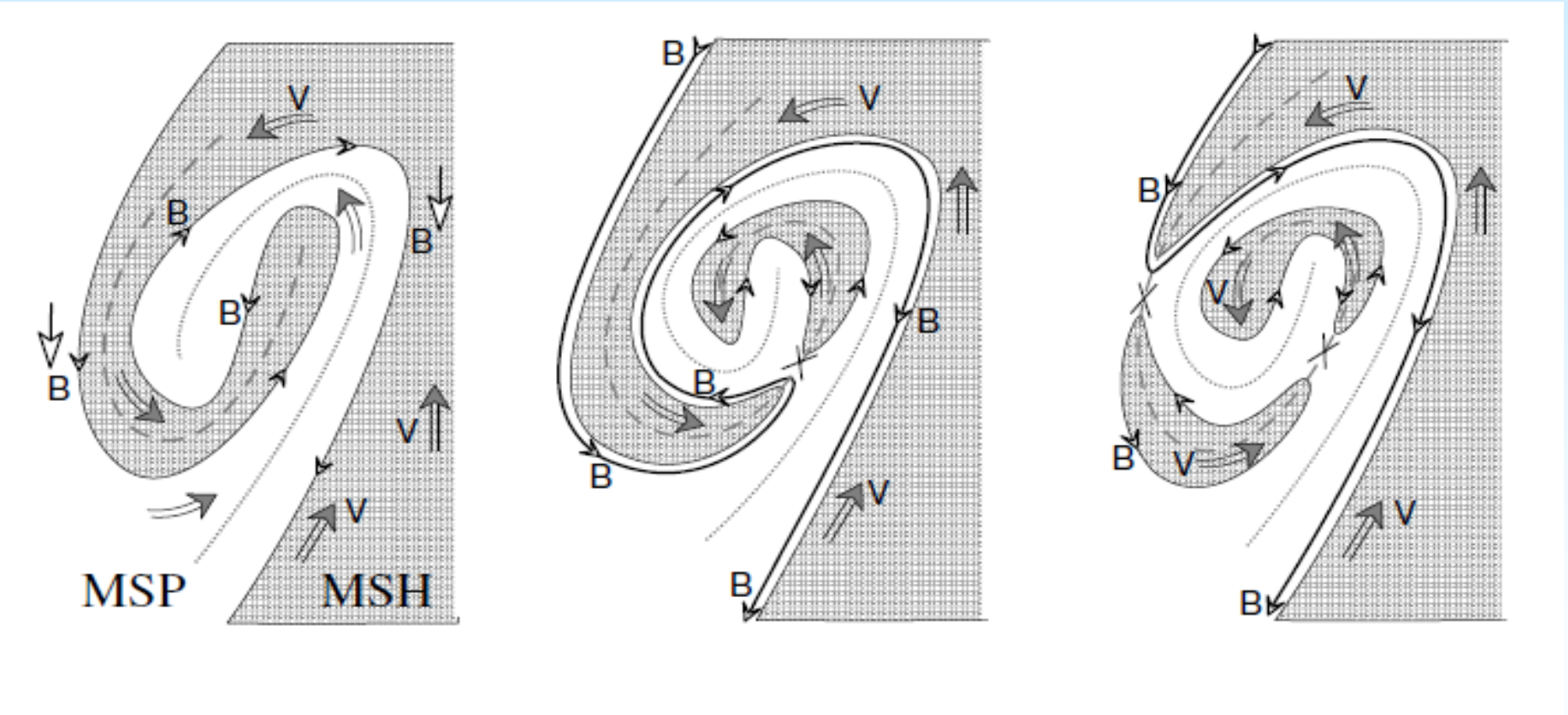

⇒ mass diffusion coefficient D=10^9 m^2s^-1

⇒ [From Otto et al.]

The open magnetosphere control

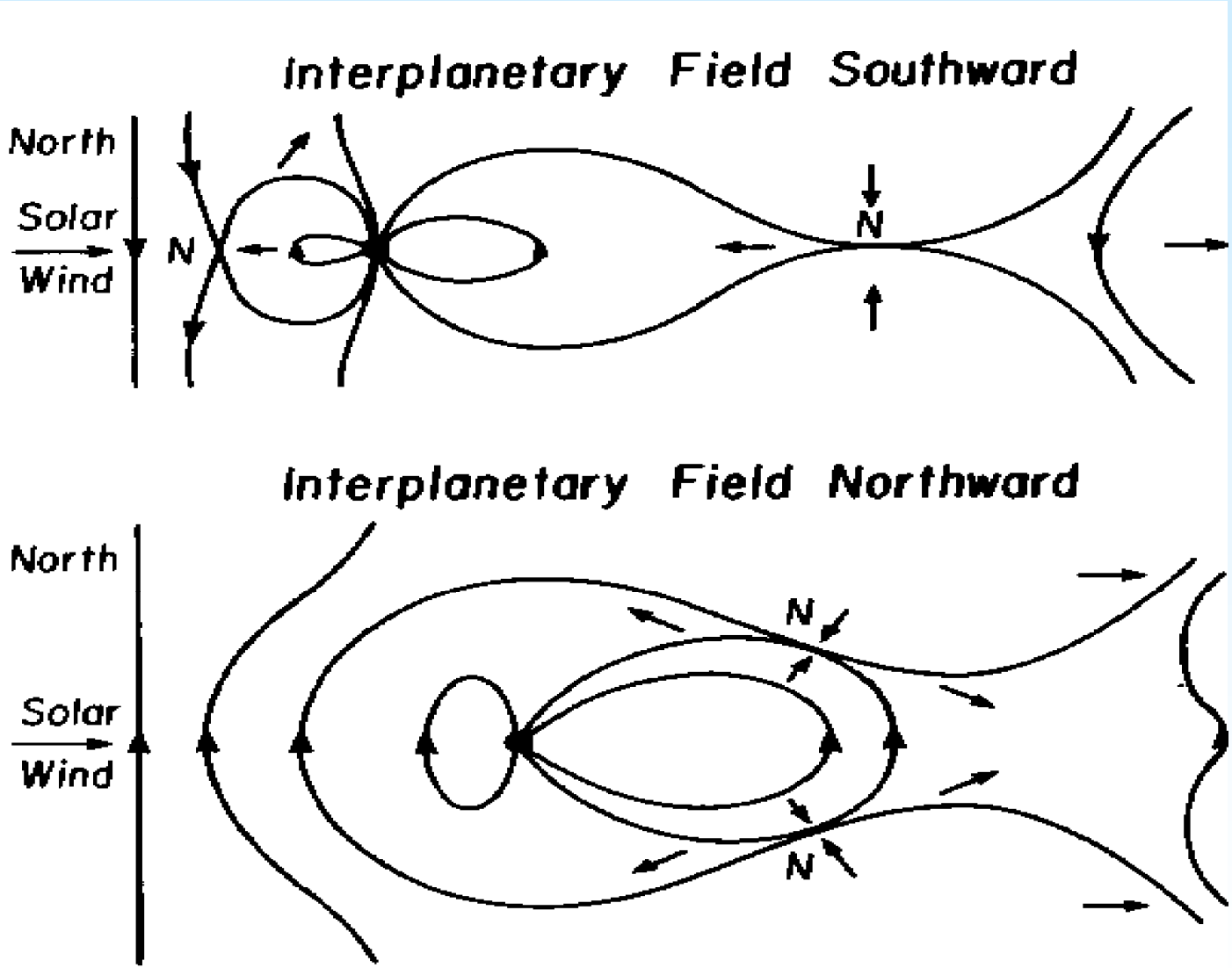

(A) Southward Interplanetary B-field -> strong dayside reconnection controls the MSP convection.

(B) Northward Interplanetary B-field -> reconnection behind the cusps of the MSP.

Suggested by [Dungey,1961]

The Earth‘s magnetotail

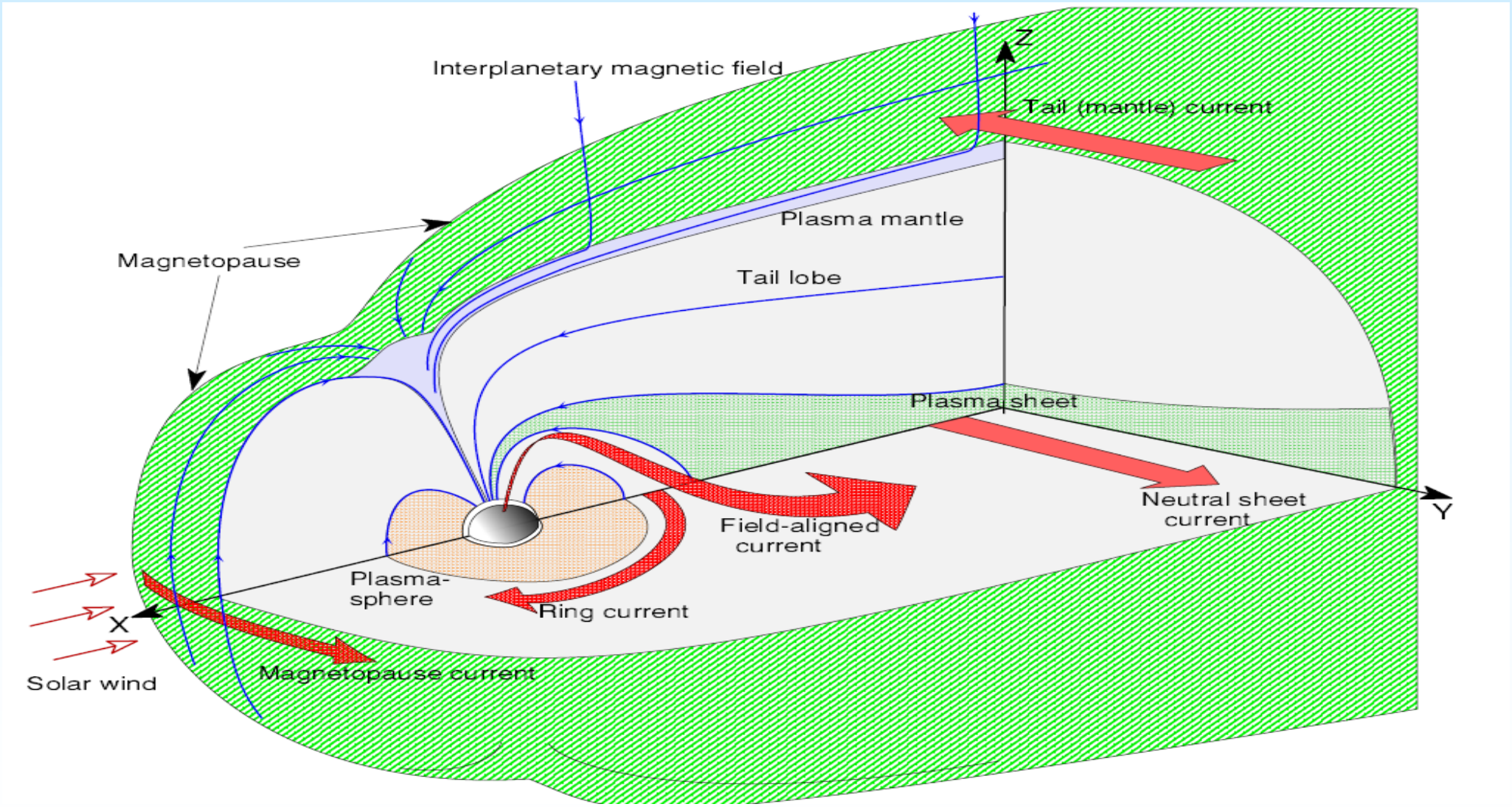

Magnetotail reconnection

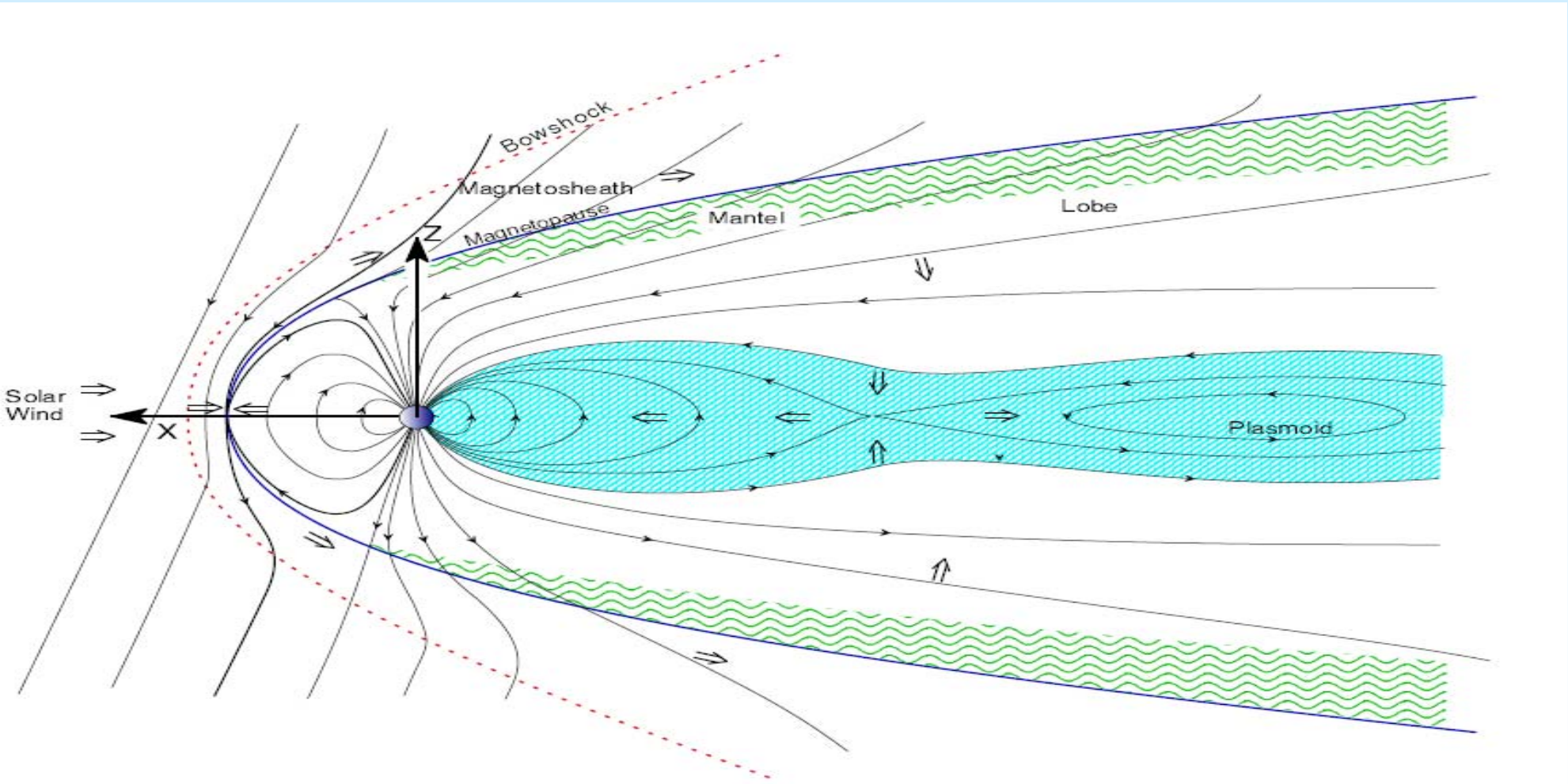

Substorm sequence

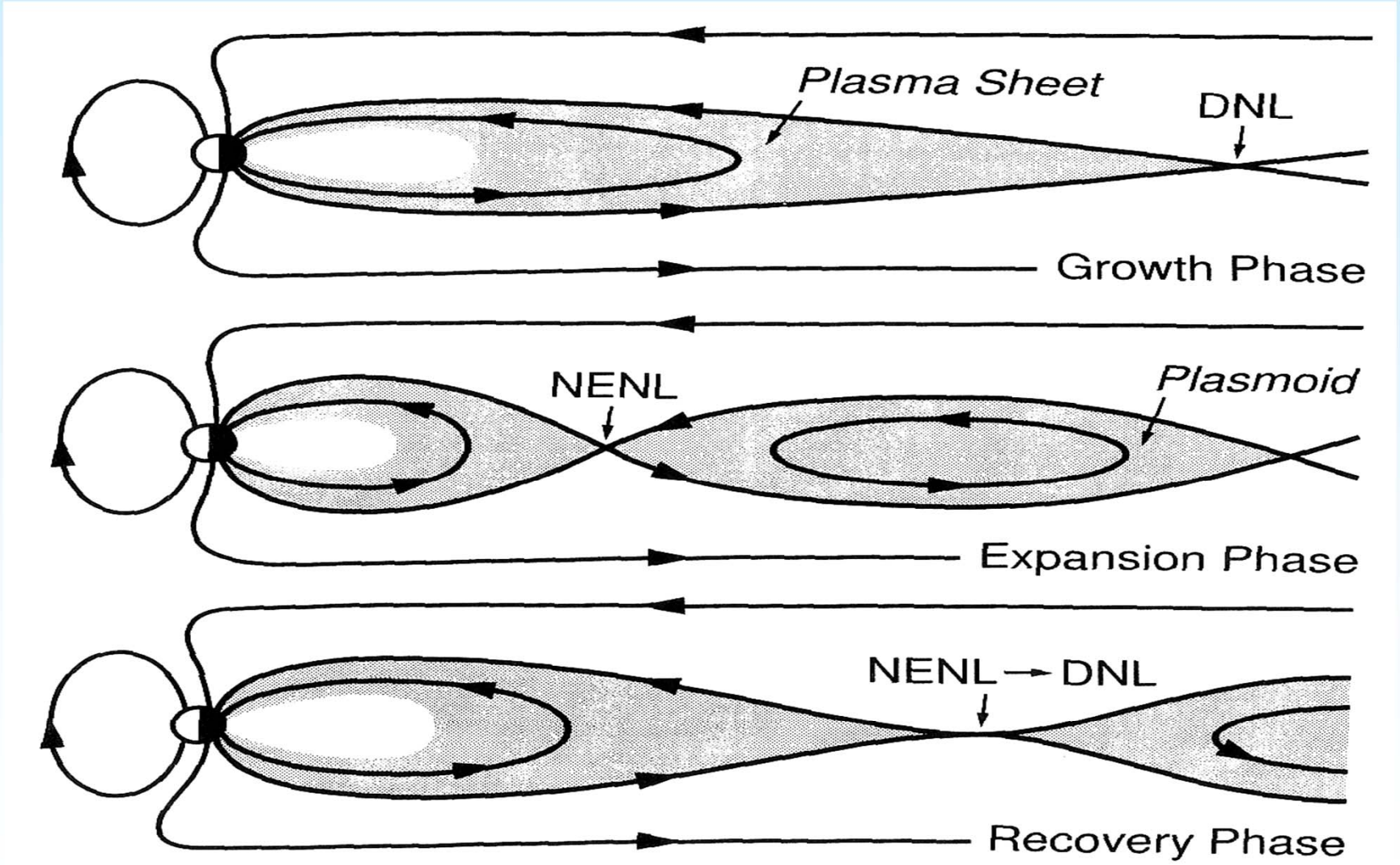

Substorms and „current-wedge“

Enhanced westward electrojet in the ionosphere

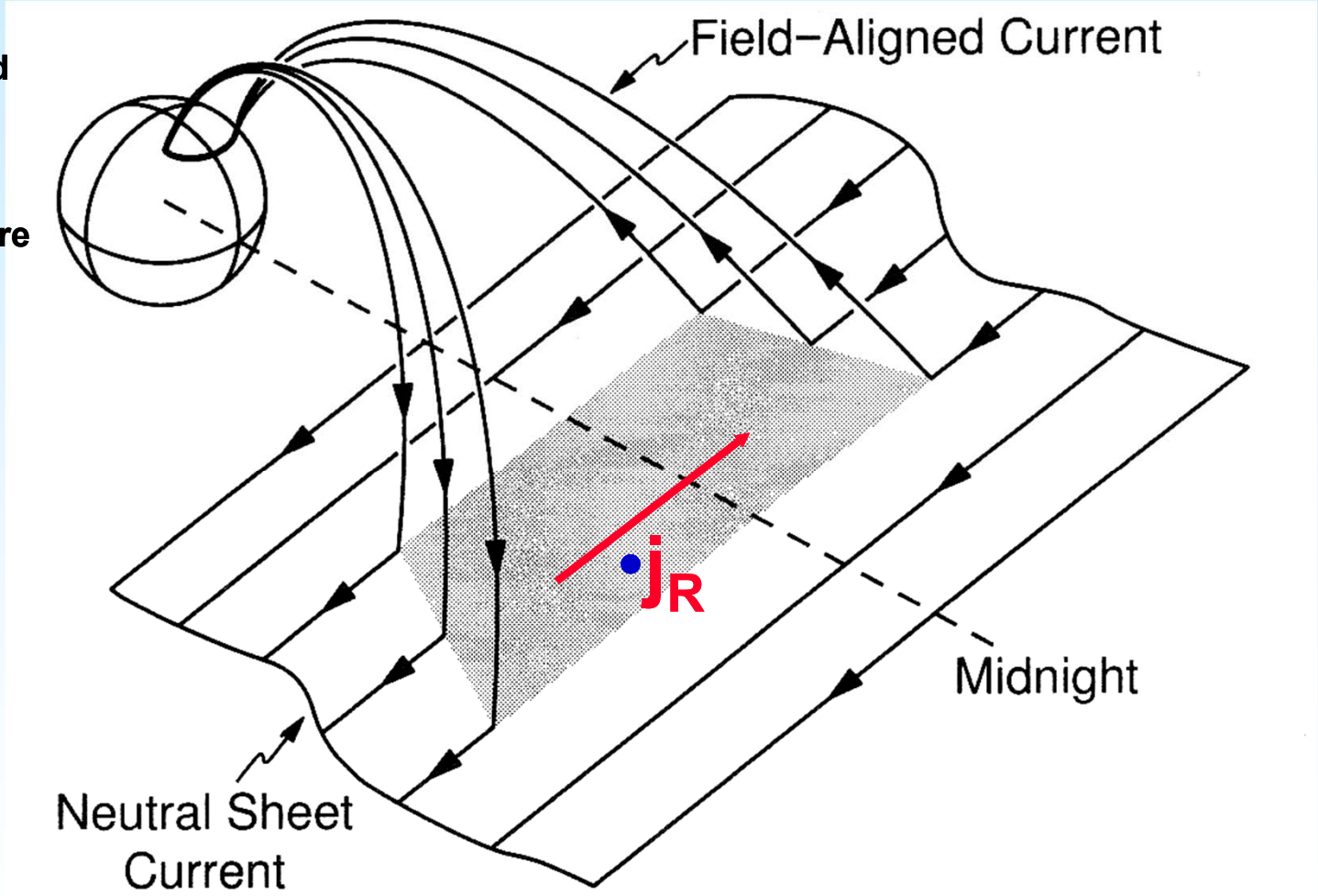

From: [R. L. McPherron, Magnetospheric substorms, Rev. Geophys. Space Phys.]

Start from an Equilibrium

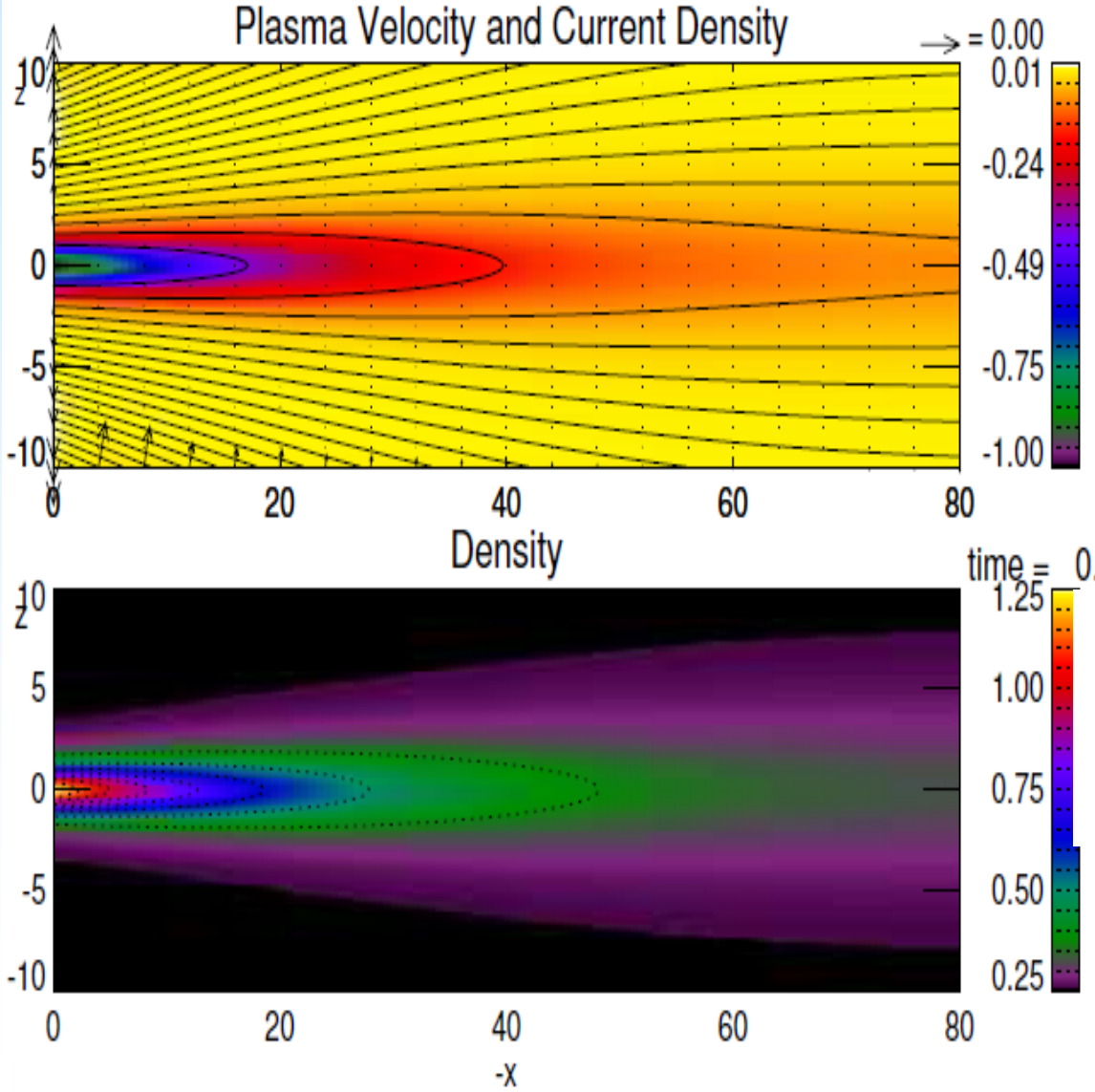

Tail-like Harris (1962) - type equilibrium

$$
\begin{aligned}
A_y &= A_c \ln\cosh(z/l(x)) + f(x) \\
B_x &= -\partial A_y/\partial z = B_0(x)\tanh(z/l(x)) \\
B_z &= \partial A_y/\partial x
\end{aligned}
$$

Simulation exercise No. 3: Magnetotail reconnection

Plasma velocity; current density; mass density

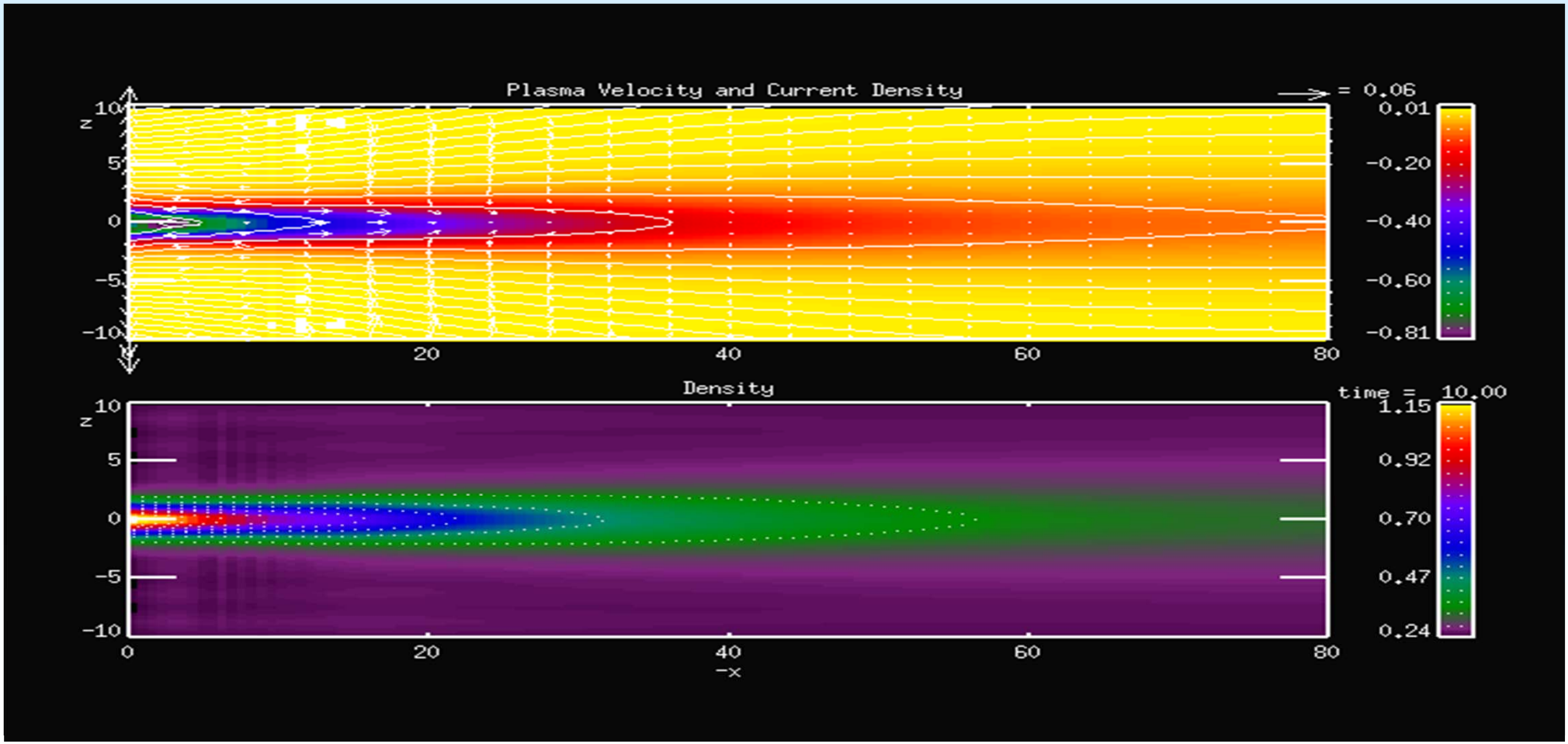

2. Kinetic plasma physics via Vlasov and PIC code simulations

Most of the astrophysical plasmas are hot and dilute (rare in the sense of large distances between the particles and a small probability of their collisions).

MHD does address the physics of individual particles and their interaction which includes resonance effects, particle acceleration, the balance of electric fields in collisionless reconnection, dissipation, microscopic origin of turbulence …

Collisionless plasma

Discrete particles: Mean free path between two particle collisions ->

$$l \approx n_o^{-1} \left(\frac{\epsilon_o \kappa T_e}{e^2} \right)^2$$

The collision frequeny ->

$$\nu \approx l^{-1} \sqrt{\frac{\kappa T_e}{m_e}}$$

... has to be compared with the continuous fluid plasma eigenfrequency ->

$$\omega_{pe} = \sqrt{\frac{n_o e^2}{m_e \epsilon_o}}$$

if the ratio of the two which vanishes if plasma is „collisionless“

With the Debye length ->

$$\lambda_D = \omega_{pe}^{-1} \sqrt{\frac{\kappa T_e}{m_e}}$$

a „graininess factor“ can be defined as the inverse of the number of particles in a Debye sphere (here: cube)

$$\frac{\nu}{\omega_{pe}} \approx \frac{1}{n_o \lambda_D^3} = g \to 0$$

When are plasmas collsionless?

Spatial condition:

$$\frac{1}{n_o \lambda_D^3} = g \to 0$$

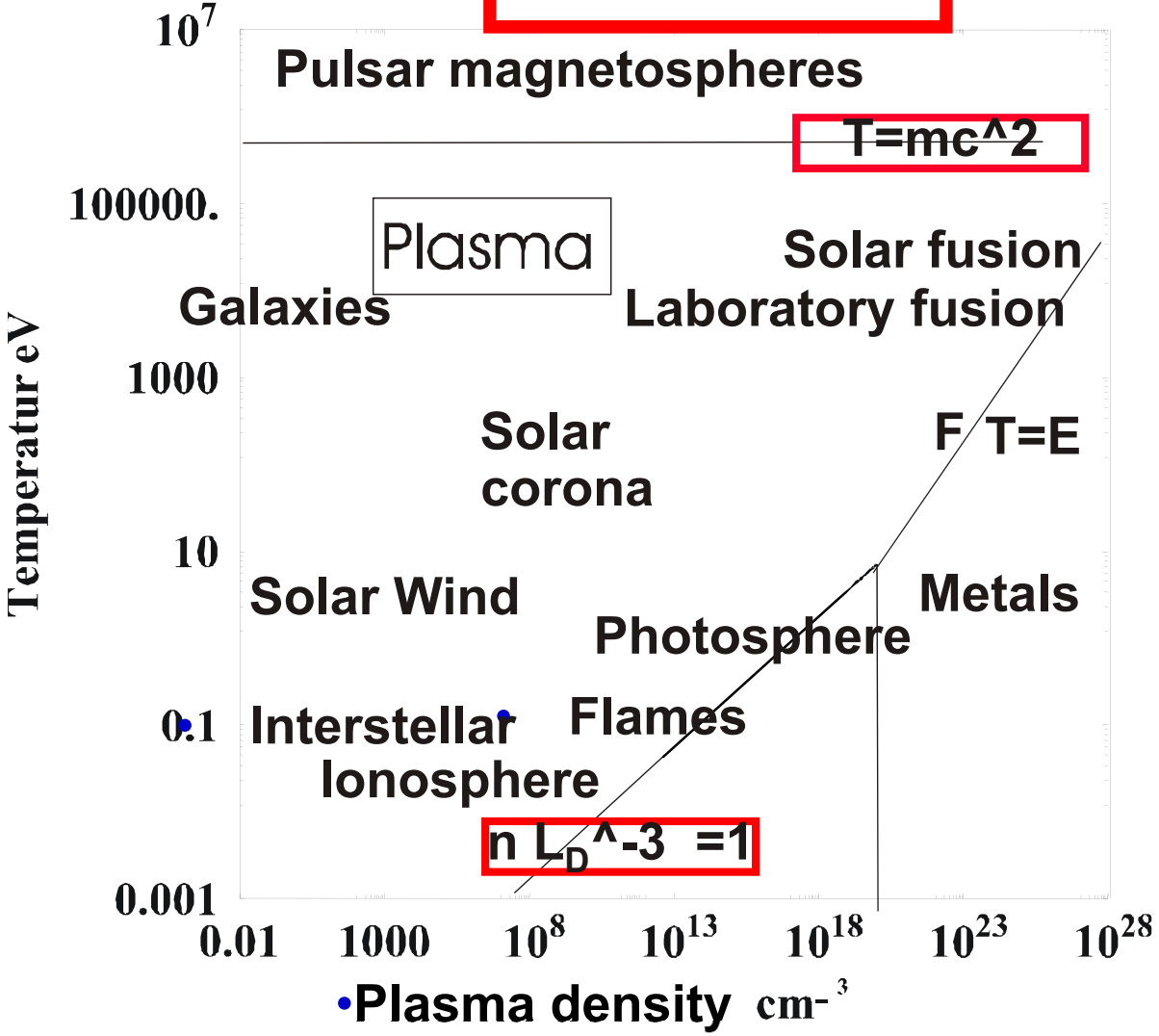

Temporal condition:

$$\tau \approx (g \cdot \omega_{pe})^{-1}$$

A plasma has to be considered collsionless for times << tau

Fusion plasmas:

$g = 10^{-9}$-10^{-7}

astrophysical plasmas:

$g = 10^{-19}$-10^{-13}

These numbers are very, very small, though finite.

Scales of typical plasma phenomena e.g. the solar corona

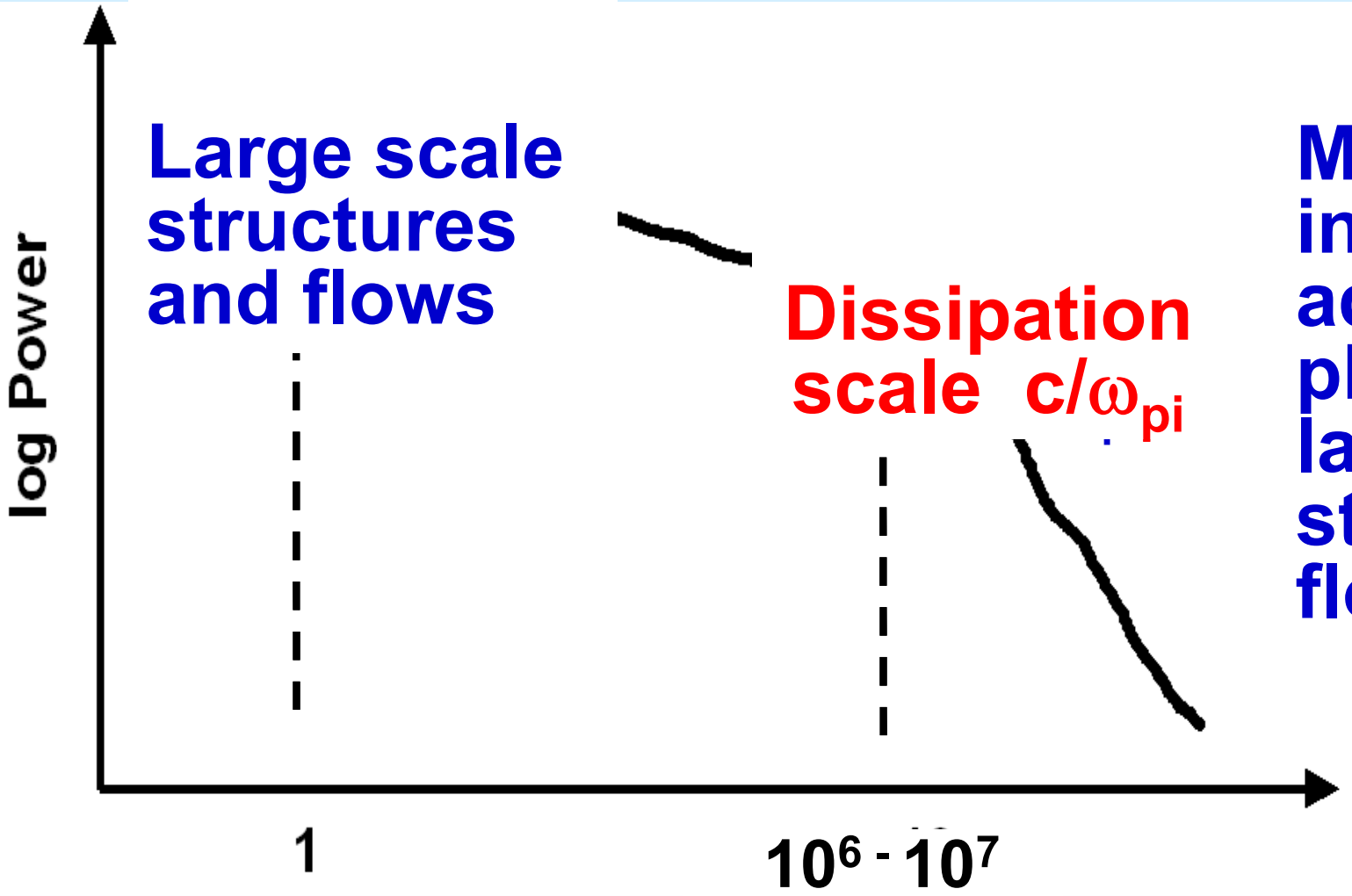

MHD investigations address the physics of large scale structures and flow.

Typical numbers for the Sun

Plasma temperature Te ~ Ti ~ 10^6 K

n	λ_{De}	c/ω_{pi}
10^8 cm^{-3}	0.7 cm	20 m
10^{11} cm^{-3}	0.02 cm	0.7 m

While the size of observed objects is: L ~ 10^7 m !

Scales and related phenomena

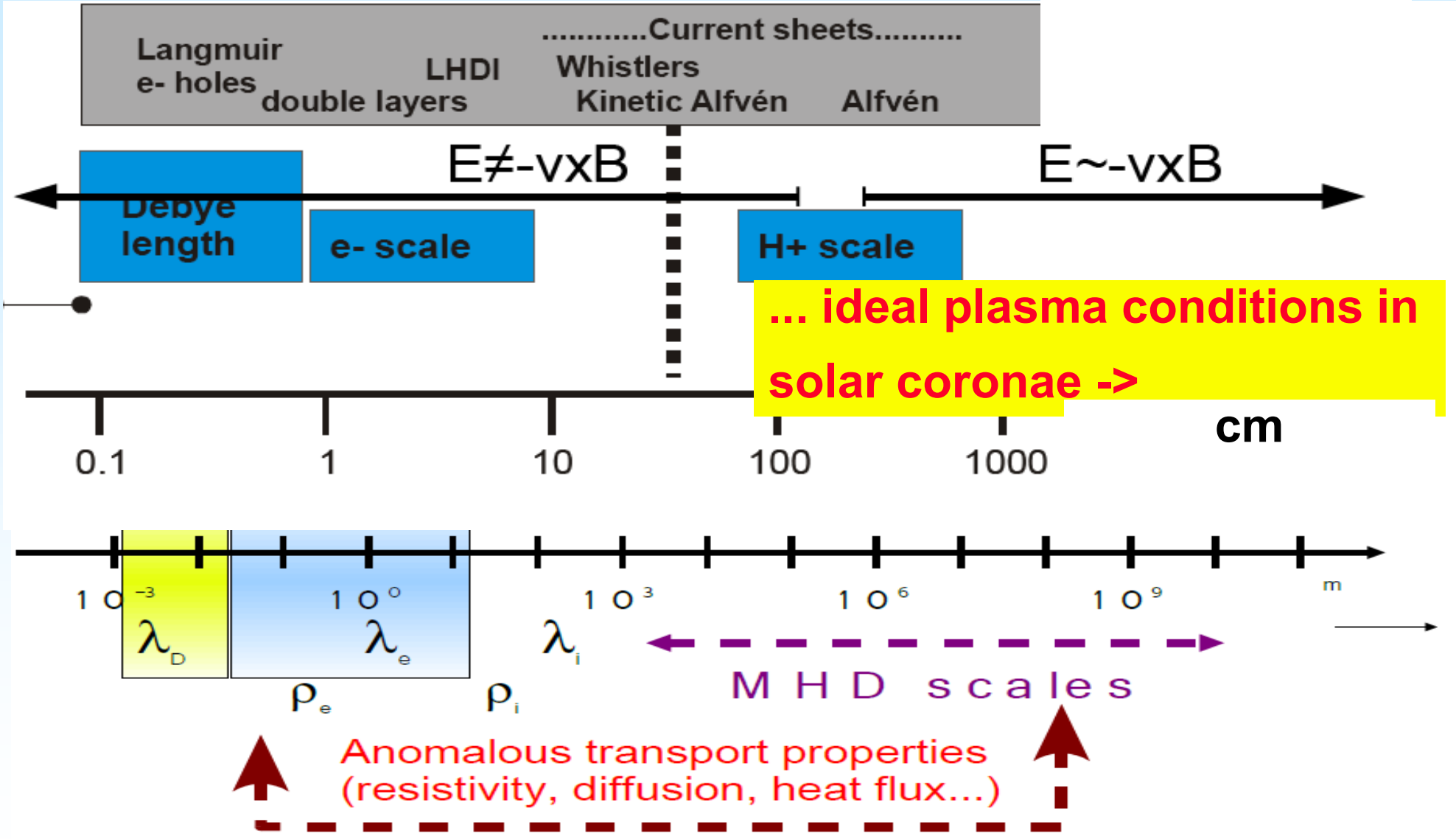

Governing: Vlasov equation

Vlasov equation for plasma species

$$\frac{df}{dt} = \frac{\partial f_\alpha}{\partial t} + \vec{v}\frac{\partial f_\alpha}{\partial \vec{r}} + \frac{q_\alpha}{m_\alpha}\left[\vec{E} + \frac{\vec{v}\times\vec{B}}{c}\right]\frac{\partial f_\alpha}{\partial \vec{v}} = 0$$

Maxwell equations for EM fields

$$\frac{1}{c}\frac{\partial \vec{E}}{\partial t} = \nabla\times\vec{B} - \frac{4\pi}{c}\sum_\alpha q_\alpha \int \vec{v} f_\alpha d\vec{v} \qquad \frac{1}{c}\frac{\partial \vec{B}}{\partial t} = -\nabla\times\vec{E}$$

$$\nabla\cdot\vec{E} = 4\pi\sum q_\alpha \int f_\alpha d\vec{v} \qquad \nabla\cdot\vec{B} = 0$$

$$f(x, y, z, v_x, v_y, v_z, t)$$

3D + 3V = 6 dimensions+time

1938: Equation used by Vlasov

Т. VIII Журнал экспериментальной и теоретической физики Вып. 3
1938

A.A. Vlasov: „About the vibrational properties of an electron gas“

J. Exp. Theor. Phys., 8, 291-318, 1938

О ВИБРАЦИОННЫХ СВОЙСТВАХ ЭЛЕКТРОННОГО ГАЗА

А. А. Власов

1. Постановка задачи. — 2. Исходные уравнения и их упрощение. — 3. Решение линеаризованных уравнений. — 4. Дисперсия продольных волн. — 5. Дисперсия продольных волн в электронном газе с функцией распределения по Ферми. — 6. Дисперсия поперечных волн. — 7. Резюме и заключение.

1. Постановка задачи

Во многих проблемах приходится иметь дело с большой совокупностью

Vlasov's equation

тельно оценка a, λ, v_{gt} остается ф...

Итак, вопрос о вибрационных свойствах допускает упрощение задачи — можно пренебречь всеми взаимодействиями посредством „удара".

Рассматриваемый круг вопросов, связанных с большими частотами, допускает еще одно упрощение в исходных уравнениях — вследствие большой массы ионов в сравнении с электронами можно их перемещением пренебречь, т. е. считать ионы фактически неподвижными. При всех этих условиях система исходных уравнений принимает вид:

$$\frac{\partial f}{\partial t} + \operatorname{div}_{\mathbf{r}} \mathbf{v} f + \frac{e}{m}\left(\mathbf{E} + \frac{1}{c}[\mathbf{v}\mathbf{H}]\right)\operatorname{grad}_{\mathbf{v}} f = 0,$$

$$\operatorname{div}\mathbf{E} = 4\pi e\left(\int_{-\infty}^{+\infty} f\,d\xi\,d\eta\,d\zeta - N\right); \quad \operatorname{rot}\mathbf{H} = \frac{1}{c}\frac{\partial \mathbf{E}}{\partial t} + \frac{4\pi e}{c}\int_{-\infty}^{+\infty} \mathbf{v} f\,d\xi\,d\eta\,d\zeta, \qquad \text{(II)}$$

$$\operatorname{div}\mathbf{H} = 0, \quad \operatorname{rot}\mathbf{E} = -\frac{1}{c}\frac{\partial \mathbf{H}}{\partial t},$$

где f — функция распределения для электронов. Таким образом в рассматри-
ваемой проблеме приходим к системе уравнений, описывающей поведение

neglects all interactions via „collisions"

- … and for high frequency applications neglect ions and describe the electron gas alone ...

Properties of the Vlasov equation

Vlasov equation: df/dt =0 means conservation of the phase total phase space density volume f (Liouville theorem)

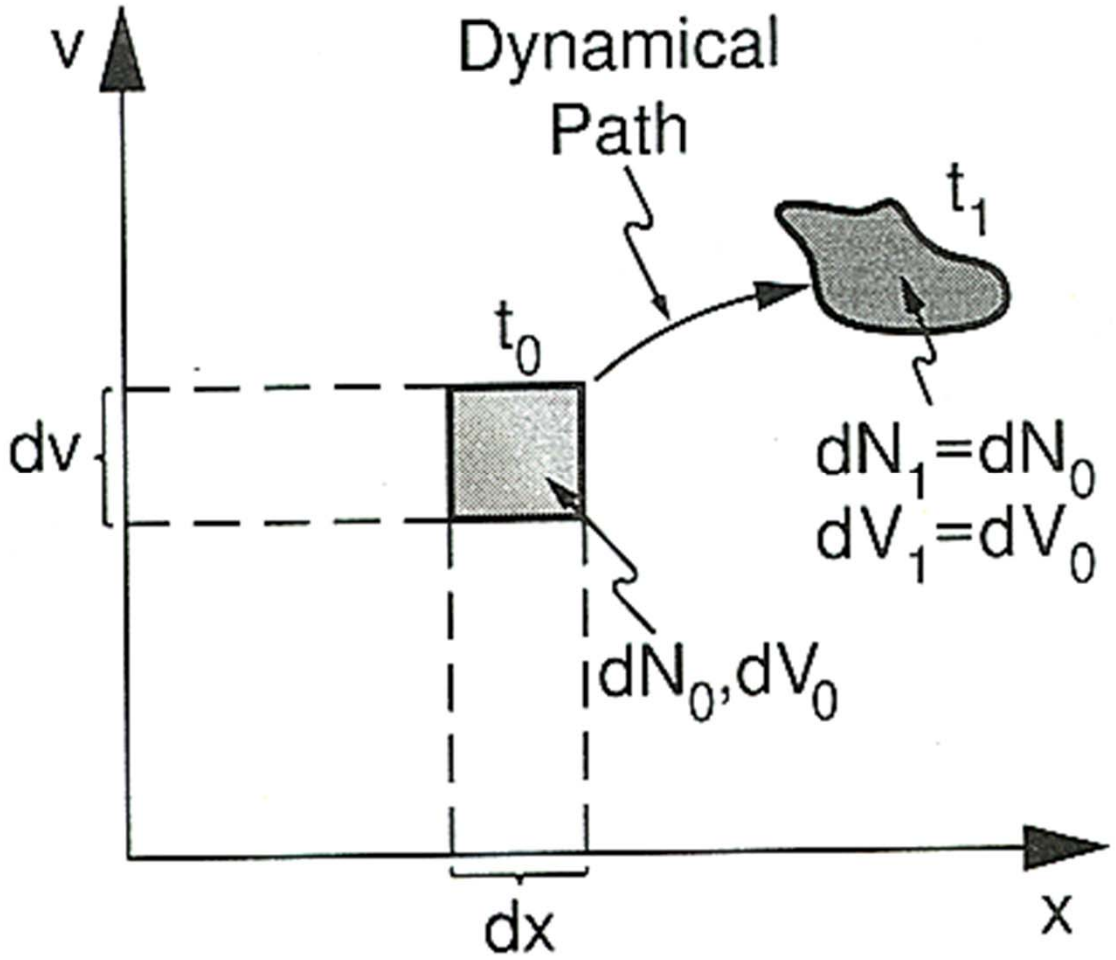

Any volume element becomes deformed under the action of electromagnetic and other forces like in an incompressible fluid. But its volume remains constant and, therefore, the number of particles contained in it.

Forms of the Vlasov's equation

Two of several possible equivalent forms for the evolution of an incompressible flow in the 6 dimensional phase space (Liouville theorem): 1.) advection form is okay for non-relativistic plasmas, velocities are independent variables:

$$\frac{\partial f_j}{\partial t} + \vec{v}\frac{\partial f_j}{\partial \vec{r}} + \frac{e_j}{m_j}\left(\vec{E} + \vec{v} \times \vec{B}\right)\frac{\partial f_j}{\partial \vec{v}} = 0$$

with E,B being the mean electric and magnetic fields, i.e

2.) Conservative form momenta as variables, good for relativistic plasmas:

$$\frac{\partial f_j}{\partial t} + \frac{\partial}{\partial \vec{r}}\left(\frac{\vec{p}}{\gamma_j m_j} f_j\right) + e_j\left[\vec{E} + \frac{\vec{p} \times \vec{B}}{\gamma_j m_j}\right]\frac{\partial}{\partial \vec{p}} f_j = 0$$

$$\gamma_j^2 = 1 + \frac{p_x^2 + p_y^2 + p_z^2}{m_j^2 c^2}$$

Vlasov equations close via Maxwell's equations -> highly nonlinear!

Specifics of Vlasov codes

- The Liouville theorem allows filamentation to infinitely small scales (property of the reversible Vlasov equation)
- 6 D phase space + time, all variables described by PDFs
- Boundary conditions:
  - needed also for distribution functions / in the velocity / momentum space
- Initial conditions:
  - Vlasov solvers are noiseless -> In initial value problems like instability analyses one needs to add noise, e.g.
    - » of the distribution functions or
    - » in the electromagnetic fields

Example: J=const. + open boundary conditions

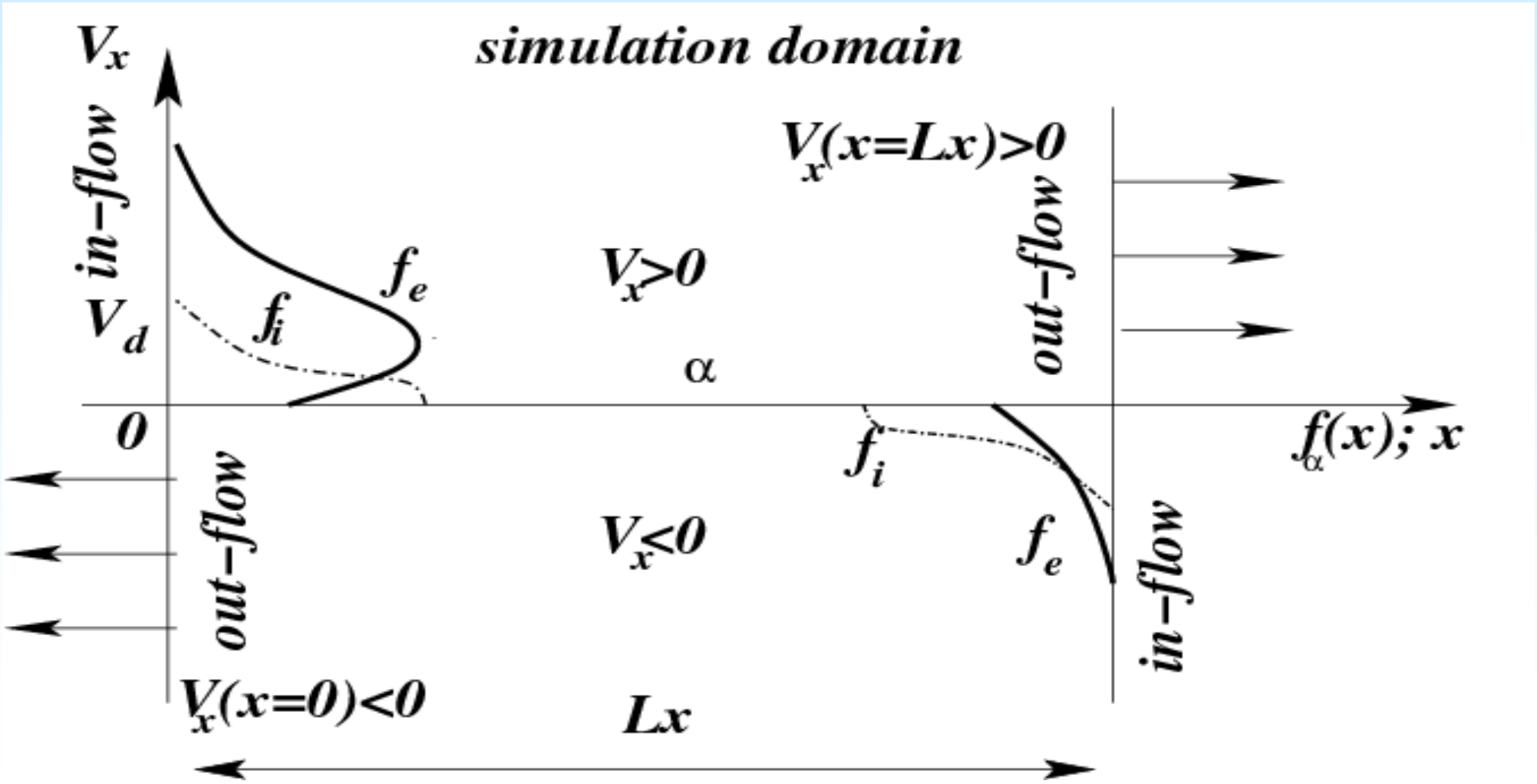

Vlasov-equation - integral form

One can use a fully conservative integral form of the Vlasov equation (due to the conservation of particle numbers, Liouville):

$$N = \int_V f(\vec{r}, \vec{v}, t) d^3r d^3v, \quad \vec{U} = \left(\dot{\vec{r}}, \dot{\vec{v}}\right)$$

$$\frac{dN}{dt} = 0 = \int_V \frac{\partial f}{\partial t} d^3r d^3v + \int_{S(V)} f\vec{U} \cdot d^5\vec{S}$$

$$\frac{\partial}{\partial t} \underbrace{\int \dots \int}_{N_d=6} f dV = - \underbrace{\int \dots \int}_{N_d-1=5} f\vec{U} \cdot \vec{n} dS$$

Finite volume discretization

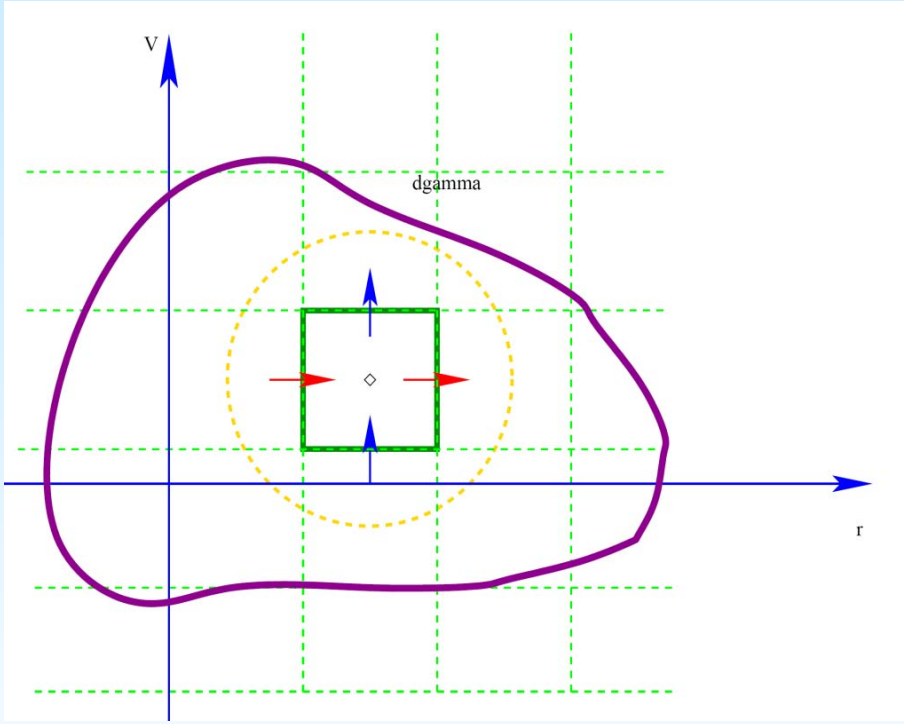

$$V = \bigcup_{i,j=1}^{N_x \times N_v} \overline{V}_{i,j}$$

$$\frac{\partial}{\partial t} \int_V f dV + \int_S F \cdot \vec{n} dS = 0$$

$$f_{i,j} = \frac{1}{|V_{i,j}|} \int_{V_{i,j}} f dV$$

From [Elkina and Büchner]

Vlasov code simulation

Here for a solver for the electromagnetic potential instad of the fields (div B = 0 is guaranteed)

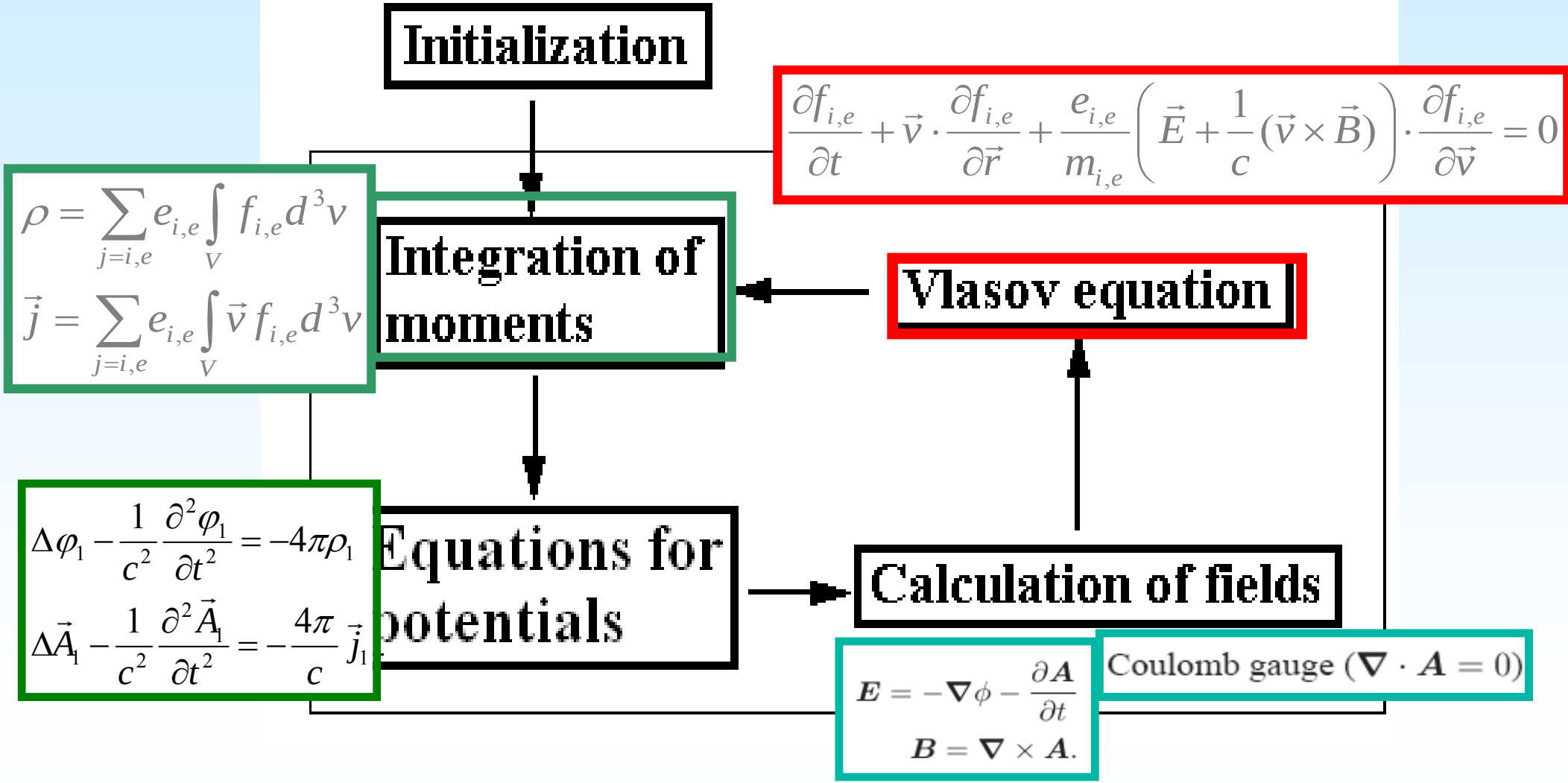

Phase space filamentation

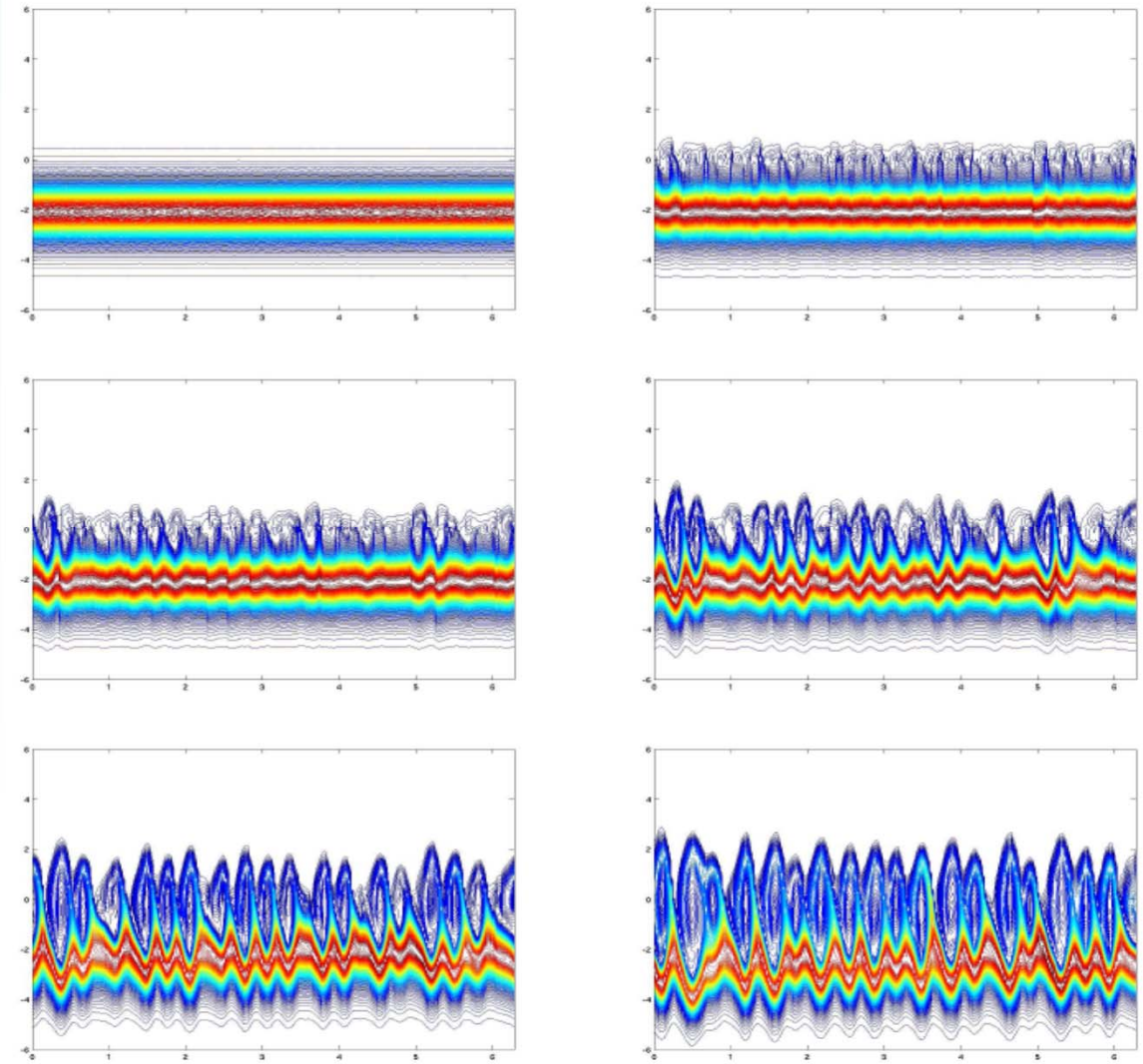

<- 1D Distribution function evolution due to wave-particle-resonant interaction:

(Vx vs. X coordinate)

-> Challenge for any numerical treatment:

With time the gradient scales reach the size of the mesh! -> Closure needed!

Vlasov code with stretched v-grid

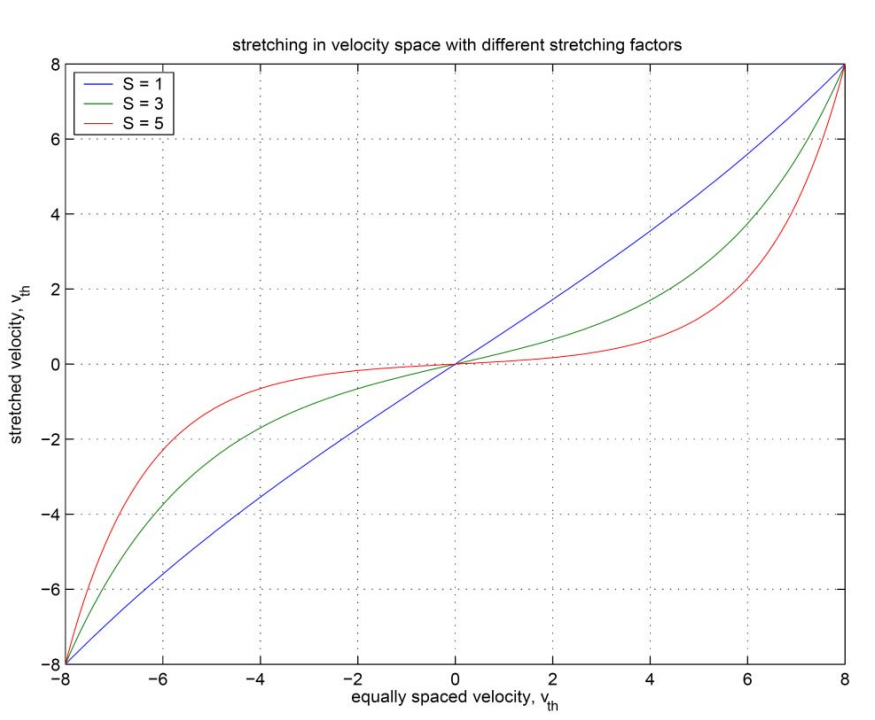

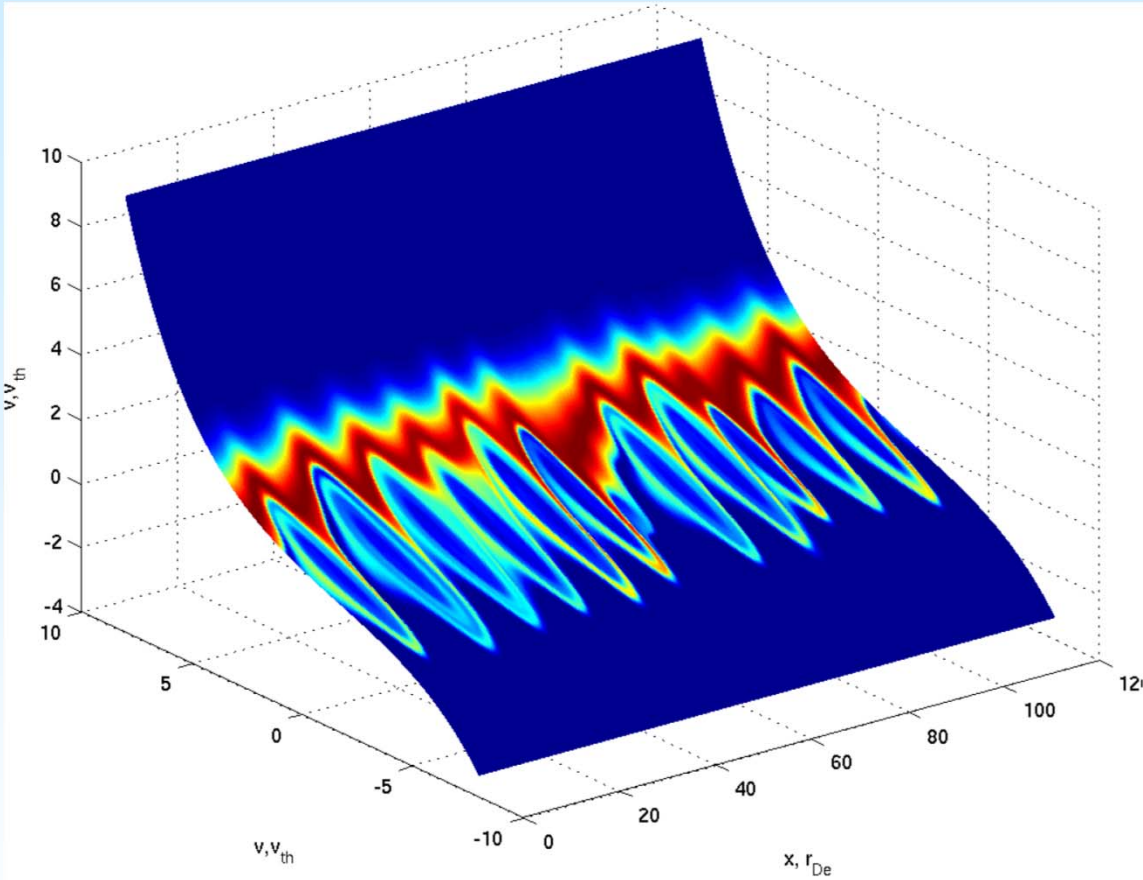

- **Str = stretching factor**

$$V_i^{str} = v^{max} \frac{\sinh\left(v_i(Str/v_{max})\right)}{\sinh(Str)}$$

Wave-particle interactions

- Shifted electron distribution ->
- Instability via „inverse Landau damping“ ->
- wave growth, but:

=> Wave saturation amplitude?

- If one neglects the modification of the distribution function:
- 1962: Vedenov, Velikhov, Sagdeev & Drummond, Pines:
- Quasilinear theory, a weak turbulence theory, if not
- large wave amplitudes / coherent structures instead of phase mixing / strongly changed distribution functions

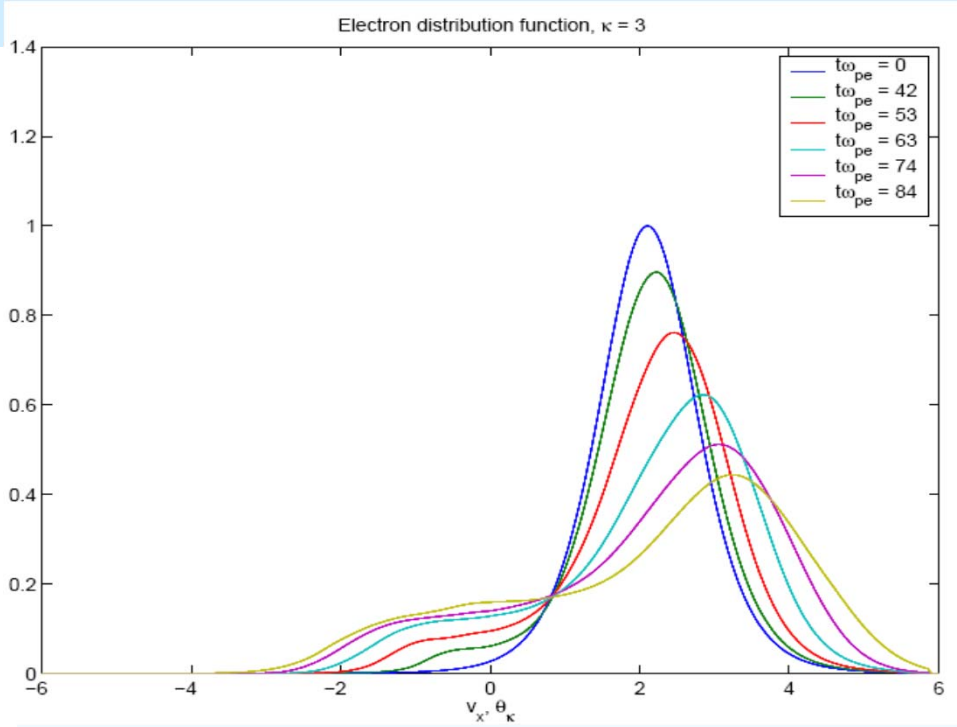

The strong nonlinearities and action on particles beyond quasi-linear theory should be investigated by numerical methods!

Linear IA instability for T_i->T_e

$$f_i = \sqrt{\frac{M}{2\pi T_i}} \exp\left(-\frac{M_i}{2}\frac{v_i^2}{v_{thi}^2}\right)$$

$$f_e = (1 + a(x))\sqrt{\frac{m_e}{2\pi T_e}} \exp\left(-\frac{(v_e - v_{de})^2}{v_{the}^2}\right)$$

a(x) is noise

Vde the drift

Linear dispersion for Te = 2Ti (not, as usual Te>> Ti)

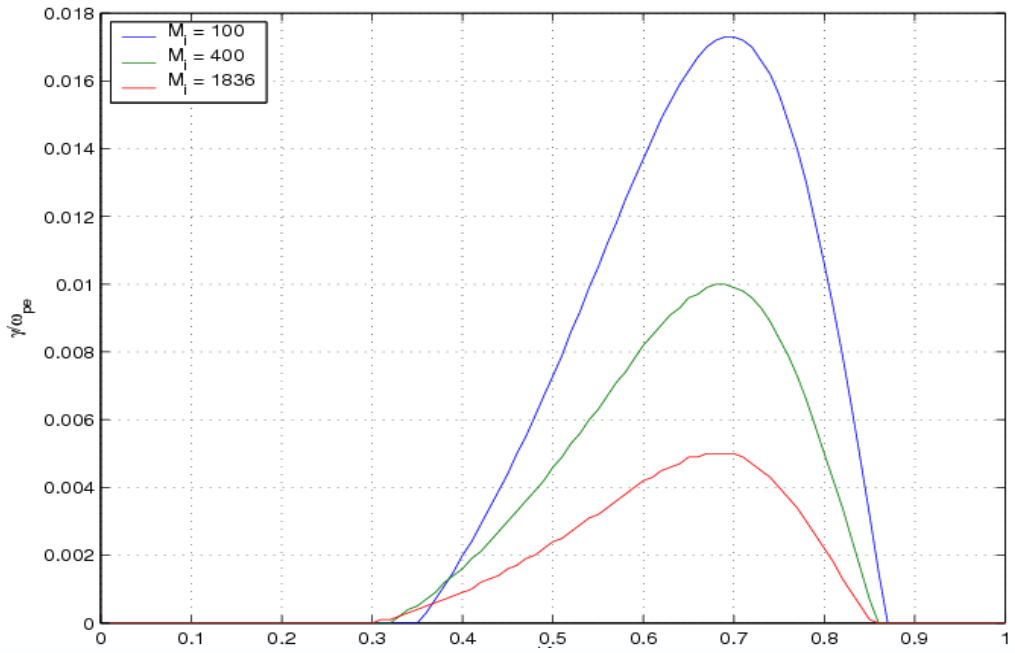

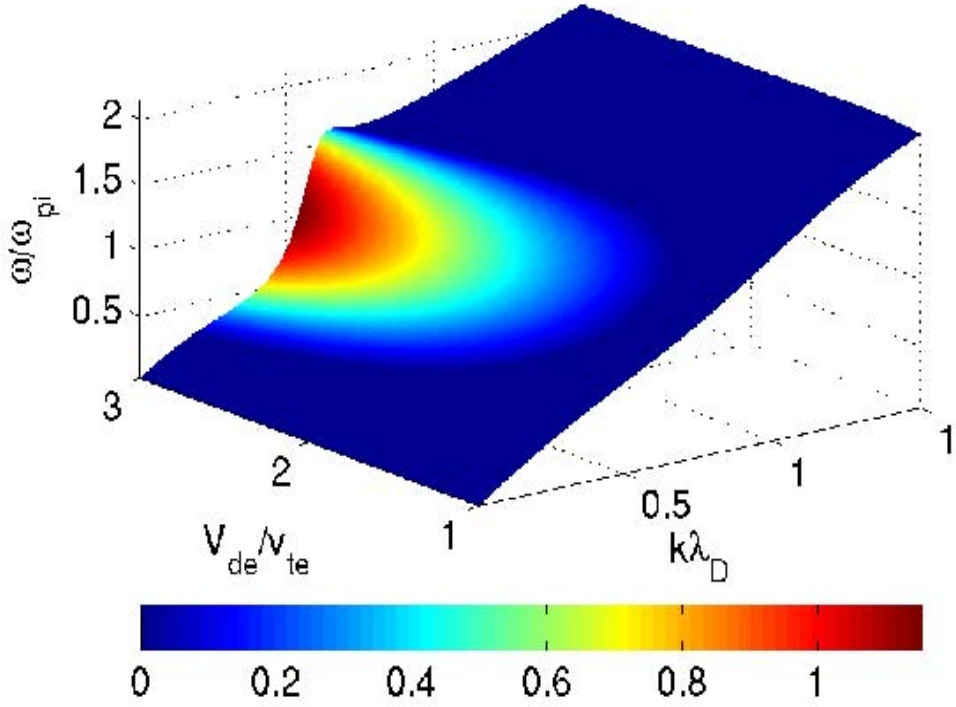

Simulated ion-acoustic instability

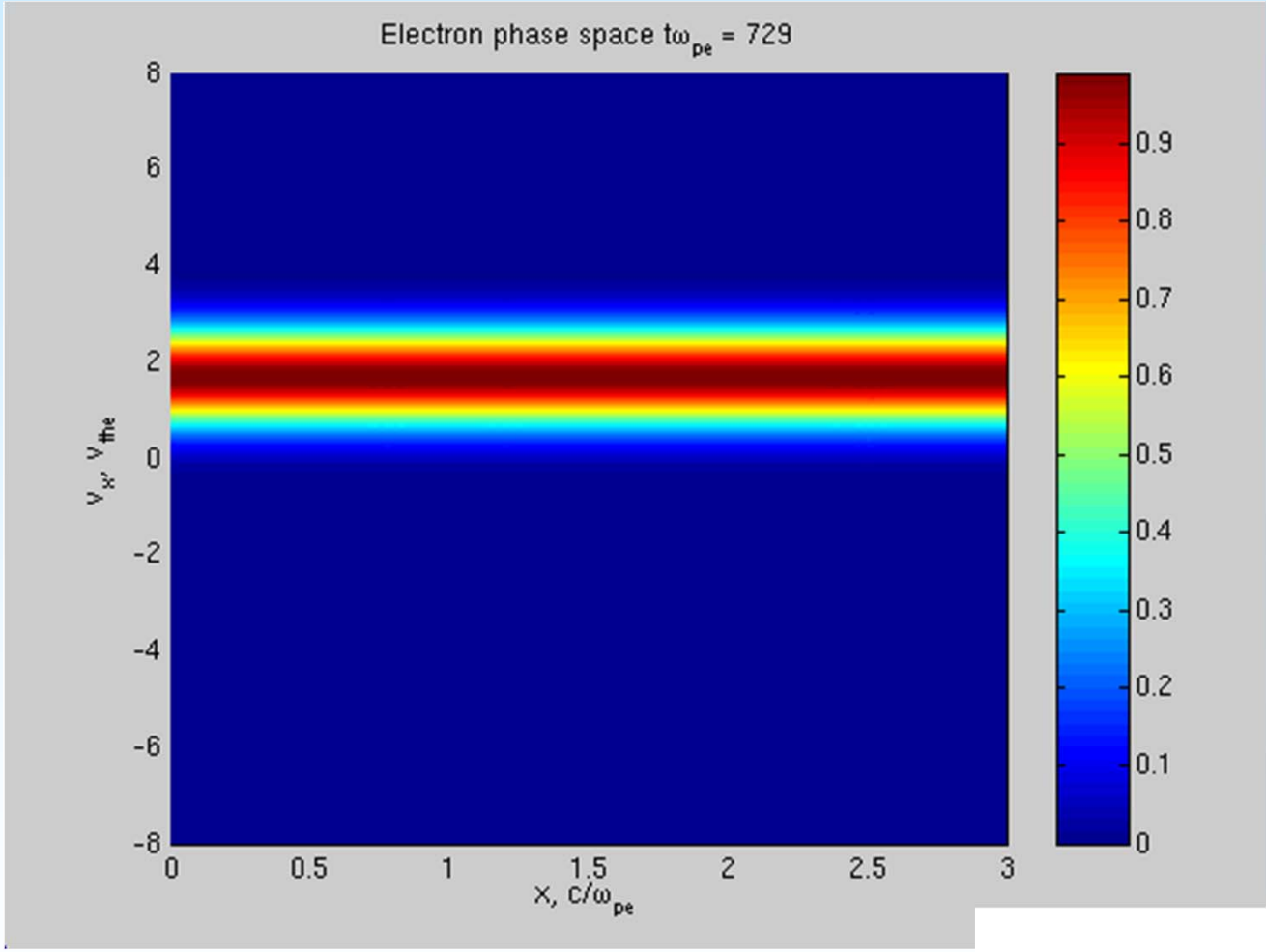

Vx vs. X

Mi/me =1800
Ti = 0.5 Te
Vde= 0.7 Vthe
Ve(max)
= +- 8 Vte
The movie shows the wave growth

$$f_i = \sqrt{\frac{M}{2\pi T_i}} \exp\left(-\frac{M_i}{2}\frac{v_i^2}{v_{thi}^2}\right)$$

$$f_e = (1 + a(x))\sqrt{\frac{m_e}{2\pi T_e}} \exp\left(-\frac{(v_e - v_{de})^2}{v_{the}^2}\right)$$

Results of wave-particle interaction

1D electron distribution in the current direction

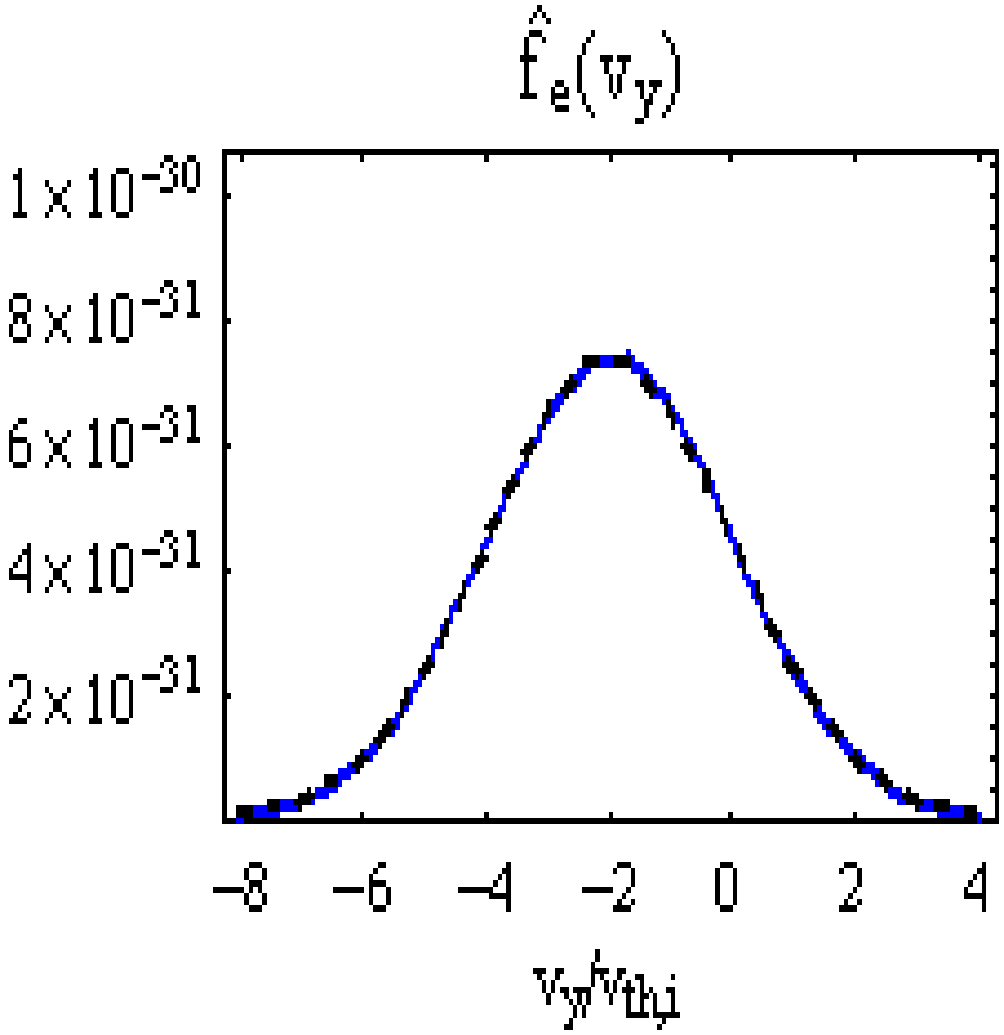

<- electrons

- **The movie shows the plateau-formation in the distribution function near the resonance velocity and electron heating**

Consequence: current reduction

Ion distribution function

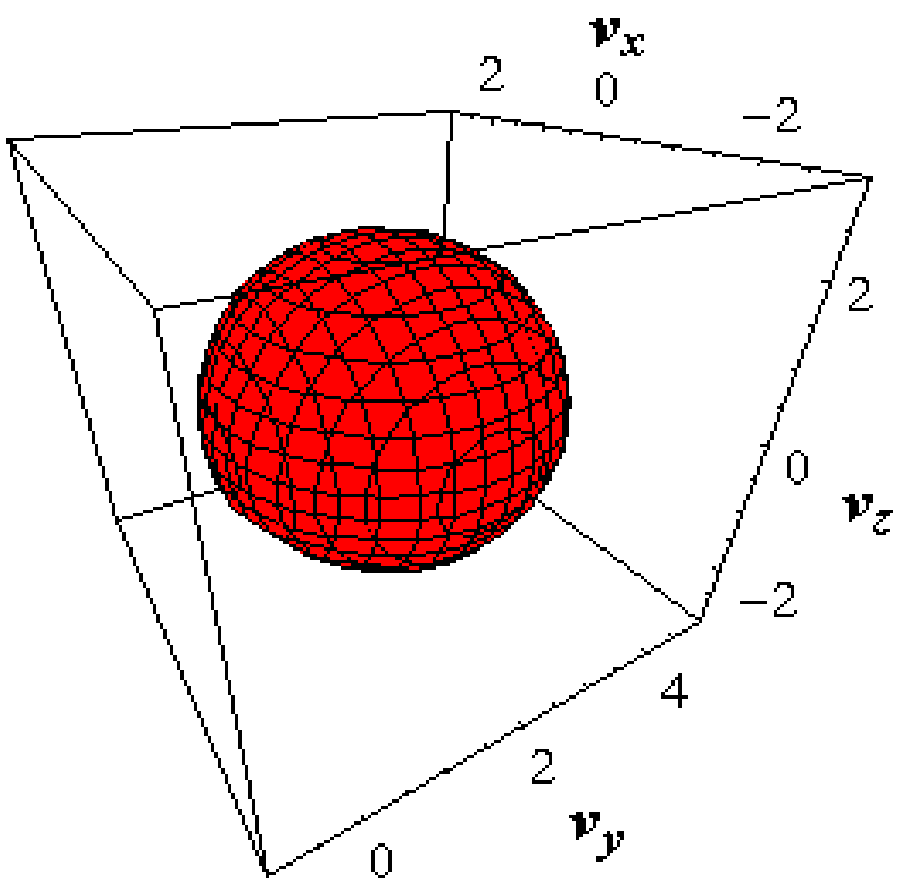

Electron distribution function

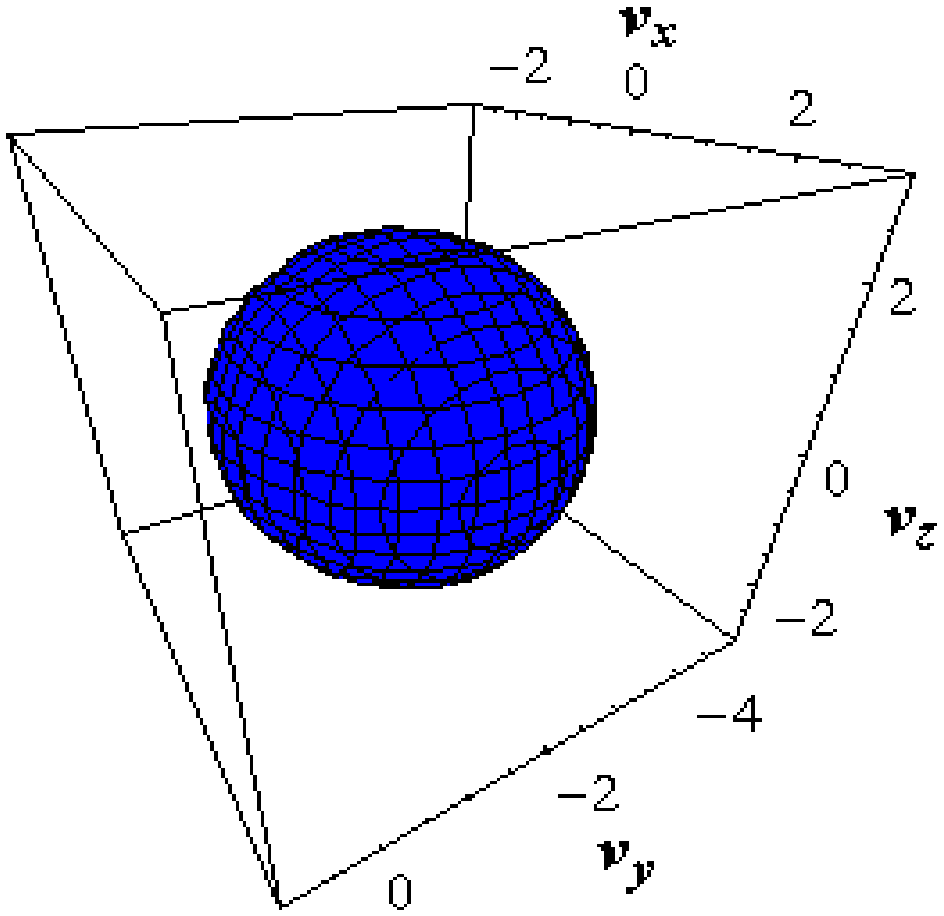

Buneman instability if Ude> Vte

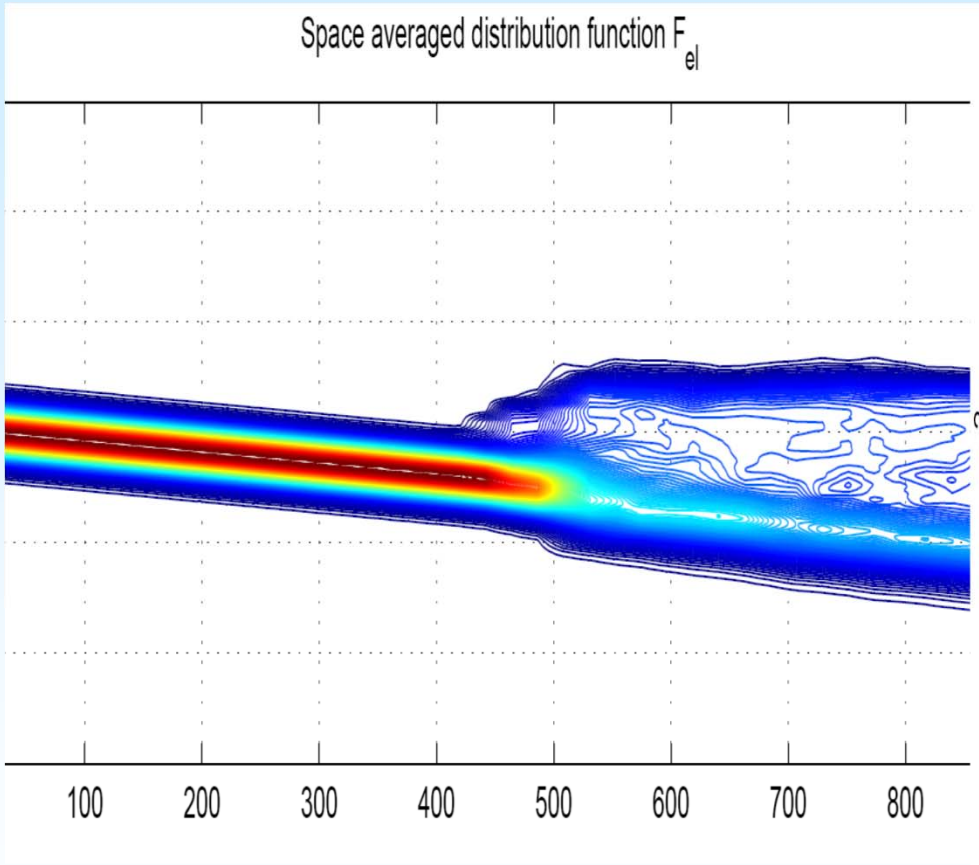

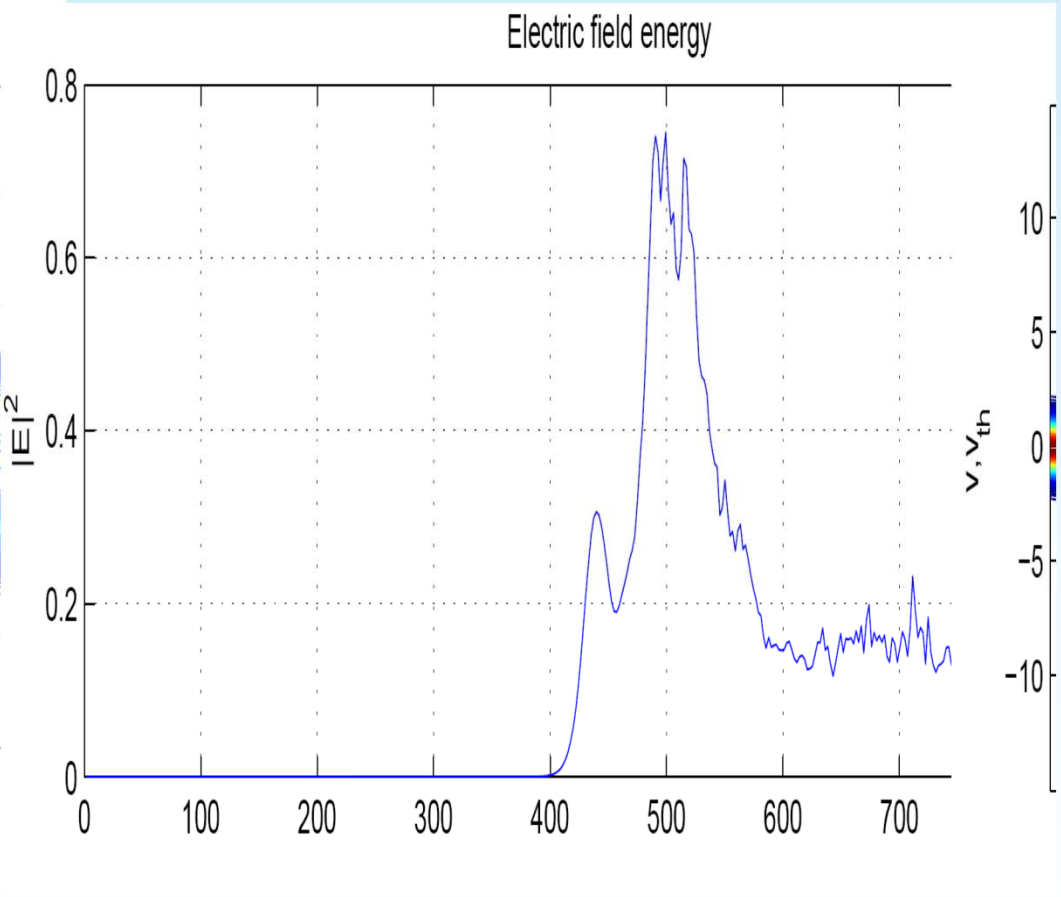

- **Te = 3 Ti**

Phase space evolution

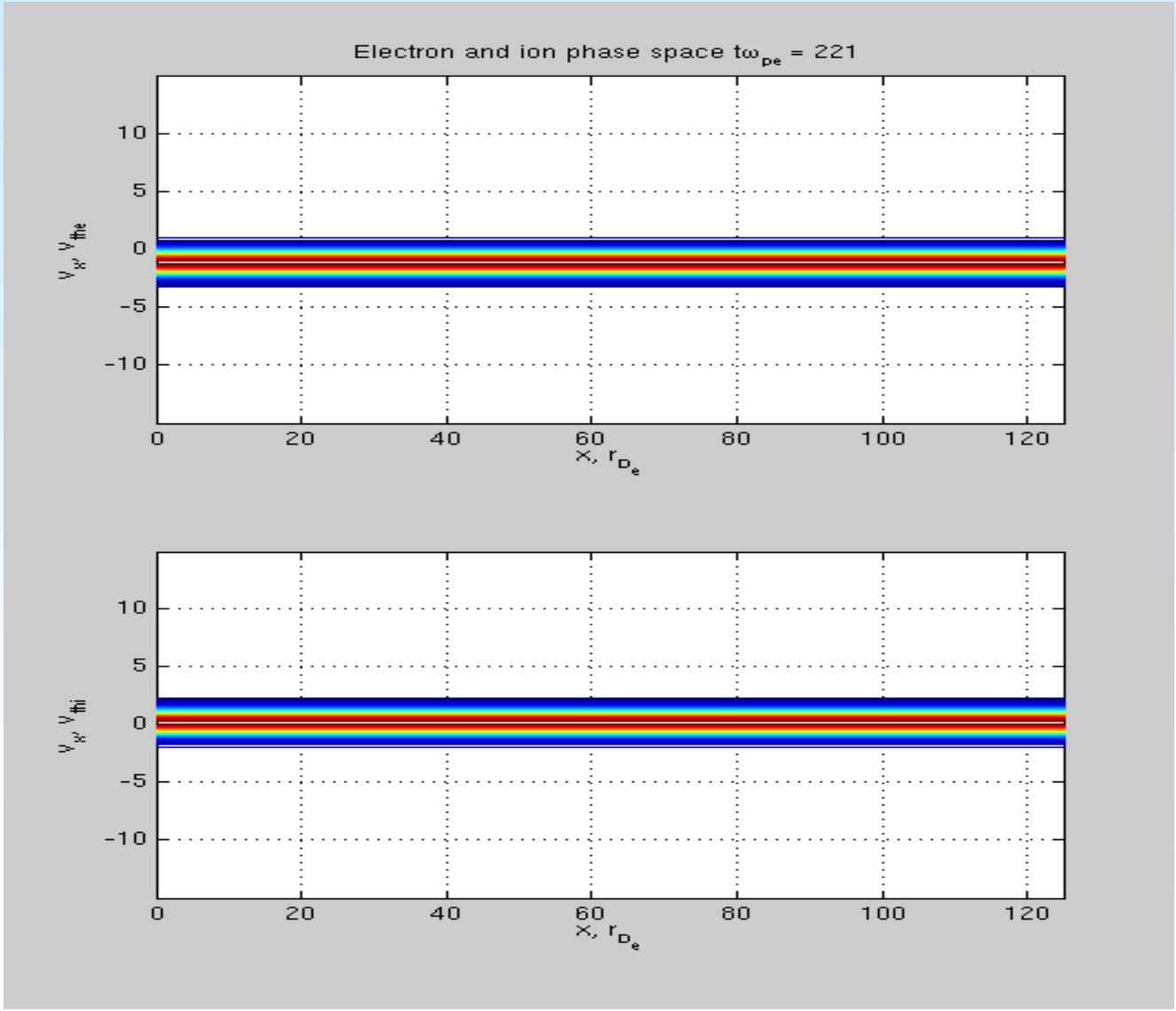

<- electrons

- The movie shows the different reaction of heavy ions and light electrons

<- ions

„Anomalous“ collision rate

The ensemble averaging of the Vlasov equation for $f_j = f_{0j} + \delta f_j.$ with

$$\langle \delta f_j \rangle = \left\langle \delta \vec{E} \right\rangle = \left\langle \delta \vec{B} \right\rangle = 0.$$

$$\frac{\partial f_{0j}}{\partial t} + \vec{v} \cdot \frac{\partial f_{0j}}{\partial \vec{r}} + \frac{e_j}{c m_j} \left(\vec{v} \times \vec{B} \right) \cdot \frac{\partial f_{0j}}{\partial \vec{v}} = \left(\frac{\partial f_j}{\partial t} \right)_{an}$$
$$= -\frac{e_j}{m_j} \left\langle \left(\delta \vec{E} + \frac{\vec{v} \times \delta \vec{B}}{c} \right) \cdot \frac{\partial \delta f_j}{\partial \vec{v}} \right\rangle.$$

$$\left(\frac{\partial}{\partial t} n_j m_j v_{y,j} \right)_{an} = \left\langle \delta E_y \delta \rho_j + \frac{\delta j_{z,j} \delta B_x - \delta j_{x,j} \delta B_z}{c} \right\rangle.$$

$$\nu_{eff,j} = \frac{1}{\langle n_j m_j v_{y,j} \rangle} \left(\frac{\partial}{\partial t} n_j m_j v_{y,j} \right)_{an}.$$

In a simulation one can directly determine the momentum exchange rate

$$\nu(t + \delta t/2) = \frac{2}{\delta t} \frac{p(t + \delta t) - p(t)}{p(t + \delta t) + p(t)}$$

Often used is a theoretical estimate of the anomalous collision frequency based on waves and their dispersion (quasilinear approach):

$$\nu = \sum_k \frac{\Delta k |\delta E(k)|^2 \omega_{pe}}{k v_{te}^2 m_e n v_d} Im \xi_e Z(\xi_e)$$

Linear instability growth

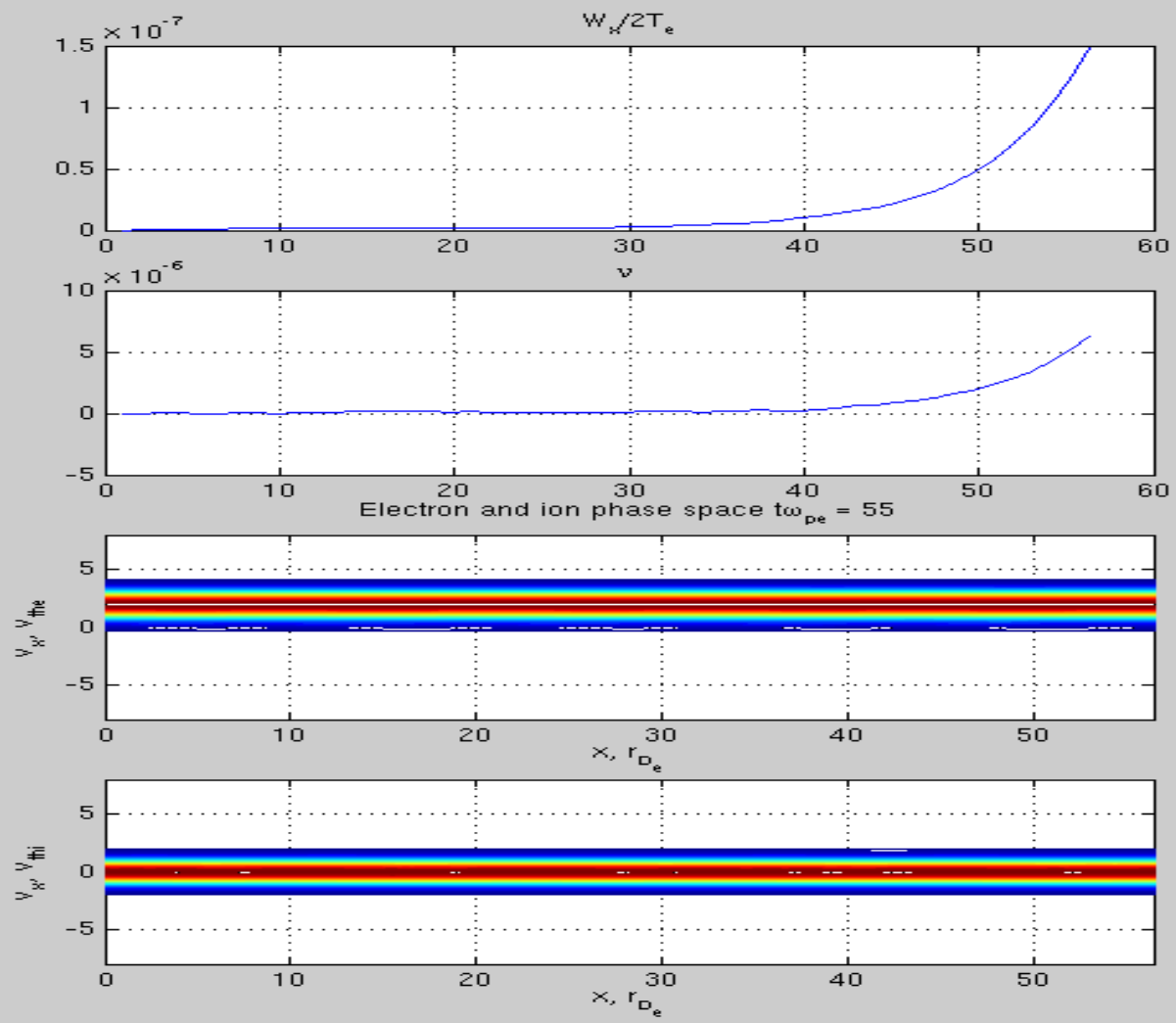

- wave energy starts to grow
- effective, i.e. collisionless "collision rate"
- f(Ve) <-> X (electron distribution function)
- f(Vi) <-> X (ion distribution function)

Quasi-linear saturation

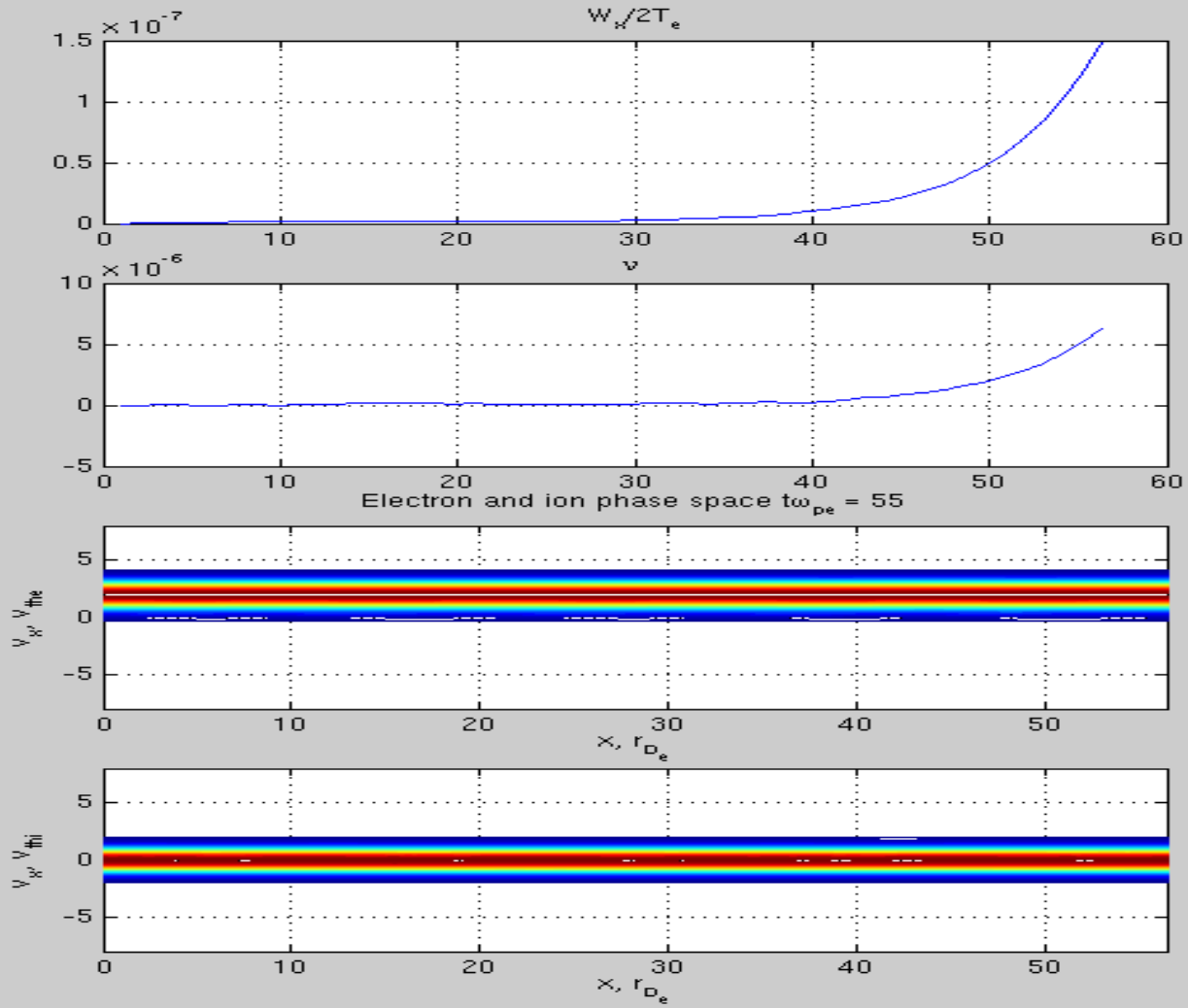

- wave energy
- anomalous collision rate
- v <-> x electrons
- v <-> x ions

Trapping in electron holes

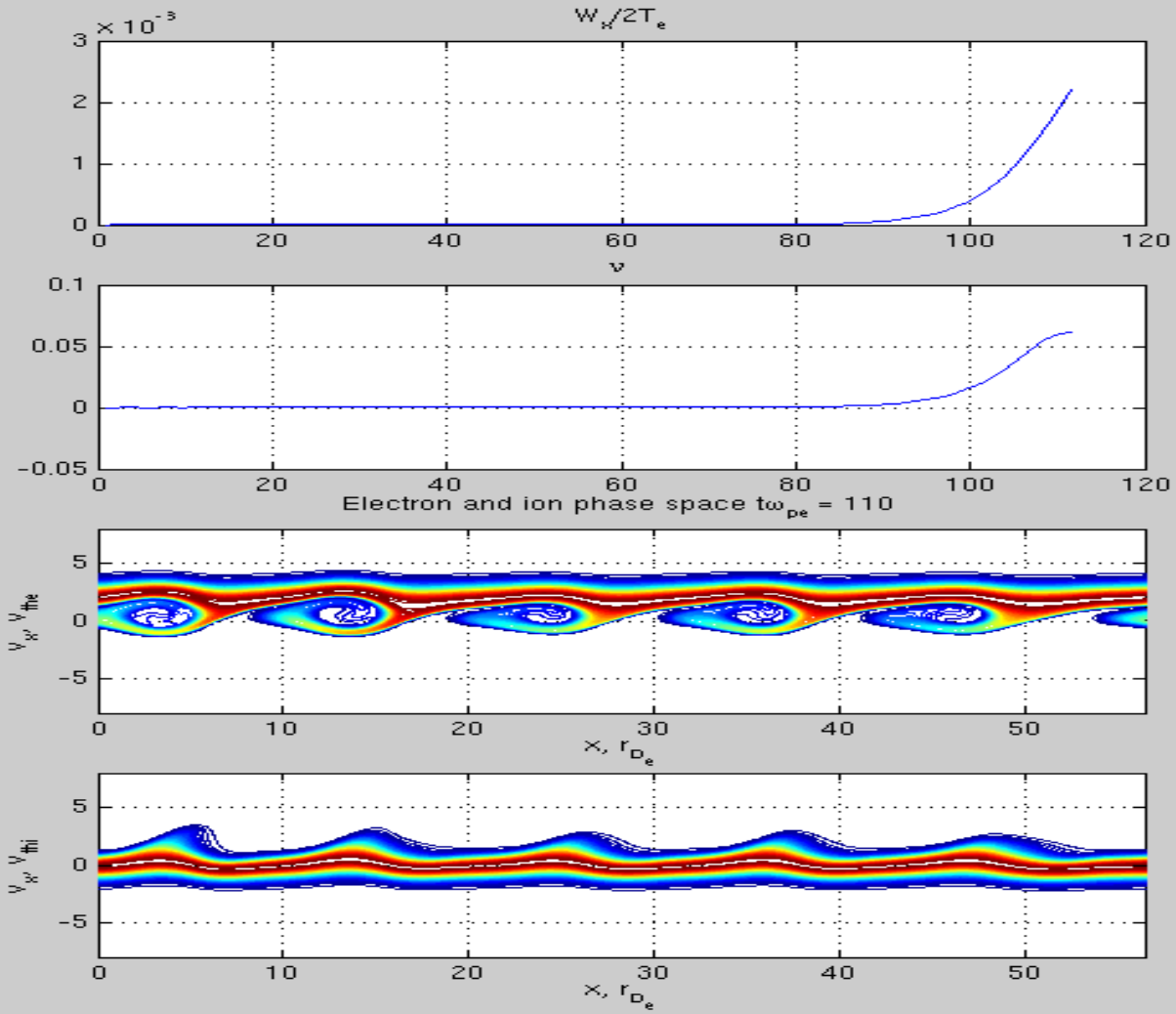

- wave energy at its maximum:
- E^2 = 0.006 n T
- the electron hole effective collision rate" nu= 0.05 ω_{pe}

is close to Sagdeev's prediction:

$$D = (\frac{c}{\omega_e})^2 \omega_e \frac{\epsilon_0 \delta E^2}{2nT}$$

$$D^{th} = 10^{-2} (\frac{c}{\omega_e})^2 \omega_i (\frac{v_d}{c_s})(\frac{T_e}{T_i})$$

Nonlinear island saturation

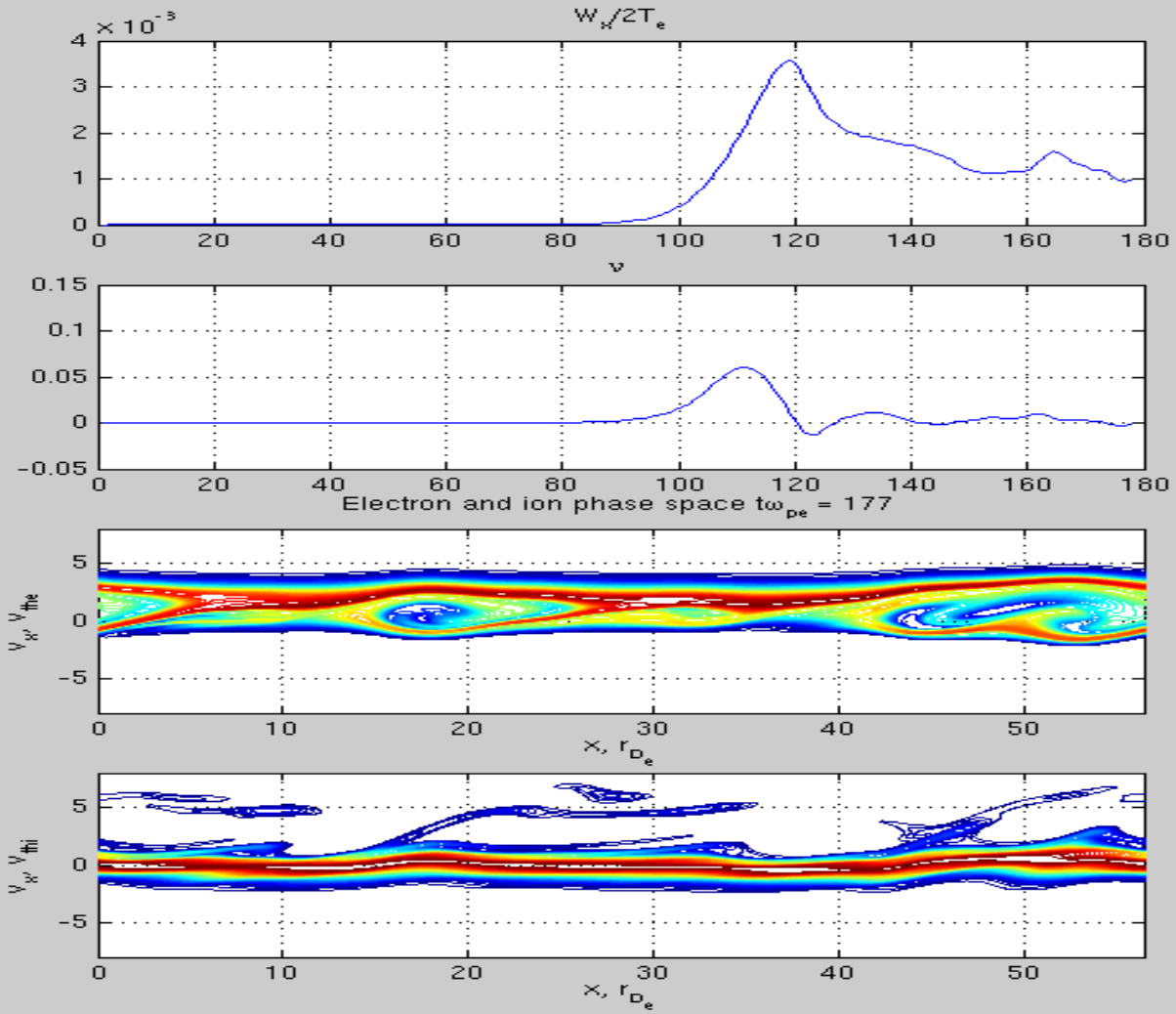

- wave energy decreased
- low "collision rate"

  the electron current is reduced, the free energy exhausted,
- islands cannot grow any further
- ions heated, but saturation at low quasilinear level

Resulting IA collision rate vs. the quasi-linear estimate (blue)

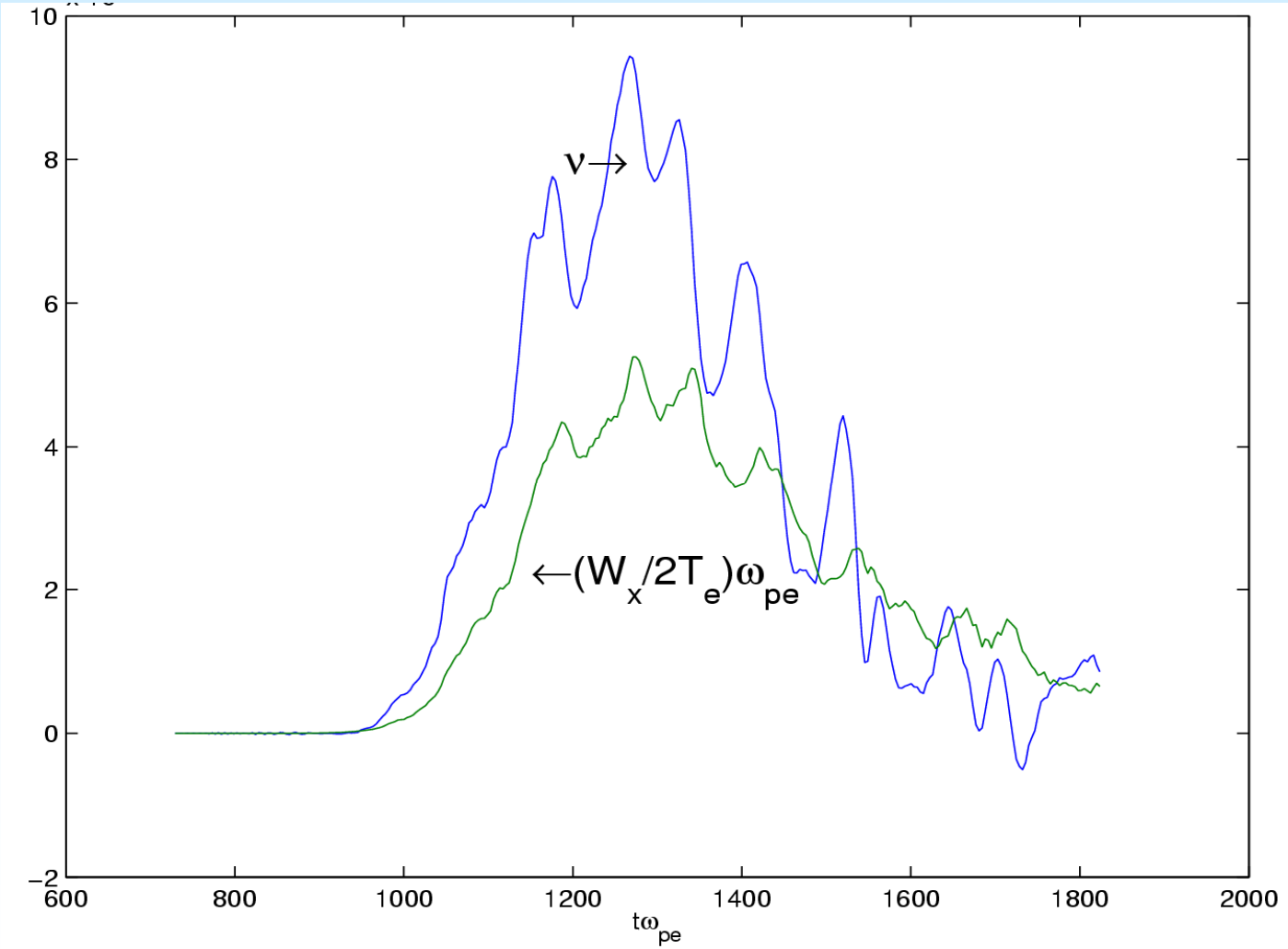

Note that, for periodic boundary conditions, after the free energy is exhausted, the anomalous collision rate decreases to zero [from Büchner & Elkina]

Collisionless balance of E +v x B

Two-fluid electron equation of motion: -> "generalized Ohm's law":

$$\frac{4\pi}{\omega_{pe}^2}\frac{d\vec{J}}{dt} = \vec{E} + \vec{v}_i \times \vec{B} - \frac{1}{ne}\vec{J} \times \vec{B} + \frac{1}{ne}\nabla p_e - \eta\vec{J}$$

In case of the corona: strong guide fields -> to the lowest order one-dimensional balance equation for Epar

$$E_{\|} = -\frac{m_e}{ne}\frac{d(nv_e)}{dt} - \frac{1}{ne}\frac{dp_e}{dx_{\|}} + \frac{1}{ne}f_{eff}$$

Electric field ⇔ Electron inertia + Pressure gradient + f_{eff} = "drag force" due to collective wave-particle interaction

Nature of the "drag force"

Representing $f_j = f_{0j} + \delta f_j \quad E_{\parallel} = \left\langle E_{\parallel} \right\rangle + \delta E_{\parallel} \quad \vec{B} = \delta \vec{B}$

for an appropriate averaging

-> the Vlasov equation reveals: $\left\langle \delta f_j \right\rangle = \left\langle \delta \vec{E} \right\rangle = \left\langle \delta \vec{B} \right\rangle = 0.$

$$\frac{\partial f_{0e}}{\partial t} + \vec{v} \cdot \frac{\partial f_{0e}}{\partial \vec{r}} + \frac{e}{m_e} \vec{E} \cdot \frac{\partial f_{0e}}{\partial \vec{v}} = -\frac{e}{m_e} \left\langle \left(\delta \vec{E} + \vec{v} \times \delta \vec{B} \right) \cdot \frac{\partial \delta f_e}{\partial \vec{v}} \right\rangle$$

after velocity-space integration, the momentum exchange rate is

$$\left(\frac{d}{dt} n m_e v_{y,e} \right)_{eff} = \langle \delta E_y \delta \rho_e + \delta j_{z,e} \delta B_x - \delta j_{x,e} \delta B_z \rangle$$

-> What fluctuations / turbulence is generated in the corona?

-> The correlations above have to be determined by kinetic numerical simulations!

Excitation beyond quasi-linearity

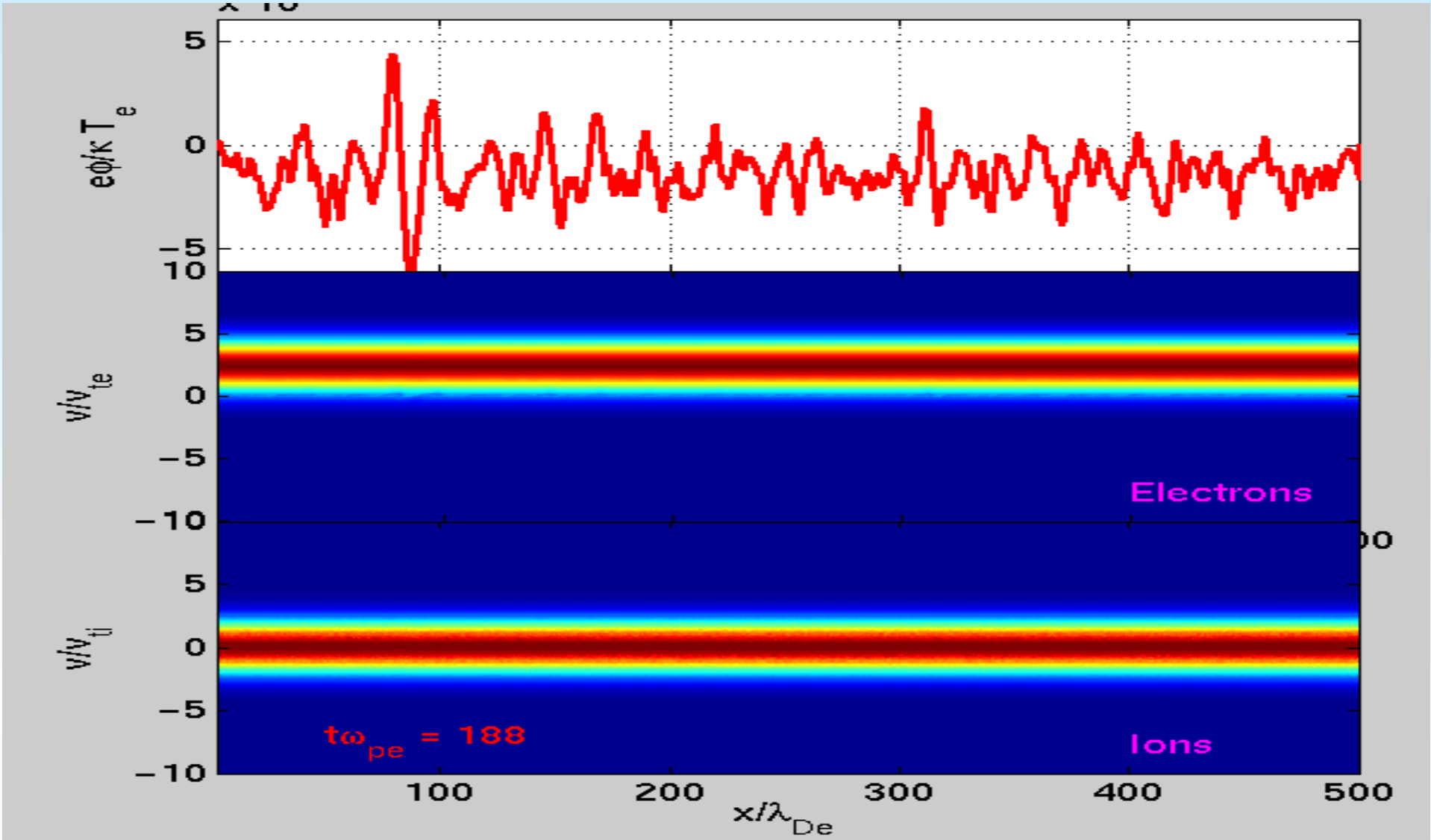

Electron phase space holes

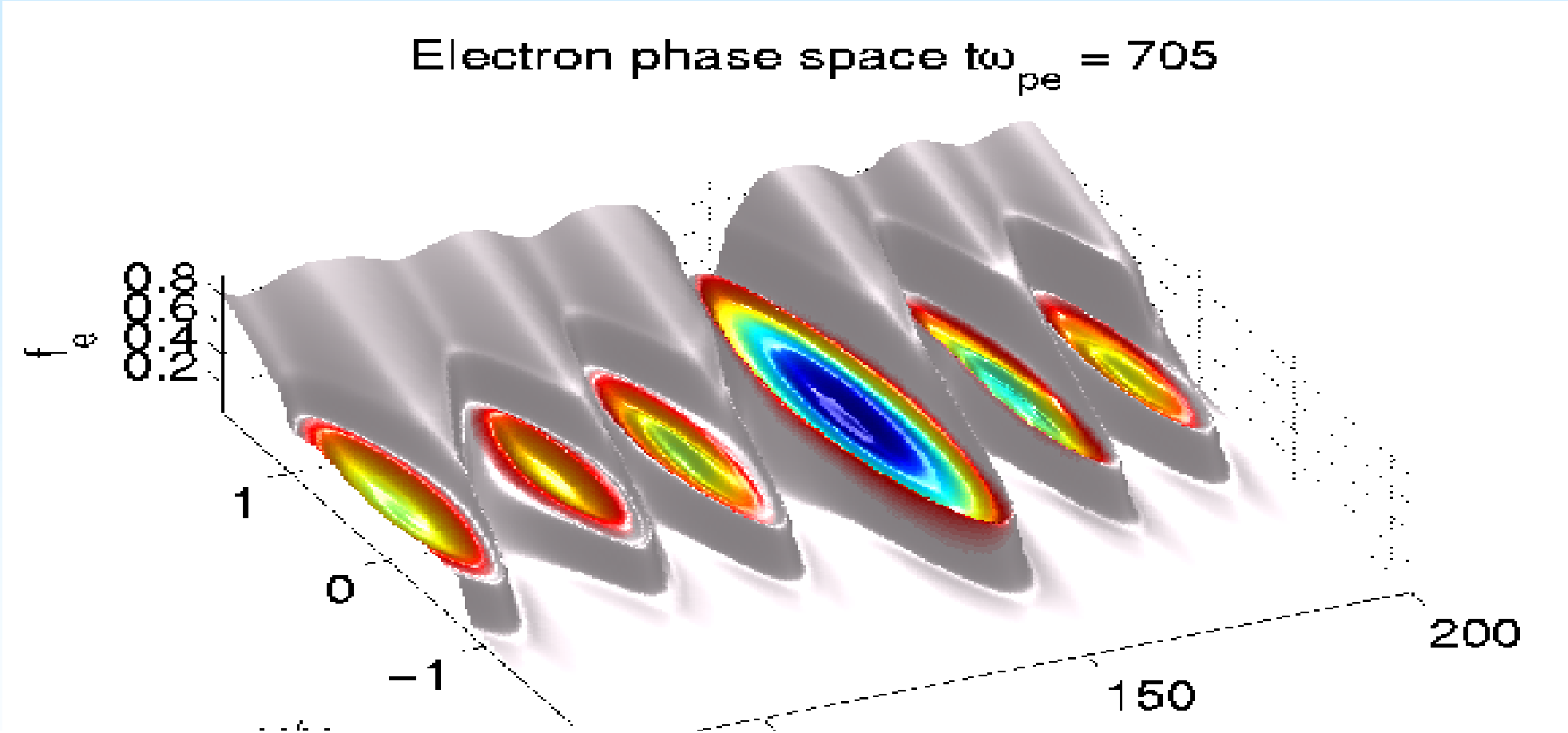

Electron phase space holes -> They grow and lead beyond the quasi-linearl (QL), weak turbulence theory level.

Later also ion density holes

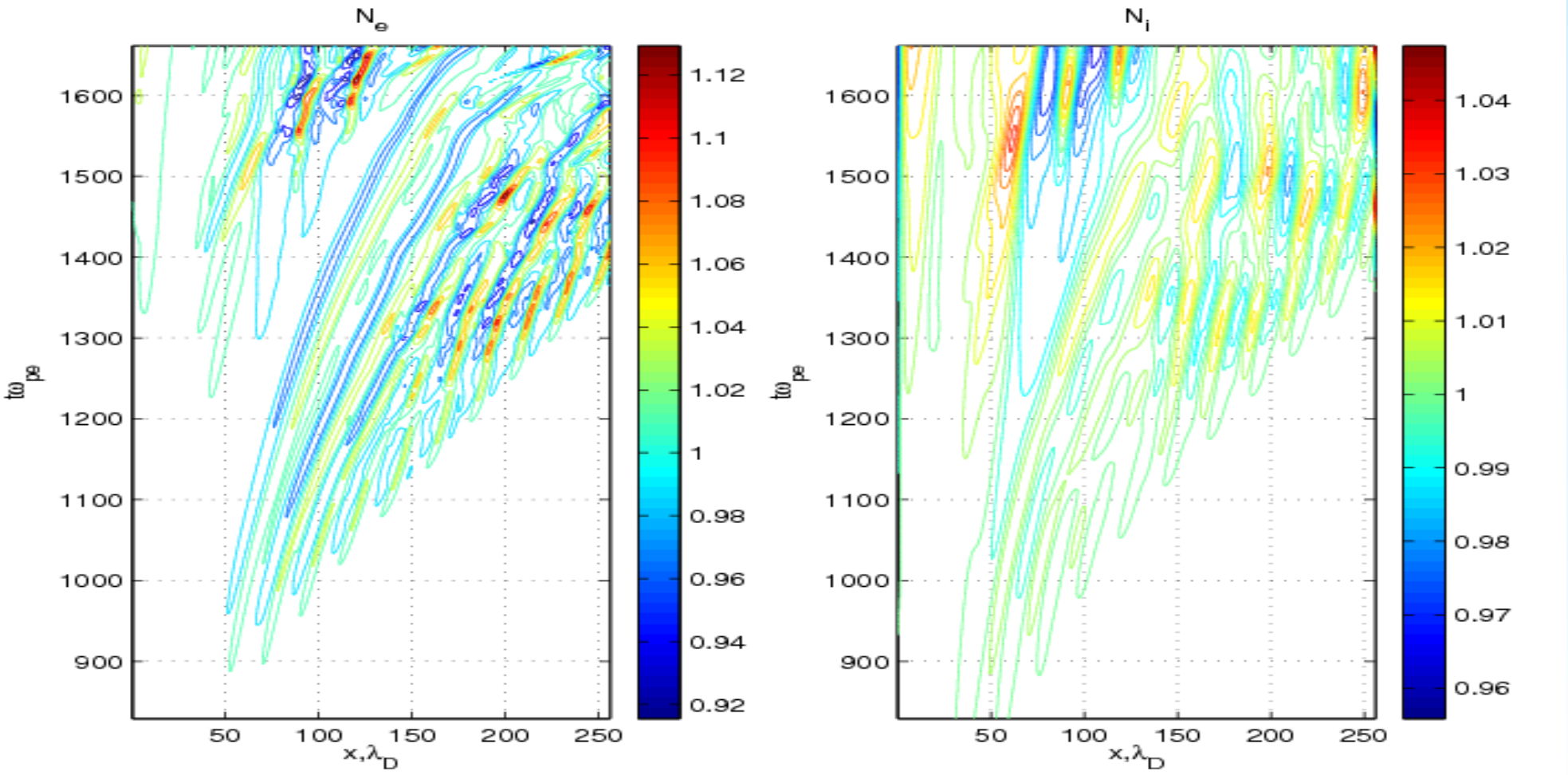

In case of open boundary conditions after electron density holes are formed (left plot) also ion holes are formed (right plot).

Hole potential-assymetric growth

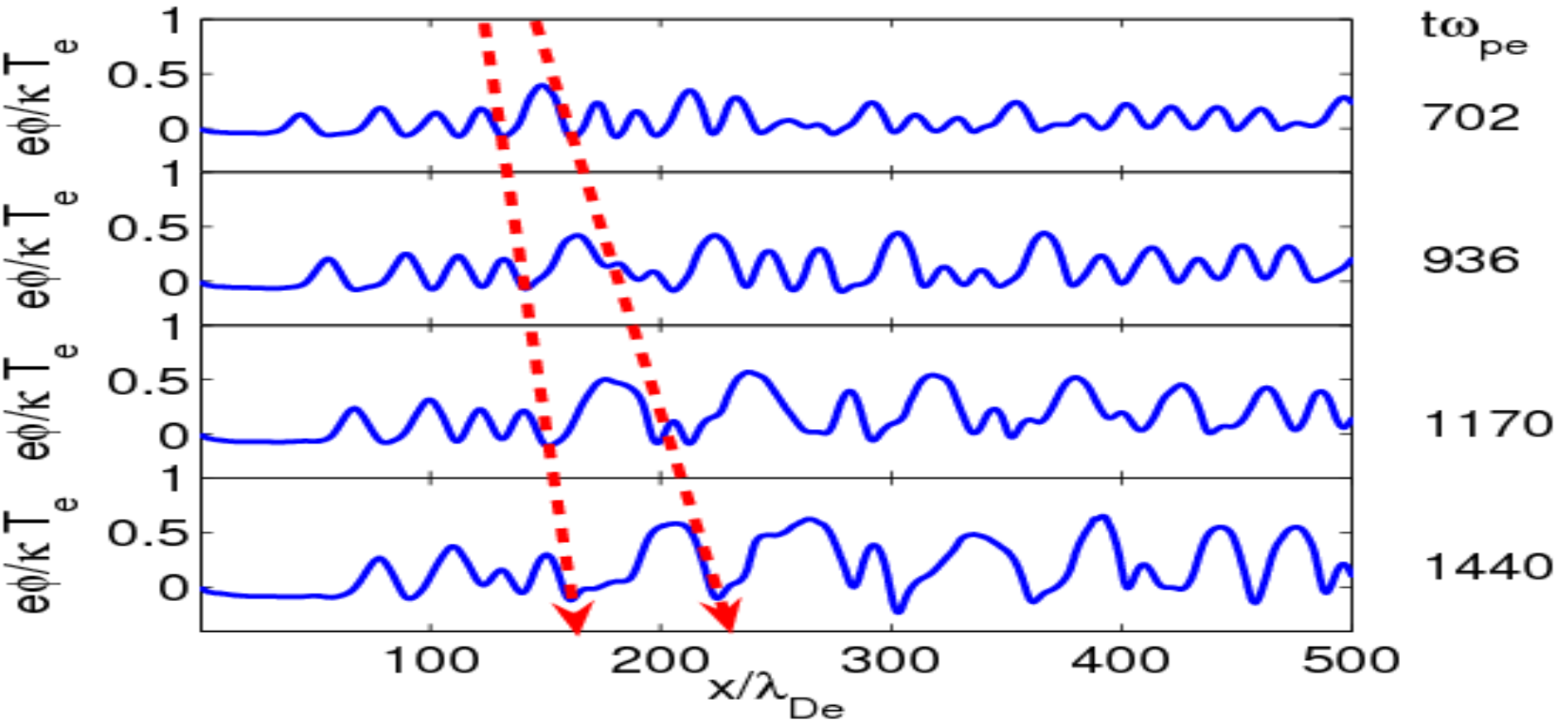

Net energy exchange becomes possible due to growing asymmetries of the electron hole potential wells with a steepening leading edge. [Büchner & Elkina]

Growth of the AC E-field power

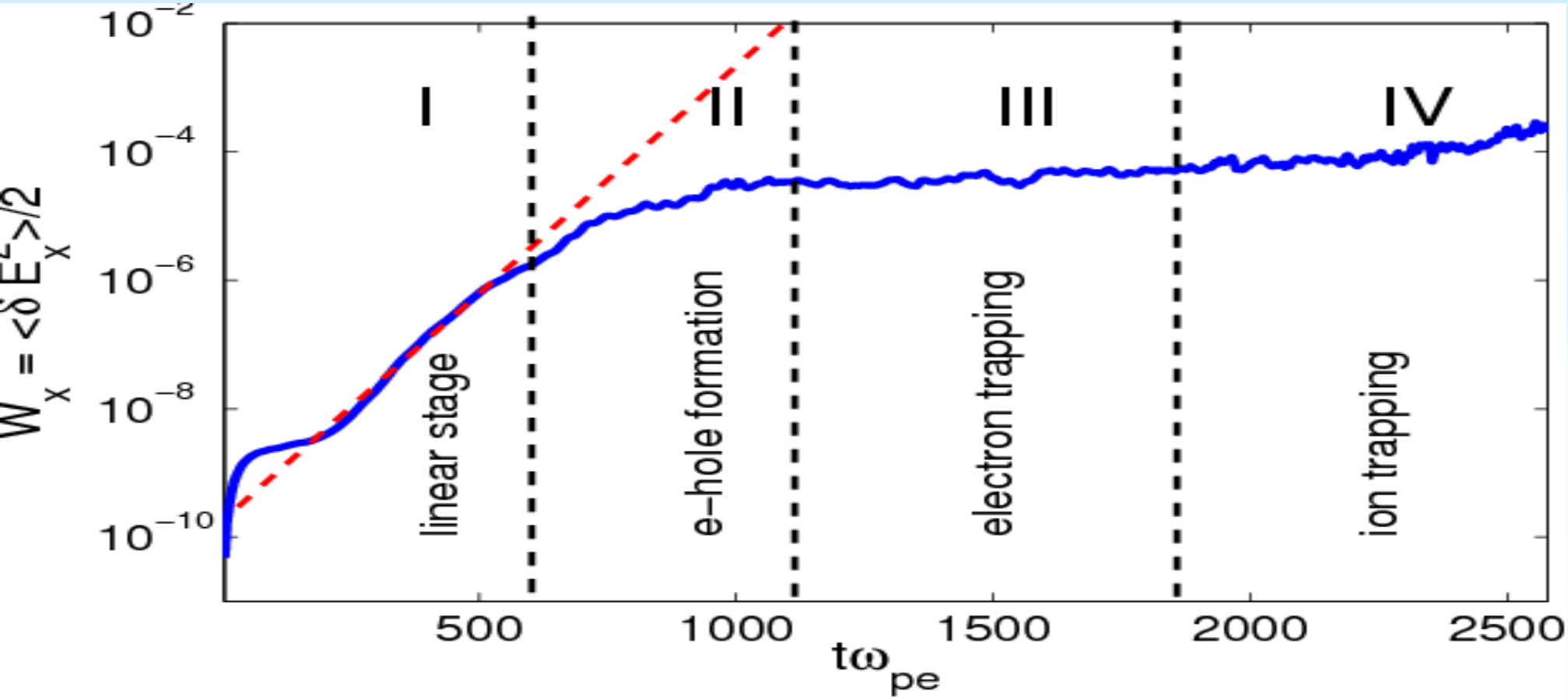

Multi-stage non-linear evolution of the current instability for open boundaries: electron holes -> ion holes -> e-s double layers

Finally – the ion holes merge into electrostatic double layers

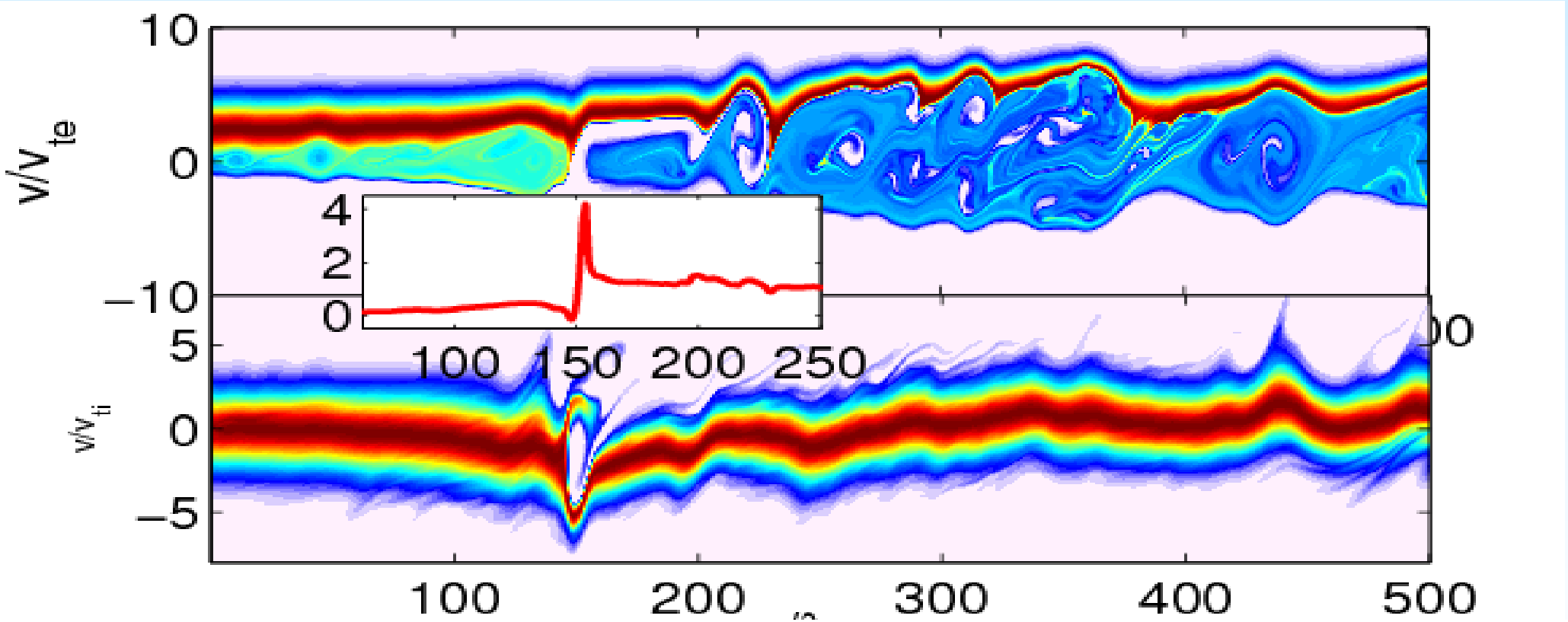

Inset: electrostatic potential around the double layer. The ion holes merge into the double layer while the electron motion becomes highly turbulent behind the layer [from Büchner & Elkina, 2006].

Quantify by „quasi-collision rates“

Using the definition: the „anomalous“ re

$$E_{\parallel} = \eta_{an} j_{\parallel} = \eta_{an} ne \left(v_i - v_e\right)$$

$$\eta_{an} = \frac{E_{\parallel}}{j_{\parallel}} = \frac{1}{ne(v_i - v_e)} \left(-\frac{m_e}{ne} \frac{d(nv_e)}{dt} - \frac{1}{ne} \frac{dp_e}{dx_{\parallel}} + \frac{1}{ne} f_{eff} \right)$$

with ..... where

$$\eta_{an} = \frac{m_e}{ne^2} \nu_{an} = \left(\epsilon_0 \omega_{pe}^2\right)^{-1} \nu_{an}$$

$$\nu_{an} = -\nu_{in} - \nu_{pg} + \nu_{eff}$$

$$\nu_{in} = \frac{1}{n(v_i - v_e)} \frac{d(nv_e)}{dt} \qquad \nu_{pg} = \frac{1}{nm_e(v_i - v_e)} \frac{dp_e}{dx_{\parallel}} \qquad \nu_{eff} = \frac{f_{eff}}{ne(v_i - v_e)}$$

Local „anomalous“ collision rates

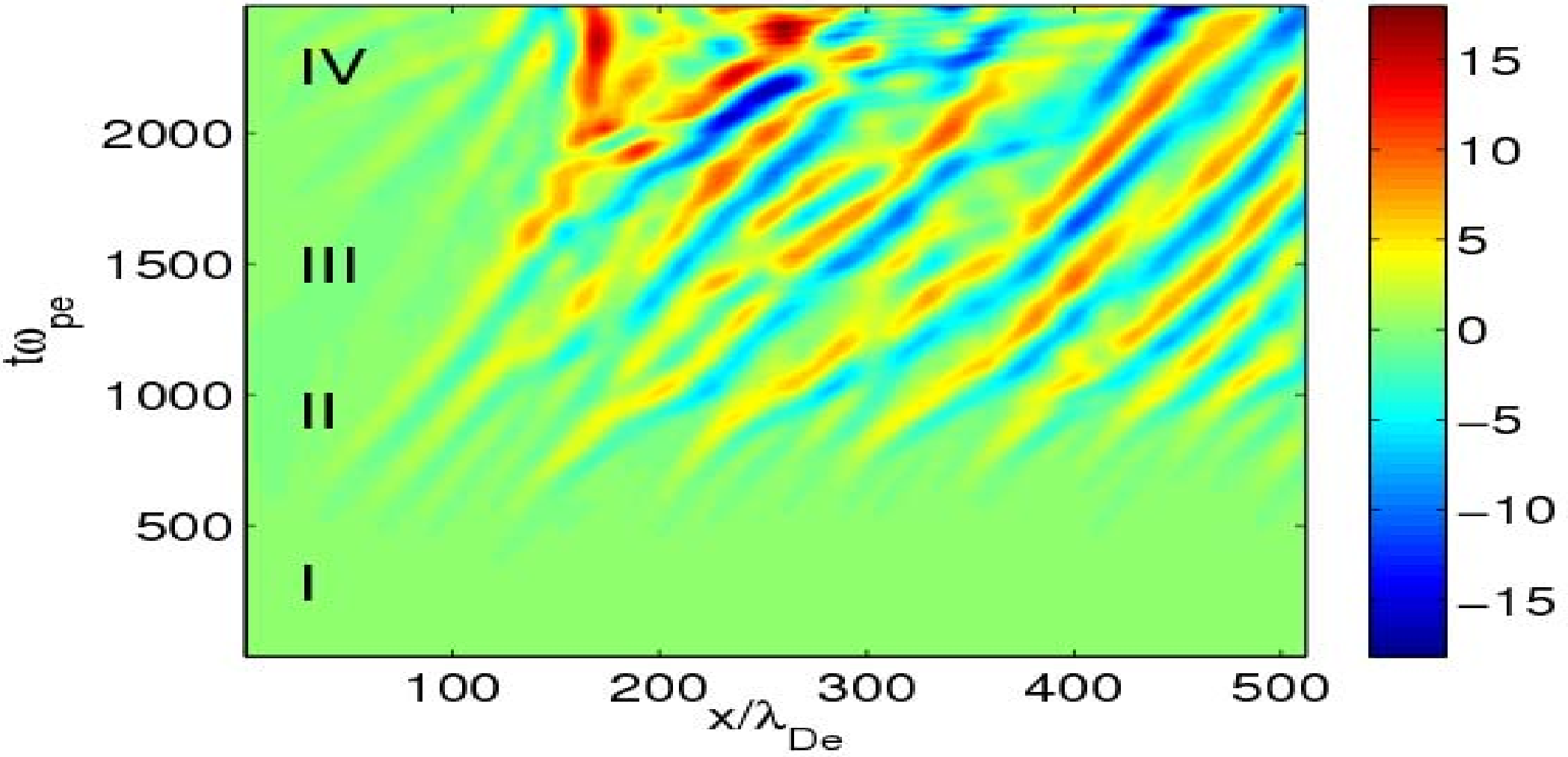

„Anomalous“ friction at phase space holes / DLs while locally particles can also gain enery -> the average matters!

Average „collision rates“

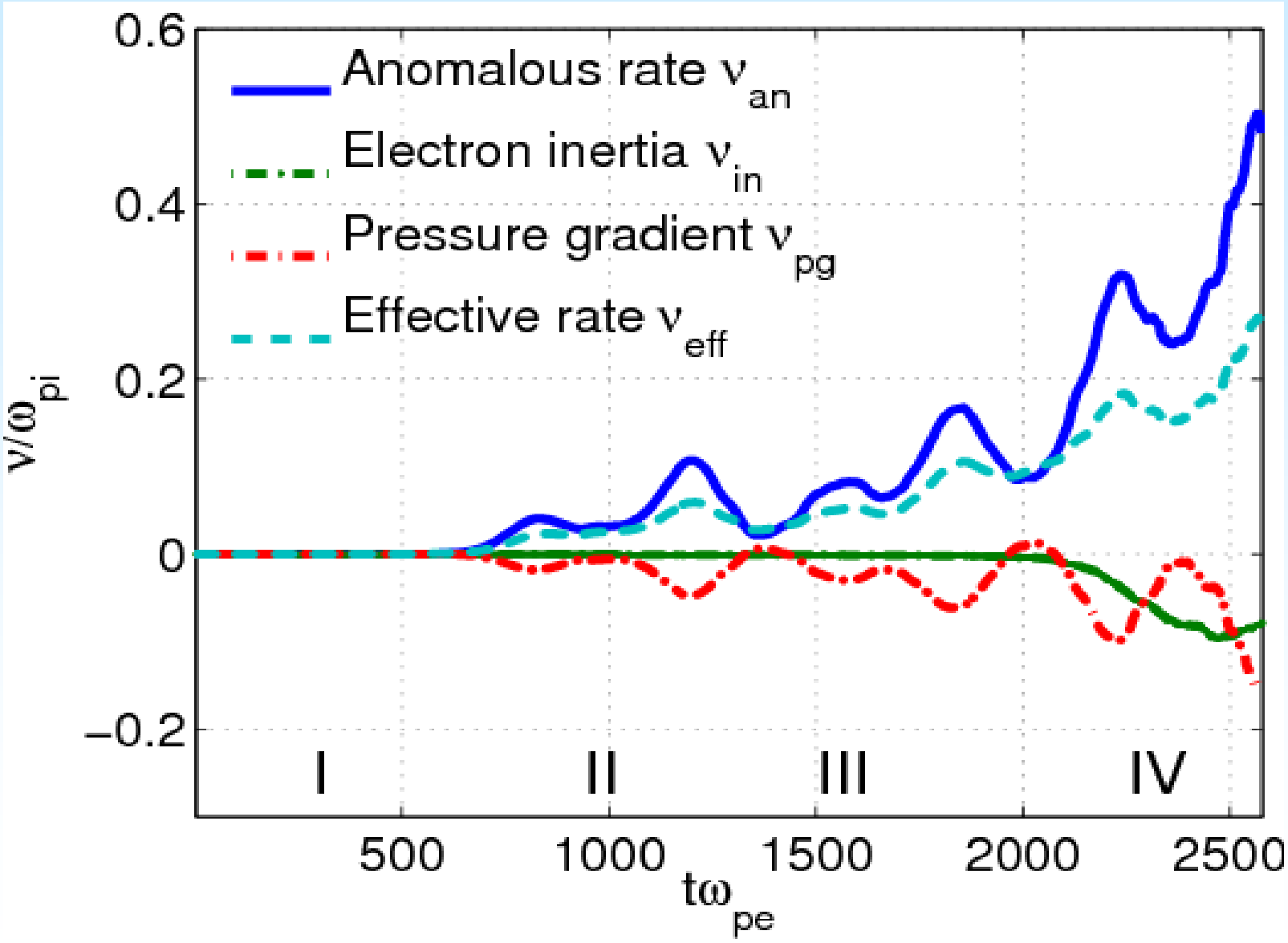

[Büchner and Elkina]:

The Rm, which corresponds to the threshold Uccv > Vte for the instability l = c / ω_pi = 20 m, V= 20 km/s and Nu=0.5 ω_pi is Rm ~ 1!

2D current sheet instability

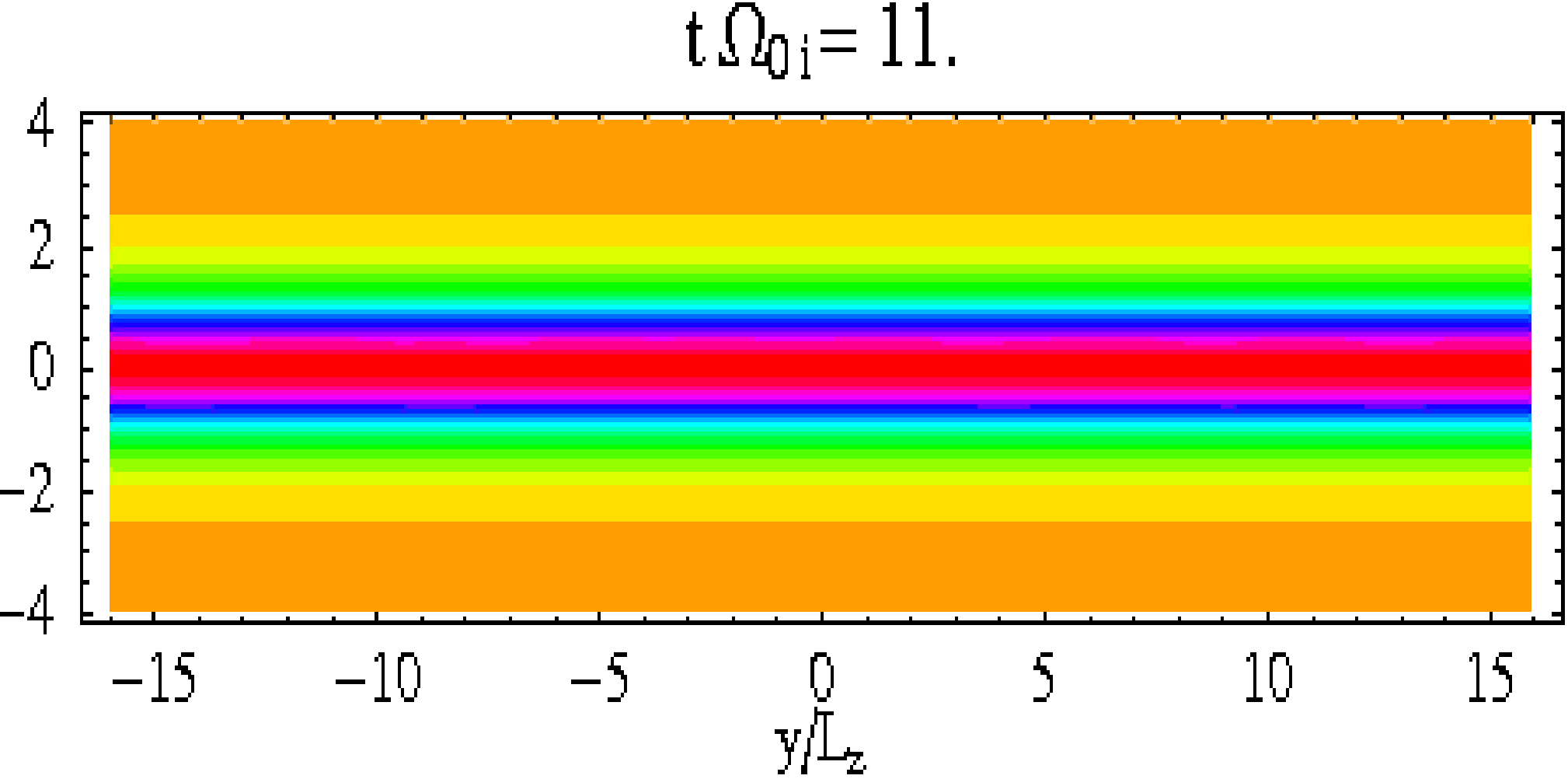

2D Current sheet „collision rates“

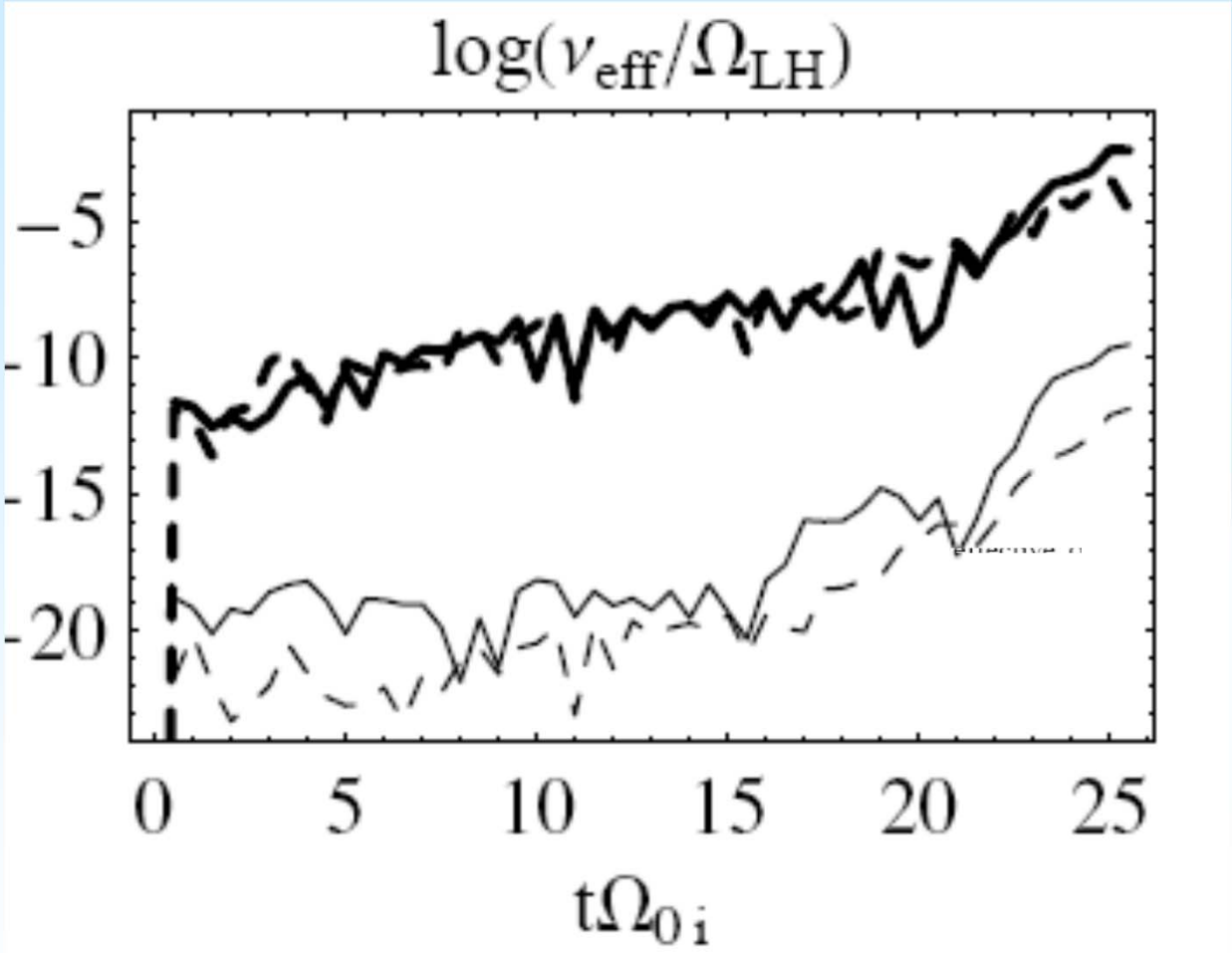

In the solar coronal plasma these rates exceed those of the 1D instability by a factor of about 6
[Silin & Büchner]

Effective „collision rates“: Solid (electric) $\delta\rho\delta E_{\shortparallel}$ and dashed (magnetic fluctuations) $\delta j \times \delta B$ lines;
(Upper - thicker lines: electrons; Lower - thinner lines: ions

3D current sheet instability

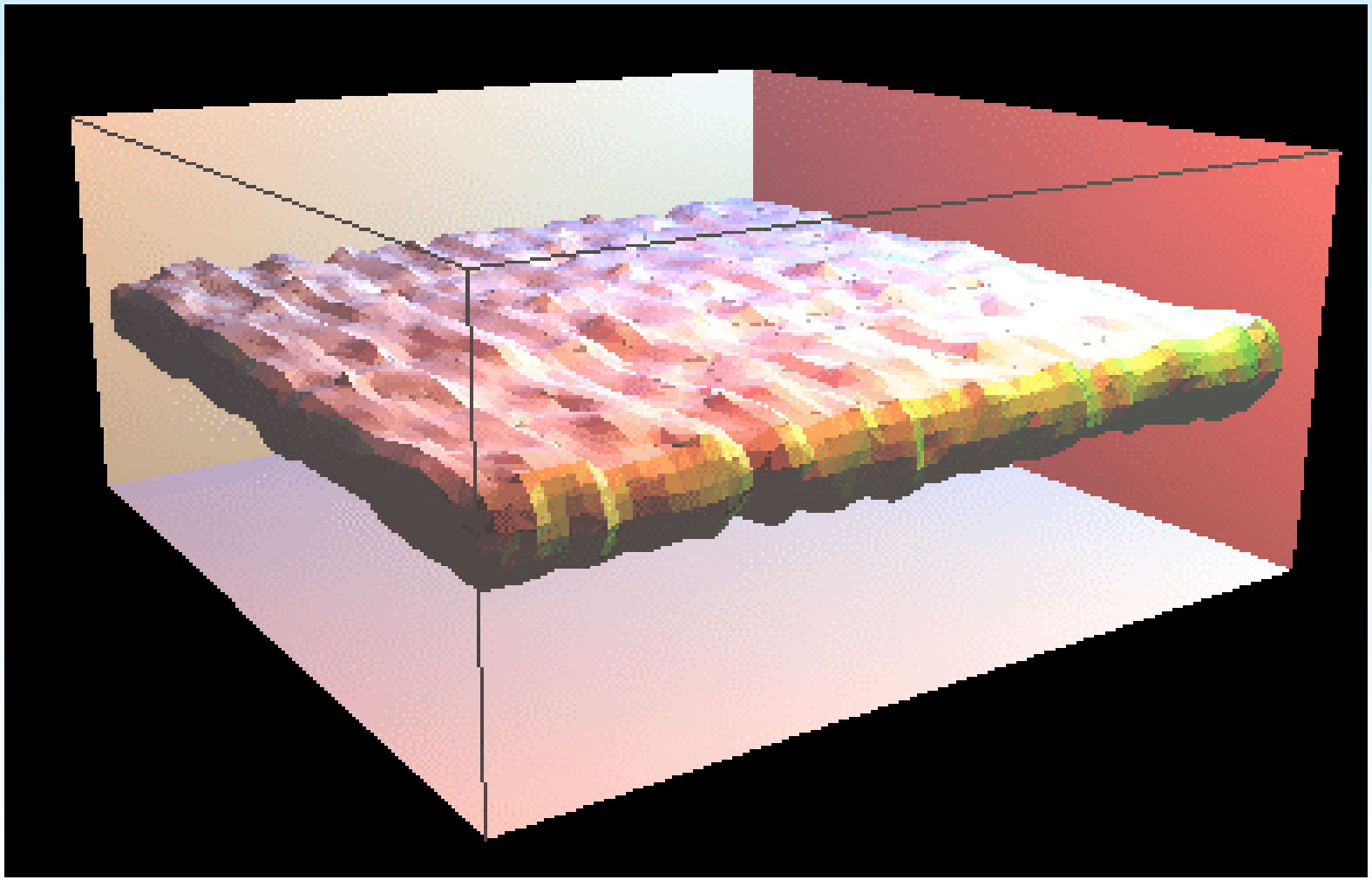

3D magnetic Nulls (simulation result by [Büchner & Kuska])

Result for the use in MHD simulations: turbulent resistivity

Magnetic diffusivity expressed via an effective „collision frequency“:

$$\eta = \frac{\nu}{\epsilon_0 \omega_{pe}^2}$$

Neglible: binary particle collision [Spitzer 56, Härm–Braginski 63]

$$\nu_{coll} \approx \frac{\omega_{pe}}{n\lambda_D^3}$$

There is no indication for the estimate of [Bunemann 1958] in the solar corona

$$\nu_{eff} \approx \omega_{pe}/2\pi$$

PIC and Vlasov code simulations revealed for the solar corona: [Büchner, Kuska, Silin, Elkina, 99-08]

– 1D small beta: IA / double layers

$$\nu_c \approx \omega_{pi}/2\pi$$

– 2D higher beta – LH turbulence

$$\nu_c \sim \omega_{LH}$$

- 3D highest beta: LH/kink sausage

$$\nu_c \approx \omega_{pi}$$

Summary

- Both MHD and kinetic simulations are important on their own rights – whatever one wants to investigate:
  - Large scale flows and instabilites, fluid turbulence -> MHD
  - particle acceleration, collisionless dissipation, collisionles balancing of electric fields in reconection, microturbulence -> kinetic approach
- Open question: What has not been achieved yet is a direct coupling of the two approaches